Modern Journal of Statistics
2(1), 32–74
DOI:https://doi.org/10.64389/mjs.2026.02140
https://sphinxsp.org/journal/index.php/mjs/

Research article

Obulezi distribution: a novel one-parameter distribution for lifetime data modeling

Okechukwu J. Obulezi

Department of Statistics, Faculty of Physical Sciences, Nnamdi Azikiwe University, P.O. Box 5025, Awka, Nigeria.

* **Correspondence:** oj.obulezi@unizik.edu.ng

ARTICLE INFO

Keywords:
Obulezi distribution
Estimation
Exponential distribution
Mixing proportion
Tail behaviour

Mathematics Subject Classification:
60E05, 62F10, 62N05

Important Dates:
Received: 7 October 2025
Revised: 5 November 2025
Accepted: 5 November 2025
Online: 6 November 2025

ABSTRACT This paper introduces the novel, single-parameter `Obulezi` distribution for modeling lifetime data. We derived its statistical and reliability properties and performed an exhaustive comparison of fifteen parameter estimation techniques via simulation and application to three real datasets. Simulation results confirmed the consistency of all estimators, while empirical analysis showed the `Obulezi` distribution consistently yielded the lowest standard errors, proving it to be the most precise and stable model compared to competitors. Goodness-of-fit metrics confirmed the `Obulezi` distribution's superior fit, particularly for data exhibiting an increasing hazard rate. The `Obulezi` distribution is thus a robust and highly competitive model for parsimonious survival and reliability analysis.

1. The Genesis

The study of lifetime distributions is a cornerstone of reliability theory, survival analysis, and demography. These models, which describe the time until an event occurs (e.g. failure of a component, death of a patient), are critical for accurate risk assessment and prediction.

The origin of constructing new and flexible lifetime models often traces back to mixing simpler and well-established distributions. Lindley [9] pioneered this approach by proposing a distribution as a mixture of exponential and gamma distributions. This technique provided a new avenue for modeling real-world data that often exhibit characteristics, such as skewness and varying hazard rates, not adequately captured by the ubiquitously used exponential distribution. The exponential distribution, while simple, is often limited

by its assumption of a constant hazard rate (memoryless property), which is unrealistic for many aging or reliability processes.

Following the seminal work of Lindley's distribution, the field of continuous probability modeling, particularly for lifetime data, has inspired a substantial proliferation of new, single-parameter continuous probability models, all designed to offer greater flexibility and improved fit over classical forms. This extensive research includes the fundamental Shanker family extensions such as Akash [18], Shanker [19], Shambhu [23], Aradhana [21], Sujatha [24], Amarenda [20], Devya [22], Rama [26], Rani [27], Akshaya [25], Suja [28], Om [35], Shukla [38], Komal [30], Pratibha [31], Kamlesh-Rama [36], Shreekant [32], Ishita [33], Sujit [15], Adya [34], and Uma [29]. Other similar distributions includes Pranav [8], Prakaamy [37], Iwueze [5], Odoma [10], Juchez [2], Hamza [1], Chris-Jerry [13], Fav-Jerry [3], Doje [14], Emrem [11] and Updated Lindley [12], all of which are often formulated through mixtures of exponential and gamma distributions. The central goal behind these diverse structural variations is to generate specialized density functions that capture different degrees of over-dispersion, kurtosis, and hazard rate shapes, thereby providing statisticians and engineers with more effective and specialized tools to achieve superior goodness-of-fit when modeling complex, real-world data across various applied sciences.

The primary advantage of the Lindley distribution and its many extensions lies in offering a more generalized, single-parameter alternative to the exponential distribution. These variants are particularly effective in describing positively skewed data frequently encountered in survival and reliability problems, providing a less restrictive, non-constant (e.g., bathtub-shaped, or first increasing then decreasing) hazard function. Furthermore, some variants are ingeniously paired with discrete models, such as the Poisson, to generate count distributions (e.g., the Poisson-Lindley), thereby extending their utility to modeling discrete data.

2. The Proposed `Obulezi` Distribution: Motivation and Contribution

While the exponential and its single-parameter extensions have expanded the toolkit for modeling lifetime data, empirical observations continue to reveal datasets with unique tail behaviors and complex hazard rate patterns that existing models struggle to fit optimally. The continued development of new distributions is motivated by the necessity to find models that are both parsimonious (few parameters) and flexible (good fit to diverse data structures) to achieve superior model performance and predictive accuracy. Specifically, datasets exhibiting extremely heavy right-skewness or complex risk profiles (i.e., non-monotonic hazard rates) often demand novel distributions.

In this study, we propose a novel distribution to model lifetime events, which we refer to as the `Obulezi` distribution. This new model is developed as a contribution to the body of single-parameter lifetime distributions, aiming to provide a more accurate and robust fit for specific types of data where established models like Lindley and Shanker may be sub-optimal. The introduction of the `Obulezi` distribution is justified by its potential to offer a superior performance, as will be demonstrated through detailed analytical properties and application to real-world data. We will thoroughly investigate its statistical properties, including moments, entropy, and reliability measures, before demonstrating its practical utility through comparative model fitting against established competitors.

A non-negative real-valued random variable X is said to follow `Obulezi` distribution with parameter $\rho > 0$, if its cumulative distribution function (CDF) is given as;

$$R(x) = 1 - \left(1 + \frac{\rho^3 x}{\rho^3 + 2}\right) e^{-\rho x}; \quad x > 0. \tag{2.1}$$

The corresponding probability density function (PDF) to Equation (2.1) is given by;

$$r(x) = \left(\rho^3 x + \rho^3 - \rho^2 + 2\right) \frac{\rho e^{-\rho x}}{\rho^3 + 2}; \quad x > 0, \tag{2.2}$$

where x is a continuous random variable, hence we write $X \sim$ `Obulezi`(ρ). The PDF in Equation (2.2) is of the form;

$$r(x) = \underbrace{\left(\frac{\rho^2}{\rho^3 + 2}\right)}_{W_1} \cdot \underbrace{\left(\rho^2 x e^{-\rho x}\right)}_{\text{Gamma}(2,\rho)\text{ PDF}} + \underbrace{\left(\frac{\rho^3 - \rho^2 + 2}{\rho^3 + 2}\right)}_{W_2} \cdot \underbrace{\left(\rho e^{-\rho x}\right)}_{\text{Exponential}(\rho)\text{ PDF}},$$

with the mixing proportions W_1 and W_2 such that $W_1 + W_2 = 1$. The Gamma$(2, \rho)$ distribution (also called Erlang$(2, \rho)$) describes the waiting time until the second event in a Poisson process with rate ρ. The Exponential(ρ) distribution describes the waiting time until the first event in the same process.

The next is the hazard function, which quantifies the instantaneous potential for an event (such as death, failure, or recovery) to occur at time x, given that the event has not occurred before time x. It represents the instantaneous rate of failure at time x, analogous to a "risk rate" or "force of mortality." While the PDF, $r(x)$, is a measure of the unconditional probability of an event around time x, the hazard function $h(x)$ is a measure of the conditional probability. More formally, for a small time interval Δx, the hazard function can be approximated by:

$$h(x) \approx \frac{P(x \leq X < x + \Delta x \,|\, X \geq x)}{\Delta x} = \frac{\rho\left(\rho^3 x + \rho^3 - \rho^2 + 2\right)}{\rho^3 x + \rho^3 + 2},$$

where T is the random variable that represents the time until the event. The profile of the hazard function

Theorem 1 (Hazard function profile)**.** *The hazard function $h(t)$ profile is summarized thus;*

$$\begin{cases} \lim\limits_{x \to 0} h(x) = \frac{\rho(\rho^3 - \rho^2 + 2)}{\rho^3 + 2} & \forall \rho \\ \lim\limits_{x \to \infty} h(x) = \rho \end{cases}. \tag{2.3}$$

Equation (2.3) implies that;

(i) The hazard rate is bounded and approaches a constant value ρ as time goes to infinity.

(ii) This suggests a long-term risk that stabilizes at the value of the parameter ρ.

Corollary 1 (The shape or monotonicity)**.** $h'(x) > 0 \quad \forall, x > 0$. *This implies that the hazard function is strictly increasing for all time x.*

Corollary 2 (Sensitivity of the profile to the parameter, ρ)**.** *Since ρ is the only parameter controlling the shape, it dictates the entire risk profile.*

1. *Long-Term Hazard Rate:* $h(\infty) = \rho$.
2. *Initial Hazard Rate:* $h(0) = \frac{\rho(\rho^3 - \rho^2 + 2)}{\rho^3 + 2}$.

Table 1. Impact of ρ on Starting and Limiting Risk

Behavior of ρ	Impact on $h(\infty)$	Impact on $h(0)$	Risk Interpretation
Small ρ ($\rho \to 0^+$)	$h(\infty) \to 0$	$h(0) \to \frac{0(0-0+2)}{0+2} = 0$	Both initial and long-term risk approach zero. The event is very rare.
Large ρ ($\rho \to \infty$)	$h(\infty) \to \infty$	$h(0) \to \lim_{\rho\to\infty} \frac{\rho^4-\rho^3+2\rho}{\rho^3+2} \approx \frac{\rho^4}{\rho^3} = \infty$	Both initial and long-term risk become very high, indicating an event occurs quickly.

The parameter ρ is a scale and severity parameter for the entire process. Increasing ρ proportionally increases both immediate and eventual risk levels. While $h'(t) > 0$ is established, studying the second derivative, $h''(t)$, is necessary to understand the rate at which the hazard function is increasing (i.e., its convexity or concavity).

The second derivative of $h'(x)$ is

$$h'(x) = \frac{\rho^6}{(\rho^3 x + \rho^3 + 2)^2},$$

$$h''(t) = \frac{-2\rho^9}{(\rho^3 x + \rho^3 + 2)^3}.$$

Corollary 3 (Analysis of curvature)**.** *Since $\rho > 0$, the numerator $-2\rho^9$ is always negative. The denominator $(\rho^3 x+\rho^3+2)^3$ is always positive for $\rho, x > 0$. Therefore, $h''(x) < 0$ for all $x > 0$. A negative second derivative means the hazard function is strictly concave. This indicates that while the risk is always increasing, the rate of increase slows down over time. The process of deterioration or aging is most rapid initially and plateaus as the function approaches its asymptote, $h(\infty) = \rho$.*

This analysis provides a complete picture of the hazard profile, revealing it is a concave, monotonically increasing function bounded between $h(0)$ and ρ.

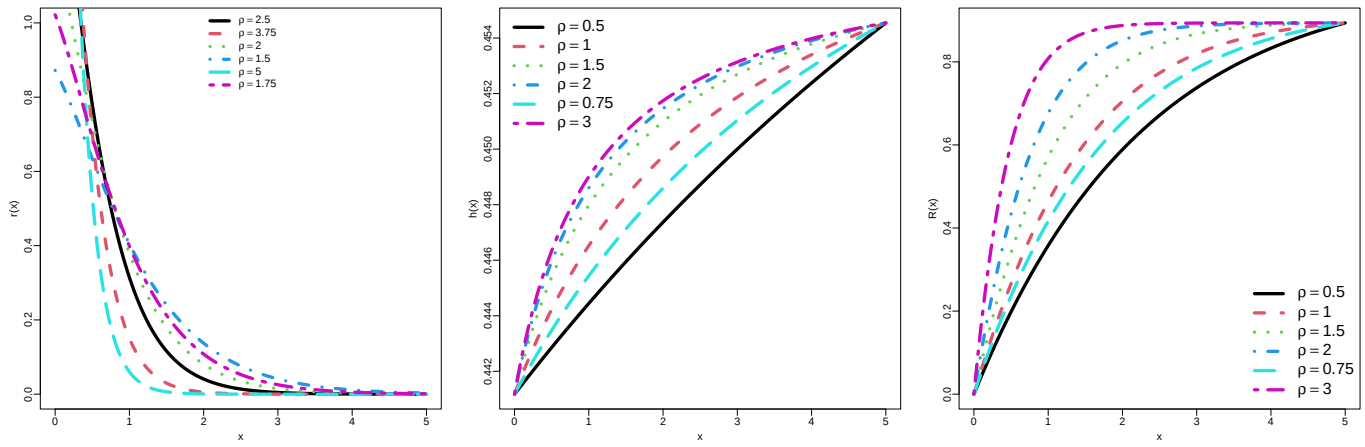

(a) **(b)** **(c)**

Figure 1. (a) PDF (b) Hazard function (c) CDF of `Obulezi`(ρ) distribution

The `Obulezi`(ρ) distribution plots, Figure 1(a), (b), and (c), demonstrate that the PDF is sharply right-skewed, peaking at $x = 0$, indicating that events are highly likely early in the process. The parameter ρ acts as a scale factor: a larger ρ causes a steeper PDF decay, signifying a smaller mean and lower variability, while a smaller ρ results in a slower decay and a larger mean. Concurrently, the Hazard Function (Figure 1(b)) exhibits an Increasing Failure Rate (IFR) as $h(x)$ rises with x, suggesting a wear-out phenomenon where risk accumulates over time. Similar to the PDF, a larger ρ consistently leads to a higher overall level

of instantaneous risk, even though the total range of hazard values remains quite narrow. The CDF plots (Figure 1(c)) confirm that ρ acts as the inverse-scale parameter for the `Obulezi` distribution. A larger ρ results in a much steeper curve, indicating that probability mass accumulates quickly, signifying a high likelihood of early events and, consequently, a smaller mean. Conversely, a smaller ρ leads to a shallower, stretched curve, suggesting a greater chance of later events and a larger mean for the distribution.

3. Statistical Properties

In this section, we study the properties of the proposed `Obulezi` distribution with the hope of demonstrating its tractability and appeal for use in modeling lifetime datasets.

3.1. Quantile function

The quantile function, $Q(u)$, is given by;

$$Q(u) = -\frac{\rho^3+2}{\rho^3} - \frac{1}{\rho}W\left[\frac{\rho^3+2}{\rho^2}(1-u)e^{-\frac{\rho^3+2}{\rho^2}}\right]; \quad u \in U(0,1), \tag{3.1}$$

where $W(\cdot)$ is the principal branch of the `Lambert W` function.

3.2. The Mode

To find the Mode of the PDF, $r(x)$, we need to find the value of $x > 0$ that maximizes $r(x)$. This is done by taking the first derivative of $\ln(r(x))$ with respect to x and setting it to zero. That is;

$$\ln r(x) = \ln\left(\frac{\rho}{\rho^3+2}\right) + \ln\left(\rho^3 x + \rho^3 - \rho^2 + 2\right) - \rho x.$$

Let $K = \frac{\rho}{\rho^3+2}$ (a positive constant) and $C = \rho^3 - \rho^2 + 2$ (a constant term). The PDF can be written as $r(x) = K(\rho^3 x + C)e^{-\rho x}$.

$$\ln r(x) = \ln K + \ln(\rho^3 x + C) - \rho x.$$

Next, find the first derivative with respect to x:

$$\frac{d}{dx}\ln r(x) = \frac{\rho^3}{\rho^3 x + C} - \rho; \quad x = \frac{2\rho^2 - \rho^3 - 2}{\rho^3}.$$

Since x must be greater than 0 ($x > 0$) for the mode to exist within the domain, we require $2\rho^2 - \rho^3 - 2 > 0$. If $2\rho^2 - \rho^3 - 2 \leq 0$, the mode occurs at the boundary $x = 0$, as $\frac{d}{dx}\ln r(x)$ will be negative for all $x > 0$.

The mode of the `Obulezi` distribution is:

$$\text{Mode} = \begin{cases} \frac{2\rho^2-\rho^3-2}{\rho^3}; & \text{if } 2\rho^2 - \rho^3 - 2 > 0 \\ 0; & \text{if } 2\rho^2 - \rho^3 - 2 \leq 0 \end{cases}.$$

3.3. Moment Generating Function

The Moment Generating Function is defined as $M_X(t) = E(e^{tX}) = \int_0^\infty e^{tx} r(x)dx$.

$$M_X(t) = \int_0^\infty e^{tx}\left(\rho^3 x + \rho^3 - \rho^2 + 2\right)\frac{\rho e^{-\rho x}}{\rho^3+2}dx = \frac{\rho}{\rho^3+2}\int_0^\infty \left[(\rho^3 - \rho^2 + 2)e^{(t-\rho)x} + \rho^3 x e^{(t-\rho)x}\right]dx.$$

We use the standard integral results: 1. $\int_0^\infty e^{-ax}dx = \frac{1}{a}$ for $a > 0$. 2. $\int_0^\infty xe^{-ax}dx = \frac{1}{a^2}$ for $a > 0$.

The integrals converge only if $t - \rho < 0$, or $t < \rho$. Let $a = \rho - t$.

$$M_X(t) = \frac{\rho}{\rho^3 + 2} \frac{(\rho^3 - \rho^2 + 2)(\rho - t) + \rho^3}{(\rho - t)^2}.$$

3.4. Complete Moment

The k-th complete moment is $\mu'_k = E(X^k) = \int_0^\infty x^k r(x)dx$.

$$\mu'_k = \frac{\rho}{\rho^3 + 2} \int_0^\infty x^k \left[(\rho^3 - \rho^2 + 2)e^{-\rho x} + \rho^3 x e^{-\rho x}\right] dx = \frac{\rho}{\rho^3 + 2} \left[(\rho^3 - \rho^2 + 2) \int_0^\infty x^k e^{-\rho x}dx + \rho^3 \int_0^\infty x^{k+1} e^{-\rho x}dx\right]$$

Using the Gamma function integral $\int_0^\infty x^n e^{-ax}dx = \frac{\Gamma(n+1)}{a^{n+1}}$, we set $a = \rho$.

$$\mu'_k = \frac{\rho}{\rho^3 + 2} \left[(\rho^3 - \rho^2 + 2)\frac{\Gamma(k+1)}{\rho^{k+1}} + \rho^3 \frac{\Gamma(k+2)}{\rho^{k+2}}\right].$$

Since $\Gamma(k + 2) = (k + 1)\Gamma(k + 1)$,

$$\mu'_k = \frac{\Gamma(k+1)}{\rho^k(\rho^3 + 2)} \left[\rho^3 - \rho^2 + k + 3\right].$$

The mean (first moment, $k = 1$) is $\mu = \mu'_1$:

$$\mu = \frac{\Gamma(2)}{\rho^1(\rho^3 + 2)} \left[\rho^3 - \rho^2 + 1 + 3\right] = \frac{1}{\rho(\rho^3 + 2)} \left[\rho^3 - \rho^2 + 4\right].$$

Table 2. Comparative Summary of Some One-Parameter Distributions

Distribution	$f(x, \rho)$	$E(X)$	$h(x)$
`Obulezi`	$\left(\rho^3 x + \rho^3 - \rho^2 + 2\right) \frac{\rho e^{-\rho x}}{\rho^3+2}$	$\frac{\rho^3+\rho^2+2}{\rho(\rho^3+2)}$	Decreasing or Unimodal
Lindley	$\frac{\rho^2}{\rho+1}(1 + x)e^{-\rho x}$	$\frac{\rho+2}{\rho(\rho+1)}$	Increasing or Bathtub
Shanker	$\frac{\rho^2}{\rho^2+1}(\rho + x)e^{-\rho x}$	$\frac{\rho+2}{\rho(\rho^2+1)}$	Increasing
xgamma	$\frac{\rho^2}{\rho+1}\left(1 + \frac{\rho}{2}x^2\right)e^{-\rho x}$	$\frac{\rho+3}{\rho(\rho+1)}$	Decreasing or Unimodal
Updated Lindley	$\frac{\rho}{2(\rho^3+2)}(4 + \rho^5 x^2)e^{-\rho x}$	$\frac{4+12\rho^3}{\rho(\rho^3+2)}$	Decreasing or Bathtub/Unimodal
Chris-Jerry	$\frac{\rho^2}{\rho+2}(1 + \rho x^2)e^{-\rho x}$	$\frac{\rho+6}{\rho(\rho+2)}$	Unimodal (Inverted Bathtub)
Fav-Jerry	$\frac{\rho}{\rho^2+2}(2 + \rho^3 x)e^{-\rho x}$	$\frac{2(\rho^2+1)}{\rho(\rho^2+2)}$	Decreasing or Unimodal
Pranav	$\frac{\rho}{\rho^4+6}\left(\rho^4 + \frac{\rho^5 x^3}{6}\right)e^{-\rho x}$	$\frac{\rho^4+24}{\rho(\rho^4+6)}$	Bathtub or Unimodal
Rani	$\frac{\rho}{\rho^4+24}\left(\rho^4 + \frac{\rho^5 x^4}{24}\right)e^{-\rho x}$	$\frac{\rho^4+120}{\rho(\rho^4+24)}$	Bathtub or Unimodal
Doje	$\frac{\rho}{\rho^6+720}\left(\rho^6 + \frac{\rho^7 x^6}{720}\right)e^{-\rho x}$	$\frac{\rho^6+5040}{\rho(\rho^6+720)}$	Bathtub or Unimodal

Table 2 contains a comparison of some one-parameter distribution.

3.5. Incomplete Moment

The k-th incomplete moment is $I_k(t) = E(X^k|X < t) = \int_0^t x^k r(x)dx$.

$$I_k(t) = \frac{\rho}{\rho^3+2}\int_0^t x^k\left[(\rho^3-\rho^2+2)e^{-\rho x}+\rho^3 x e^{-\rho x}\right]dx = \frac{\rho}{\rho^3+2}\left[(\rho^3-\rho^2+2)\int_0^t x^k e^{-\rho x}dx+\rho^3\int_0^t x^{k+1}e^{-\rho x}dx\right]$$

Using the lower incomplete Gamma function $\gamma(n,z) = \int_0^z t^{n-1}e^{-t}dt$, we have $\int_0^t x^n e^{-\rho x}dx = \frac{\gamma(n+1,\rho t)}{\rho^{n+1}}$.

$$I_k(t) = \frac{1}{\rho^k(\rho^3+2)}\left[(\rho^3-\rho^2+2)\gamma(k+1,\rho t)+\rho^2\gamma(k+2,\rho t)\right].$$

3.6. Mean Residual Life Function

The Mean Residual Life function is $MRL(x) = E(X-x|X>x) = \frac{1}{S(x)}\int_x^\infty S(t)dt$.

$$\int_x^\infty S(t)dt = \int_x^\infty\left(1+\frac{\rho^3 t}{\rho^3+2}\right)e^{-\rho t}dt = \int_x^\infty e^{-\rho t}dt+\frac{\rho^3}{\rho^3+2}\int_x^\infty te^{-\rho t}dt$$

Using the standard integral results $\int_x^\infty e^{-at}dt = \frac{e^{-ax}}{a}$ and $\int_x^\infty te^{-at}dt = \frac{e^{-ax}(ax+1)}{a^2}$:

$$\int_x^\infty S(t)dt = \frac{e^{-\rho x}}{\rho}+\frac{\rho^3}{\rho^3+2}\frac{e^{-\rho x}(\rho x+1)}{\rho^2} = e^{-\rho x}\left[\frac{1}{\rho}+\frac{\rho}{\rho^3+2}(\rho x+1)\right]$$

$$MRL(x) = \frac{1}{S(x)}\int_x^\infty S(t)dt = \frac{e^{-\rho x}\left[\frac{1}{\rho}+\frac{\rho}{\rho^3+2}(\rho x+1)\right]}{\left(1+\frac{\rho^3 x}{\rho^3+2}\right)e^{-\rho x}} = \frac{\frac{1}{\rho}+\frac{\rho(\rho x+1)}{\rho^3+2}}{\frac{\rho^3 x+\rho^3+2}{\rho^3+2}}$$

$$MRL(x) = \frac{\frac{\rho^3+2+\rho^2(\rho x+1)}{\rho(\rho^3+2)}}{\frac{\rho^3 x+\rho^3+2}{\rho^3+2}} = \frac{\rho^3+2+\rho^3 x+\rho^2}{\rho(\rho^3+2)}\cdot\frac{\rho^3+2}{\rho^3 x+\rho^3+2} = \frac{\rho^3 x+\rho^3+\rho^2+2}{\rho(\rho^3 x+\rho^3+2)}.$$

3.7. Order statistics

Let $X_1, X_2, \ldots, X_n$ be a random sample from the Obulezi distribution, and $X_{(1)} < X_{(2)} < \ldots < X_{(n)}$ be the corresponding order statistics.

The PDF of the j-th order statistic $X_{(j)}$ is:

$$r_j(x) = \frac{n!}{(j-1)!(n-j)!}[R(x)]^{j-1}[S(x)]^{n-j}r(x).$$

Substituting the functions:

$$r_j(x) = \frac{n!}{(j-1)!(n-j)!}\left[1-\left(1+\frac{\rho^3 x}{\rho^3+2}\right)e^{-\rho x}\right]^{j-1}\left[\left(1+\frac{\rho^3 x}{\rho^3+2}\right)e^{-\rho x}\right]^{n-j}\left[\left(\rho^3 x+\rho^3-\rho^2+2\right)\frac{\rho e^{-\rho x}}{\rho^3+2}\right].$$

3.8. Stochastic Ordering

A random variable X is said to be smaller than a random variable Y in the stochastic order (denoted $X \leq_{st} Y$) if $S_X(x) \leq S_Y(x)$ for all x. Since the Obulezi distribution has a single parameter ρ, we compare X_{ρ_1} and X_{ρ_2}.

Let $S_\rho(x) = \left(1 + \frac{\rho^3 x}{\rho^3+2}\right) e^{-\rho x}$. We examine $\frac{\partial S_\rho(x)}{\partial \rho}$.

$$\frac{\partial S_\rho(x)}{\partial \rho} = \frac{\partial}{\partial \rho}\left[e^{-\rho x}\left(1 + \frac{\rho^3 x}{\rho^3+2}\right)\right]$$

Using the product rule, $u'v + uv'$:

$$= (-xe^{-\rho x})\left(1 + \frac{\rho^3 x}{\rho^3+2}\right) + e^{-\rho x}\frac{\partial}{\partial \rho}\left(1 + \frac{\rho^3 x}{\rho^3+2}\right)$$

The derivative term is:

$$\frac{\partial}{\partial \rho}\left(\frac{\rho^3 x}{\rho^3+2}\right) = x \cdot \frac{3\rho^2(\rho^3+2) - \rho^3(3\rho^2)}{(\rho^3+2)^2} = x\frac{3\rho^5 + 6\rho^2 - 3\rho^5}{(\rho^3+2)^2} = \frac{6\rho^2 x}{(\rho^3+2)^2}$$

Substituting back:

$$\frac{\partial S_\rho(x)}{\partial \rho} = -xe^{-\rho x}\left(\frac{\rho^3 x + \rho^3 + 2}{\rho^3+2}\right) + e^{-\rho x}\frac{6\rho^2 x}{(\rho^3+2)^2}$$

$$= \frac{xe^{-\rho x}}{(\rho^3+2)^2}\left[-(\rho^3+2)(\rho^3 x + \rho^3 + 2) + 6\rho^2\right]$$

Since $\rho, x > 0$, $\frac{xe^{-\rho x}}{(\rho^3+2)^2} > 0$. The sign is determined by the bracketed term:

$$T = -(\rho^3+2)(\rho^3 x + \rho^3 + 2) + 6\rho^2$$

For small x, $T \approx -(\rho^3+2)(\rho^3+2) + 6\rho^2 = -(\rho^6 + 4\rho^3 + 4) + 6\rho^2$. The sign of T is generally negative for typical ρ values. For example, if $\rho = 1$, $T = -3(3+x) + 6 = -3x - 3$, which is negative. If $T \leq 0$ for all x, then $\frac{\partial S_\rho(x)}{\partial \rho} \leq 0$.

If $\rho_1 > \rho_2$, then $S_{\rho_1}(x) \leq S_{\rho_2}(x)$, which implies $X_{\rho_1} \leq_{st} X_{\rho_2}$. The Obulezi distribution is stochastically ordered with respect to its parameter ρ.

3.9. Rényi Entropy

The Rényi entropy is defined as $H_\delta = \frac{1}{1-\delta}\log\left(\int_0^\infty [r(x)]^\delta dx\right)$ for $\delta \neq 1$.

$$[r(x)]^\delta = \left(\left(\rho^3 x + \rho^3 - \rho^2 + 2\right)\frac{\rho e^{-\rho x}}{\rho^3+2}\right)^\delta = \left(\frac{\rho}{\rho^3+2}\right)^\delta e^{-\delta\rho x}\left(\rho^3 x + \rho^3 - \rho^2 + 2\right)^\delta.$$

The integral $\int_0^\infty [r(x)]^\delta dx$ does not simplify to a closed-form expression.

Therefore, the Rényi entropy is not in a closed form and requires numerical integration.

3.10. Extropy

The Extropy is defined as $J = -\frac{1}{2}\int_0^\infty [r(x)]^2 dx$.

$$J = -\frac{1}{2}\int_0^\infty \left(\frac{\rho}{\rho^3+2}\right)^2 e^{-2\rho x}\left(\rho^3 x + \rho^3 - \rho^2 + 2\right)^2 dx$$

$$J = -\frac{1}{2}\left(\frac{\rho}{\rho^3+2}\right)^2 \int_0^\infty e^{-2\rho x}\left[(\rho^3 x)^2 + 2(\rho^3 x)(\rho^3 - \rho^2 + 2) + (\rho^3 - \rho^2 + 2)^2\right] dx$$

$$J = -\frac{\rho^2}{2(\rho^3+2)^2}\left[\rho^6 \int_0^\infty x^2 e^{-2\rho x} dx + 2\rho^3(\rho^3 - \rho^2 + 2)\int_0^\infty x e^{-2\rho x} dx + (\rho^3 - \rho^2 + 2)^2 \int_0^\infty e^{-2\rho x} dx\right]$$

Using $\int_0^\infty x^n e^{-ax} dx = \frac{n!}{a^{n+1}}$ with $a = 2\rho$:

$$\int_0^\infty x^2 e^{-2\rho x} dx = \frac{2!}{(2\rho)^3} = \frac{2}{8\rho^3} = \frac{1}{4\rho^3}$$

$$\int_0^\infty x e^{-2\rho x} dx = \frac{1!}{(2\rho)^2} = \frac{1}{4\rho^2}$$

$$\int_0^\infty e^{-2\rho x} dx = \frac{0!}{(2\rho)^1} = \frac{1}{2\rho}$$

$$J = -\frac{\rho^2}{2(\rho^3+2)^2}\left[\rho^6\left(\frac{1}{4\rho^3}\right) + 2\rho^3(\rho^3 - \rho^2 + 2)\left(\frac{1}{4\rho^2}\right) + (\rho^3 - \rho^2 + 2)^2\left(\frac{1}{2\rho}\right)\right]$$

$$J = -\frac{\rho^2}{2(\rho^3+2)^2}\left[\frac{\rho^3}{4} + \frac{\rho}{2}(\rho^3 - \rho^2 + 2) + \frac{(\rho^3 - \rho^2 + 2)^2}{2\rho}\right].$$

3.11. Stress-Strength Reliability

The stress-strength reliability is $R_{S,T} = P(S < T) = \int_0^\infty r_S(x) R_T(x) dx$, where S and T are independent random variables from the Obulezi distribution with parameters ρ_1 and ρ_2, respectively.

$$R_{S,T} = \int_0^\infty r_{\rho_1}(x) S_{\rho_2}(x) dx$$

$$R_{S,T} = \int_0^\infty \left[\left(\rho_1^3 x + \rho_1^3 - \rho_1^2 + 2\right)\frac{\rho_1 e^{-\rho_1 x}}{\rho_1^3 + 2}\right]\left[\left(1 + \frac{\rho_2^3 x}{\rho_2^3 + 2}\right)e^{-\rho_2 x}\right] dx$$

$$R_{S,T} = \frac{\rho_1}{\rho_1^3 + 2}\frac{1}{\rho_2^3 + 2}\int_0^\infty e^{-(\rho_1+\rho_2)x}\left(\rho_1^3 x + \rho_1^3 - \rho_1^2 + 2\right)\left(\rho_2^3 x + \rho_2^3 + 2\right) dx$$

Let $\lambda = \rho_1 + \rho_2$. The integral is of the form $\int_0^\infty e^{-\lambda x}(Ax + B)(Cx + D) dx$, where $A = \rho_1^3$, $B = \rho_1^3 - \rho_1^2 + 2$, $C = \rho_2^3$, and $D = \rho_2^3 + 2$.

$$\int_0^\infty e^{-\lambda x}(ACx^2 + (AD + BC)x + BD) dx$$

$$= AC\frac{\Gamma(3)}{\lambda^3} + (AD + BC)\frac{\Gamma(2)}{\lambda^2} + BD\frac{\Gamma(1)}{\lambda^1}$$

$$= \frac{2AC}{\lambda^3} + \frac{AD + BC}{\lambda^2} + \frac{BD}{\lambda}$$

Substituting A, B, C, D, λ back will yield the closed-form expression for $R_{S,T}$.

4. Estimation and Computational Details

This section explores fifteen distinct non-Bayesian estimation methods for determining the unknown parameter ρ of the `Obulezi` distribution. These methods are broadly classified into likelihood-based, distance-based, and spacing-based approaches. They include the Maximum Likelihood (MLE), Anderson-Darling (ADE), Cramér-von Mises (CVME), Maximum Product of Spacings (MPSE), Ordinary Least Squares (OLSE), Right-Tail Anderson-Darling (RTADE), Weighted Least Squares (WLSE), Left-Tail Anderson-Darling (LTADE), Minimum Spacing Absolute Distance (MSADE), Minimum Spacing Absolute-Log Distance (MSALDE), Anderson-Darling Second-Order Left-Tail (ADSOE), Kolmogorov (KE), Minimum Spacing Square Distance (MSSDE), Minimum Spacing Squared-Log Distance (MSSLDE), and Minimum Spacing Linex Distance (MSLNDE) estimators. The objective functions for each approach are detailed below.

4.1. Maximum Likelihood Estimation (MLE)

The Maximum Likelihood method, whose foundations were established by [6] and [7], is widely used due to its favorable asymptotic properties, such as consistency and asymptotic normality. The estimator $\hat{\rho}$ is the value that maximizes the log-likelihood function $\ell(\rho|\mathbf{x})$. Given a random sample $x_1, \ldots, x_n$ of size n from the `Obulezi` distribution with PDF $r(x;\rho)$, the likelihood function $\mathcal{L}(\rho)$ is:

$$\mathcal{L}(\rho|\mathbf{x}) = \prod_{i=1}^{n} r(x_i;\rho) = \prod_{i=1}^{n} \left[\left(\rho^3 x_i + \rho^3 - \rho^2 + 2\right) \frac{\rho e^{-\rho x_i}}{\rho^3 + 2} \right].$$

The log-likelihood function, $\ell(\rho|\mathbf{x}) = \ln(\mathcal{L}(\rho|\mathbf{x}))$, is:

$$\ell(\rho|\mathbf{x}) = n\ln(\rho) - n\ln(\rho^3 + 2) + \sum_{i=1}^{n} \ln\left(\rho^3 x_i + \rho^3 - \rho^2 + 2\right) - \rho \sum_{i=1}^{n} x_i.$$

The Maximum Likelihood Estimator ($\hat{\rho}$) is the value that maximizes $\ell(\rho|\mathbf{x})$, which is achieved by numerically minimizing the negative log-likelihood function, $-\ell(\rho|\mathbf{x})$. The estimation equation, found by setting the partial derivative with respect to ρ to zero, is:

$$\frac{\partial \ell}{\partial \rho} = \frac{\partial}{\partial \rho} \left[n\ln(\rho) - n\ln(\rho^3 + 2) + \sum_{i=1}^{n} \ln\left(\rho^3 x_i + \rho^3 - \rho^2 + 2\right) - \rho \sum_{i=1}^{n} x_i \right] = 0.$$

$$\frac{\partial \ell}{\partial \rho} = \frac{n}{\rho} - \frac{3n\rho^2}{\rho^3 + 2} + \sum_{i=1}^{n} \frac{3\rho^2 x_i + 3\rho^2 - 2\rho}{\rho^3 x_i + \rho^3 - \rho^2 + 2} - \sum_{i=1}^{n} x_i = 0.$$

4.2. Anderson-Darling Estimation (ADE)

The ADE approach minimizes a weighted statistic, $A(\rho)$, which measures the discrepancy between the theoretical CDF $R(x)$ and the empirical CDF, placing greater weight on the tails. The estimate $\hat{\rho}$ is derived by numerically minimizing the Anderson-Darling statistic, $A(\rho)$:

$$A(\rho) = -n - \frac{1}{n} \sum_{i=1}^{n} (2i-1) \left[\log R(x_{i:n}) + \log S\left(x_{n-i+1:n}\right) \right],$$

where $x_{i:n}$ are the order statistics, $R(x)$ is the `Obulezi` CDF, and $S(x) = 1 - R(x)$ is the `Obulezi` survival function.

4.3. Cramér-von Mises Estimation (CVME)

The CVME approach minimizes a criterion sensitive to discrepancies across the entire distribution range. The parameter $\hat{\rho}$ is obtained by numerically minimizing the Cramér-von Mises statistic, $C(\rho)$:

$$C(\rho) = \frac{1}{12n} + \sum_{i=1}^{n} \left[R(x_{i:n}) - \frac{2i-1}{2n} \right]^2.$$

4.4. Ordinary Least Squares Estimation (OLSE)

The OLSE technique minimizes the sum of squared differences between the theoretical CDF $R(x_{i:n})$ and the plotting position $\frac{i}{n+1}$. The parameter $\hat{\rho}$ is estimated by numerically minimizing the Ordinary Least Squares statistic, $V(\rho)$:

$$V(\rho) = \sum_{i=1}^{n} \left[R(x_{i:n}) - \frac{i}{n+1} \right]^2.$$

4.5. Right-Tail Anderson-Darling Estimation (RTADE)

The RTADE method prioritizes goodness-of-fit in the upper (right) tail. The parameter $\hat{\rho}$ is found by numerically minimizing the RTADE statistic, $R(\rho)$:

$$R(\rho) = \frac{n}{2} - 2\sum_{i=1}^{n} R(x_{i:n}) - \frac{1}{n}\sum_{i=1}^{n} (2i-1) \log S(x_{i:n}).$$

4.6. Weighted Least Squares Estimation (WLSE)

The WLSE method uses weights to reduce the influence of extreme observations. The parameter estimate $\hat{\rho}$ is derived by numerically minimizing the Weighted Least Squares statistic, $W(\rho)$:

$$W(\rho) = \sum_{i=1}^{n} \frac{(n+1)^2(n+2)}{i(n-i+1)} \left[R(x_{i:n}) - \frac{i}{n+1} \right]^2.$$

4.7. Left-Tail Anderson-Darling Estimation (LTADE)

The LTADE method focuses on optimizing the fit in the lower (left) tail. The parameter $\hat{\rho}$ is estimated by numerically minimizing the LTADE statistic, $L(\rho)$:

$$L(\rho) = -\frac{3}{2}n + 2\sum_{i=1}^{n} R(x_{i:n}) - \frac{1}{n}\sum_{i=1}^{n} (2i-1) \log R(x_{i:n}).$$

4.8. Anderson-Darling Second-Order Left-Tail (ADSOE)

This method penalizes a poor fit near the origin. The parameter $\hat{\rho}$ is estimated by numerically minimizing the ADSOE statistic, $LTS(\rho)$:

$$LTS(\rho) = 2\sum_{i=1}^{n} \log R(x_{i:n}) + \frac{1}{n}\sum_{i=1}^{n} \frac{(2i-1)}{R(x_i)}.$$

4.9. Kolmogorov Estimation (KE)

The Kolmogorov method minimizes the maximum absolute distance (supremum norm). The parameter $\hat{\rho}$ is estimated by numerically minimizing the Kolmogorov statistic, $KM(\rho)$:

$$KM(\rho) = \underset{1\le i\le n}{\mathrm{MAX}}\left[\frac{i}{n} - R(x_{i:n}), R(x_{i:n}) - \frac{i-1}{n}\right].$$

4.10. Maximum Product of Spacings Estimation (MPSE)

The MPSE method minimizes the negative log-product of spacings. The parameter $\hat{\rho}$ is found by numerically minimizing the negative log-product of spacings, $\delta(\rho)$:

$$\delta(\rho) = -\frac{1}{n+1}\sum_{i=1}^{n+1} \log I_i(\rho),$$

where $I_i = R(x_{i:n}) - R(x_{i-1:n})$, with $R(x_{0:n}) = 0$ and $R(x_{n+1:n}) = 1$.

4.11. Minimum Spacing Absolute Distance (MSADE)

The MSADE approach minimizes the L_1-norm between observed spacings and their expected value. The MSADE statistic, ζ, is numerically minimized to find $\hat{\rho}$:

$$\zeta(\rho) = \sum_{i=1}^{n+1}\left|I_i - \frac{1}{n+1}\right|.$$

4.12. Minimum Spacing Absolute-Log Distance (MSALDE)

The MSALDE method minimizes the absolute difference of the log-spacings from the log-expected spacing. The parameter $\hat{\rho}$ is estimated by numerically minimizing the MSALDE statistic, Υ:

$$\Upsilon(\rho) = \sum_{i=1}^{n+1}\left|\log I_i - \log\frac{1}{n+1}\right|.$$

4.13. Minimum Spacing Square Distance (MSSDE)

The MSSDE method minimizes the L_2-norm (sum of squared differences) between the observed spacings and their expected value. The parameter $\hat{\rho}$ is estimated by numerically minimizing the MSSDE statistic, ϕ:

$$\phi(\rho) = \sum_{i=1}^{n+1}\left(I_i - \frac{1}{n+1}\right)^2.$$

4.14. Minimum Spacing Squared-Log Distance (MSSLDE)

The MSSLDE approach minimizes the squared differences of the log-transformed spacings. The parameter $\hat{\rho}$ is derived by numerically minimizing the MSSLDE statistic, Ψ:

$$\Psi(\rho) = \sum_{i=1}^{n+1} \left(\log I_i - \log \frac{1}{n+1} \right)^2.$$

4.15. Minimum Spacing Linex Distance (MSLNDE)

The MSLNDE technique employs an asymmetric Linex-type loss function. The parameter $\hat{\rho}$ is estimated by numerically minimizing the MSLNDE statistic, Δ:

$$\Delta(\rho) = \sum_{i=1}^{n+1} \left[e^{I_i - \frac{1}{n+1}} - \left(I_i - \frac{1}{n+1} \right) - 1 \right].$$

4.16. Computational and Convergence Diagnostics Algorithm

Since the estimating equations for all methods lack closed-form solutions, the parameter estimate $\hat{\rho}$ must be obtained via numerical optimization subject to the constraint $\rho > 0$. For smooth and differentiable objective functions (MLE, ADE, CVME, OLSE, MPSE, etc.), the Broyden-Fletcher-Goldfarb-Shanno (BFGS) quasi-Newton method or its bounded version (L-BFGS-B) is utilized to find the minimum (or maximum, in the case of log-likelihood). For non-differentiable objectives, specifically the Kolmogorov (KE), MSADE, and MSALDE estimators, the robust Nelder-Mead simplex algorithm is preferred. To ensure global convergence and stability, a grid search over a feasible range of ρ is used to determine a robust starting value (ρ_0). Convergence is declared successful when the relative change in the objective function value between successive iterations is less than a prescribed tolerance, typically 10^{-6}, and the optimization routine returns a status code indicating a successful search.

5. Simulation

This section evaluates the efficacy of several estimation techniques for the single parameter, ρ, of the `Obulezi` distribution using simulated data. We generated random datasets for various sample sizes (n = 15, 50, 120, 180, 250, and 350) using the model's quantile function in Equation (3.1). The primary objective is to assess the accuracy, precision, and computing efficiency of each estimation method. By conducting a comprehensive examination across diverse sample sizes, we aim to identify the most reliable and suitable estimation approach for the `Obulezi` distribution in various real-world contexts. The effectiveness of each methodology is evaluated using criteria such as:

$$\begin{cases} \text{Bias :} & |\text{Bias}(\widehat{\rho})| &= \frac{1}{D}\sum_{i=1}^{D} |\widehat{\rho} - \rho|, \\ \text{Mean Squared Errors :} & \text{MSE} &= \frac{1}{D}\sum_{i=1}^{D} (\widehat{\rho} - \rho)^2, \\ \text{Mean Relative Errors :} & \text{MRE} &= \frac{1}{D}\sum_{i=1}^{D} |\widehat{\rho} - \rho|/\rho, \\ \text{Average Absolute Difference :} & D_{\text{abs}} &= \frac{1}{n\,D}\sum_{i=1}^{D}\sum_{j=1}^{n} |R(x_{ij}|\rho) - R(x_{ij}|\widehat{\rho})|, \\ \text{Maximum Absolute Difference :} & D_{\text{max}} &= \frac{1}{D}\sum_{i=1}^{D} \max_{j} |R(x_{ij}|\rho) - R(x_{ij}|\widehat{\rho})|, \end{cases}$$

Algorithm 1 Numerical Estimation Algorithm for $\hat{\rho}$ of the `Obulezi` Distribution

Require: Random sample $\mathbf{x} = \{x_1, \ldots, x_n\}$; Objective function $Q(\rho)$; Tolerance $\tau = 10^{-6}$; Constraint $\rho > 0$.
Ensure: Parameter estimate $\hat{\rho}$; Success flag.

Grid Search for Initial Value (ρ_0):
Define a grid of initial candidates $\rho_{\text{grid}} \subset (\rho_{\min}, \rho_{\max})$.
Calculate $Q(\rho^{(j)})$ for all $\rho^{(j)} \in \rho_{\text{grid}}$.
$\rho_0 \leftarrow \arg\min_{\rho^{(j)} \in \rho_{\text{grid}}} Q(\rho^{(j)})$.
$\hat{\rho}^{(0)} \leftarrow \rho_0$.
Select Optimization Method:
if $Q(\rho)$ is differentiable (e.g., MLE, ADE, CVME, MPSE) **then**
    Method $\leftarrow$ BFGS or L-BFGS-B (Bounded Quasi-Newton)
else {For non-differentiable $Q(\rho)$ (e.g., KE, MSADE, MSALDE)}
    Method $\leftarrow$ Nelder-Mead (Simplex Method)
end if
Execute Numerical Optimization:
$k \leftarrow 0$
repeat
    Compute next estimate $\hat{\rho}^{(k+1)}$ using Method on $Q(\rho)$.
    Enforce Constraint: If $\hat{\rho}^{(k+1)} \leq 0$, adjust to a small positive value ϵ.
    Check Convergence: ConvCheck $\leftarrow \left| \frac{Q(\hat{\rho}^{(k+1)}) - Q(\hat{\rho}^{(k)})}{Q(\hat{\rho}^{(k)})} \right|$
    $k \leftarrow k + 1$
until ConvCheck $< \tau$ OR Max Iterations Reached
Final Diagnostics:
if ConvCheck $< \tau$ **AND** Optimizer Status = Success **then**
    $\hat{\rho} \leftarrow \hat{\rho}^{(k)}$
    Flag $\leftarrow$ Successful Convergence
else
    $\hat{\rho} \leftarrow$ NULL
    Flag $\leftarrow$ Failure
end if

The plot, Figure 6, is a partial rank heatmap showing the performance of fifteen estimation methods across five metrics for the `Obulezi` distribution, repeated over six different sample sizes (n) for simulation case 3. The color intensity indicates rank, where lighter colors (yellow/peach) represent better performance (Rank 1) and darker colors (purple/black) represent worse performance (highest rank). The heatmap demonstrates that, generally, the estimation methods' performance tends to improve (lighter ranks) as the sample size (n) increases, particularly for the parameter-dependent metrics, while some GoF methods (like D_{abs} and D_{max}) show less consistent ranking improvement.

The core finding from both the detailed simulation measures (Table 3) and the calculated partial and overall ranks (Table 4) is the superior performance of the MLE and the MPSE. Across all sample sizes ($n = 15$ to $n = 350$), the MLE method consistently achieves the lowest sum of ranks, securing the first rank ({1}) for the vast majority of individual metrics (Bias, MSE, MRE, D_{abs}, and D_{max}) and across the board in the final overall $\sum$ Ranks. The only consistent exception is at $n = 120$ where the MPSE slightly outperforms the MLE and takes the overall first rank. The second-best overall performance alternates primarily between MPSE and the ADE, with MPSE generally placing second or third in the aggregate ranking. The WLSE also shows competitive results, often placing in the top five. As the sample size (n) increases, the performance of the estimators improves across all metrics, with values for Bias and MSE decreasing substantially, which is expected. However, the relative ranking of the methods remains largely stable, affirming the robustness of the MLE and MPSE methods for estimating the parameter ρ.

Conversely, methods such as the RTADE, the KE, and the ADSOE consistently show the poorest performance, occupying the highest rank sums (ranks {13}, {14}, and {15}) across all sample sizes and metrics. The plots in Figures 2, 3, 4 and 5 align perfectly with the above discussion.

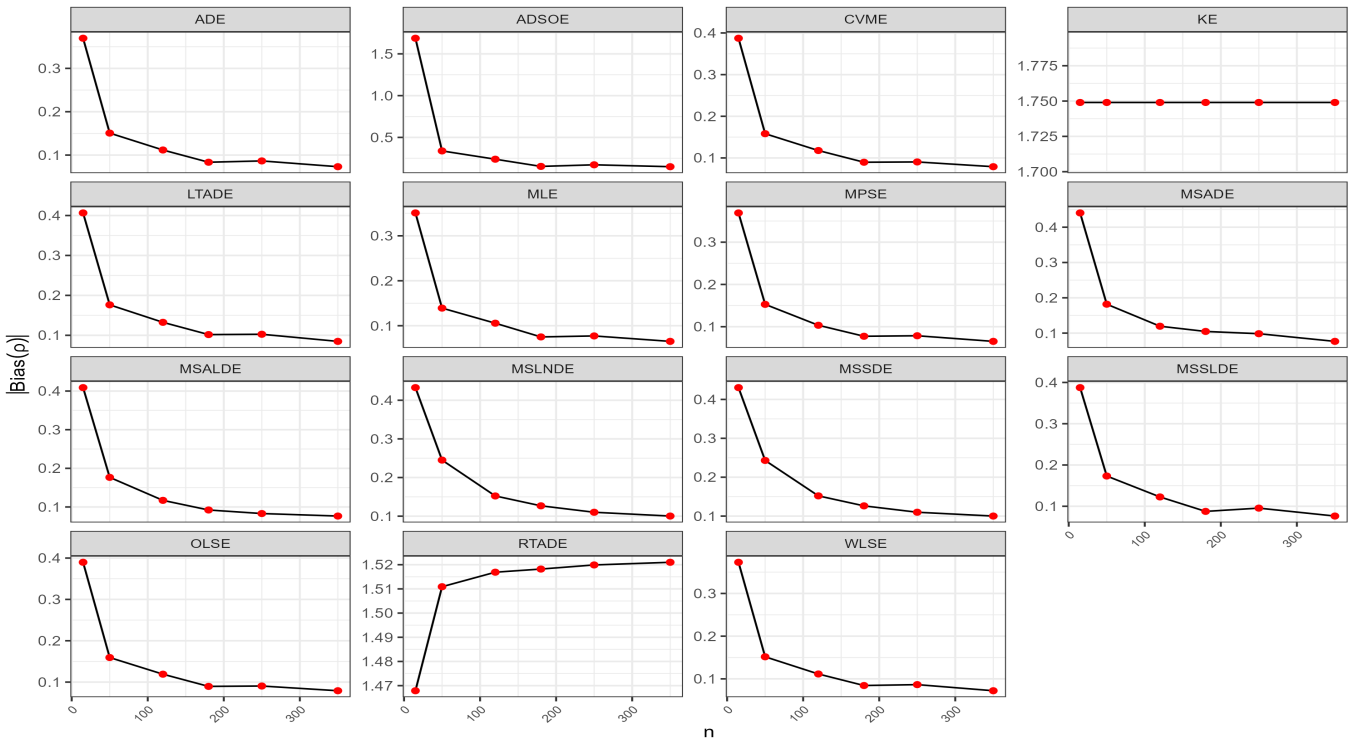

Figure 2. Graphical representations for the Bias values presented in Table 3.

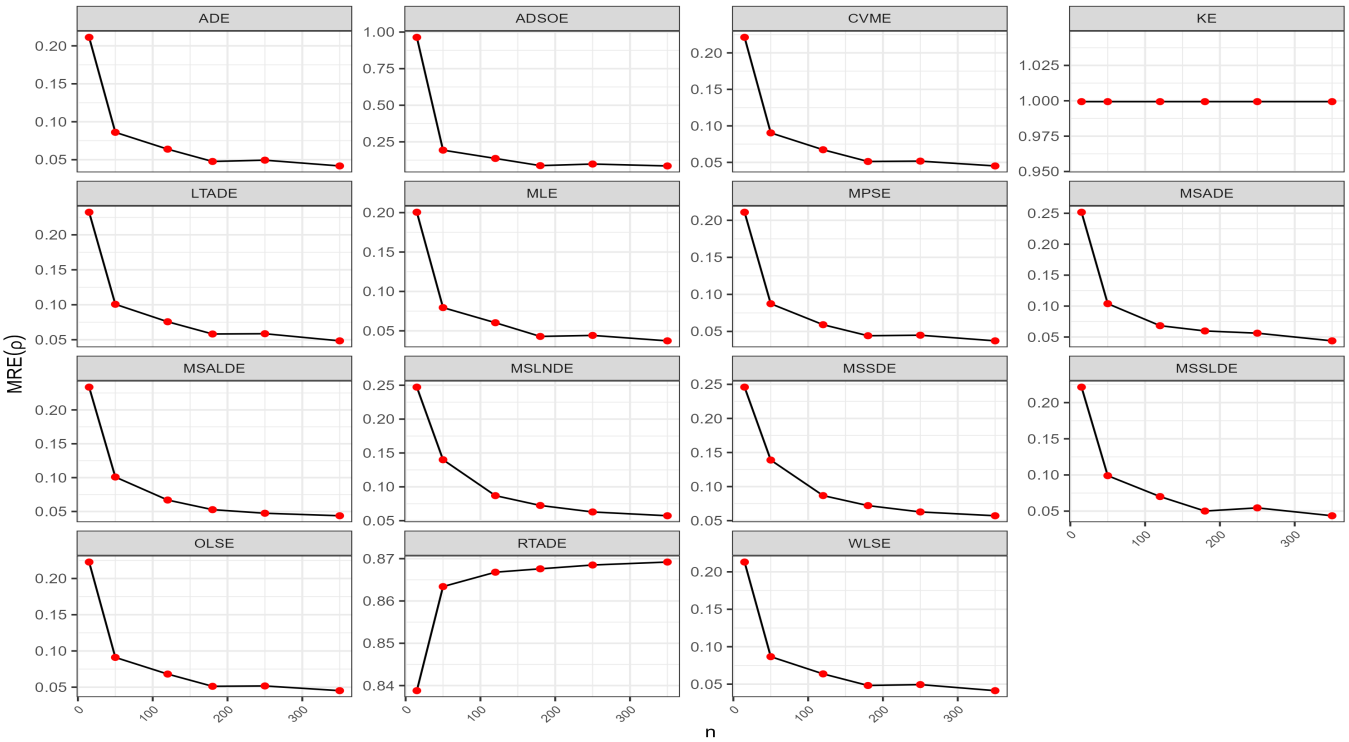

Figure 3. Graphical representations for the MRE values presented in Table 3.

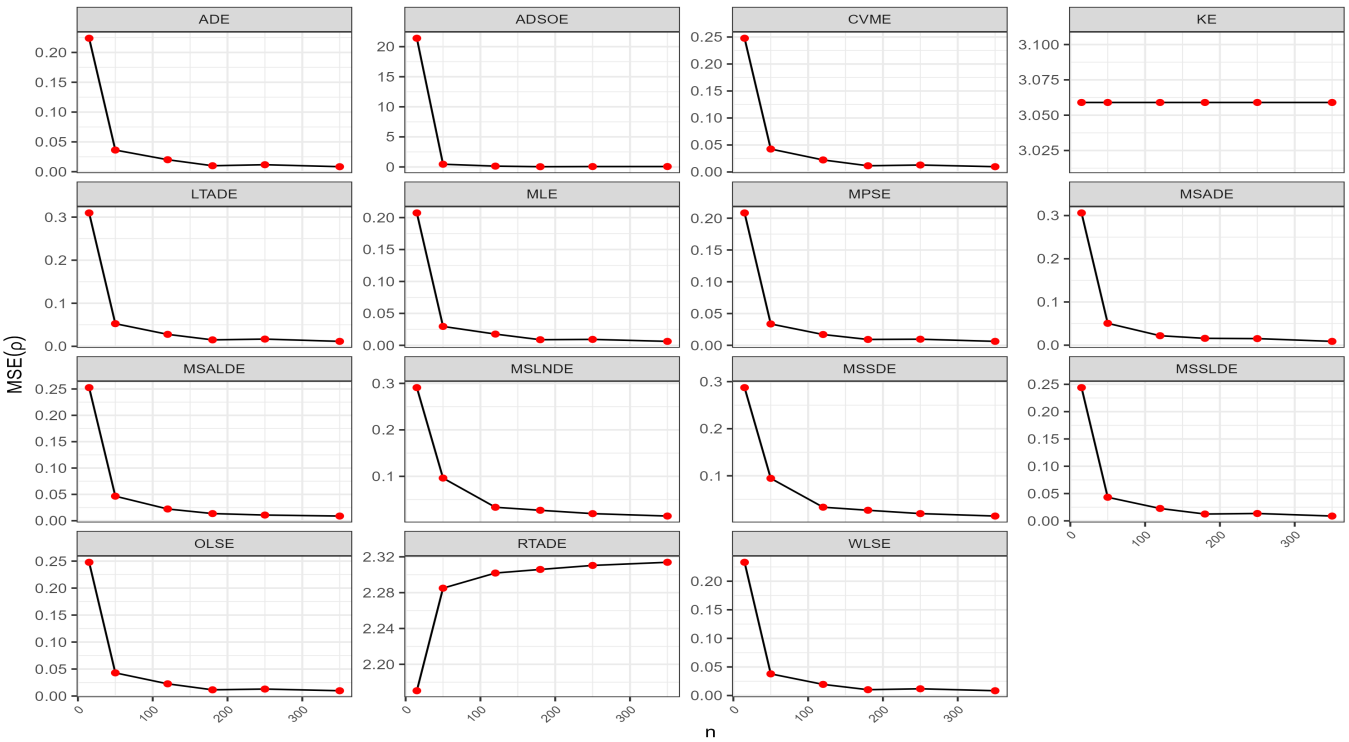

Figure 4. Graphical representations for the MSE values presented in Table 3.

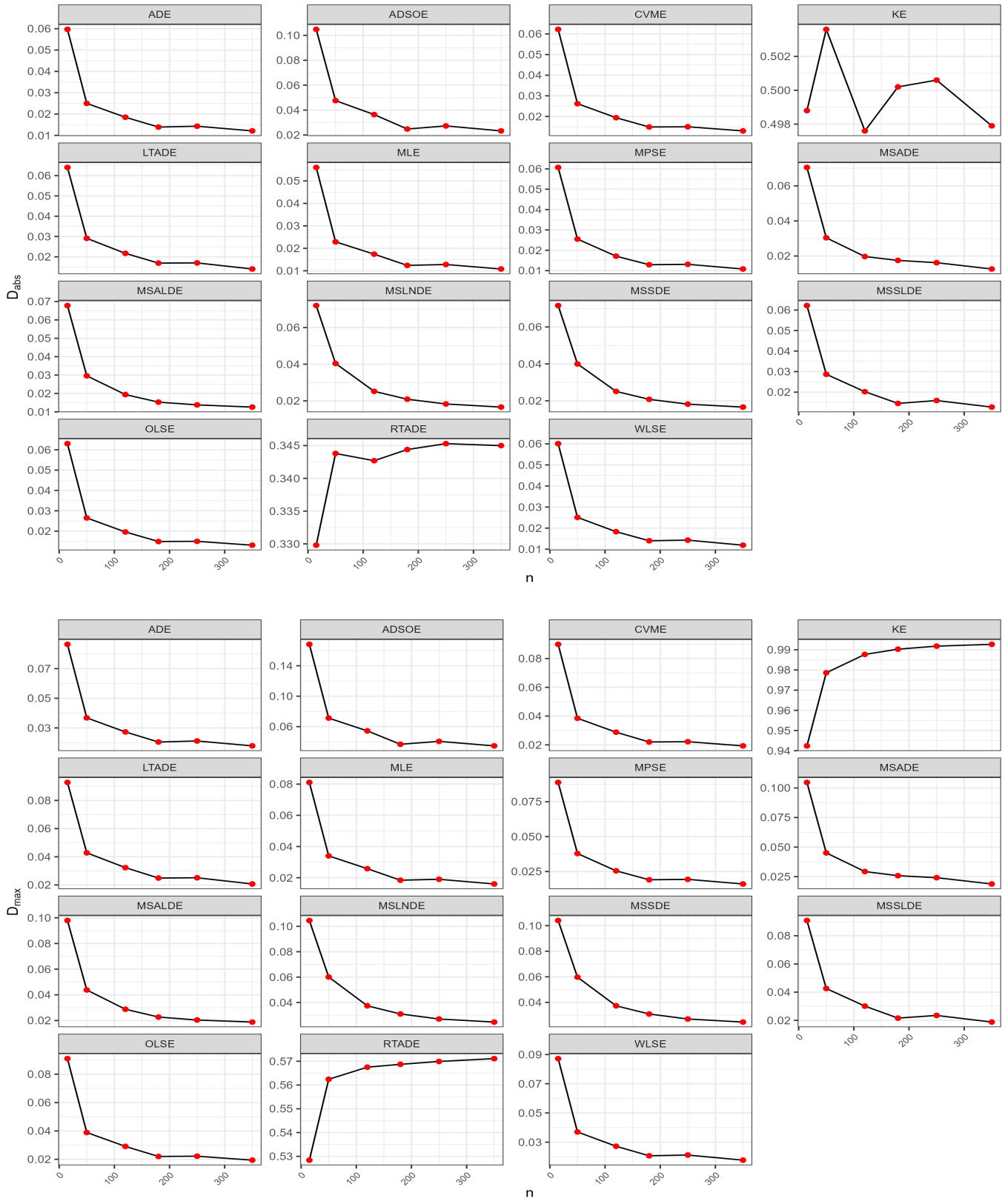

Figure 5. Graphical representations for the D_{abs} and D_{max} values presented in Table 3.

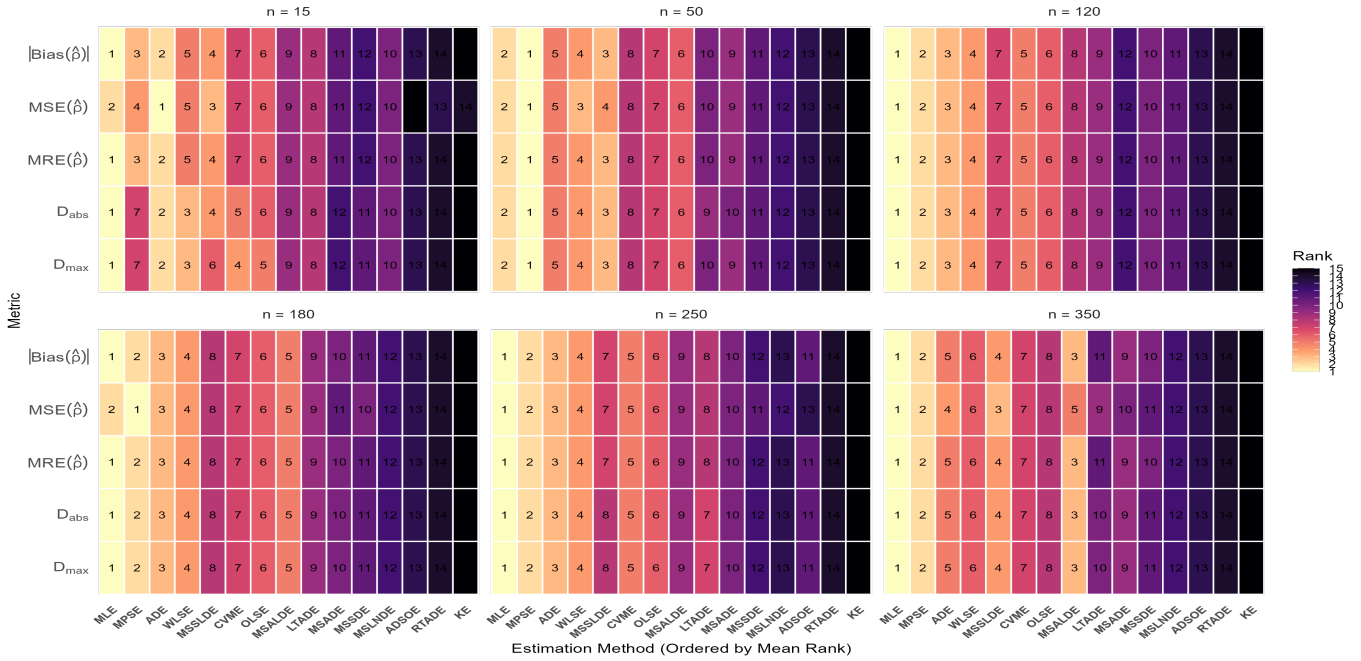

Figure 6. Partial Rank Heatmap for Simulation 3.

The plot, Figure 11, is a partial rank heatmap comparing fifteen estimation methods across five metrics for the `Obulezi` distribution at six different sample sizes (n) for simulation case 5. Lighter colors (yellow/peach) represent Rank 1 (best performance), while darker colors (purple/black) represent the worst rank. Performance generally improves (lighter ranks) as the sample size (n) increases, although the goodness-of-fit metrics (D_{abs} and D_{max}) show less change than the parameter-dependent metrics.

The simulation results in Tables 5 and 6 clearly establish a group of superior performers among the estimators. The MPSE and the MLE dominate the overall ranking, with the MPSE slightly outperforming the MLE across most sample sizes ($n = 120, 180, 250$), and the `MLE` excelling at the largest and smallest samples ($n = 15$ and $n = 350$). Both consistently occupy the first or second rank in the aggregate $\sum$ Ranks. This indicates that, for $\rho = 2.50$, these two estimators are the most precise and accurate options overall. A third strong contender is the MSSLDE. This method consistently achieves a top-three overall rank, which is particularly notable for $n = 15$ and $n = 50$ and again at $n = 350$, where it places second overall. The ADE and the WLSE round out the top five, demonstrating good, though less consistent, performance across the increasing sample sizes. As the sample size (n) increases from 15 to 350, the values of all metrics—$|\text{Bias}(\hat{\rho})|$, $\text{MSE}(\hat{\rho})$, $\text{MRE}(\hat{\rho})$, D_{abs}, and D_{max}—systematically decrease for all estimation methods. This confirms the desired property of consistency, meaning the estimators become more accurate and precise as more data is available. Crucially, while the performance itself improves with n, the general relative ranking of the estimators remains remarkably stable, with the same few methods consistently grouping at the top and the bottom.

Conversely, several estimation methods perform poorly regardless of sample size. The RTADE and the KE consistently yield the highest values for all metrics, resulting in the worst overall aggregate rank (ranks {14} and {15}) across all sample sizes, suggesting they are the least reliable methods for this distribution and parameter value. The plots in Figures 7, 8, 10 and 9 align perfectly with the results in Tables 5 and 6.

Table 3. Numerical values of simulation measures for $\rho = 1.75$.

n	Metric	MLE	ADE	CVME	MPSE	OLSE	RTADE	WLSE	LTADE	MSADE	MSALDE	ADSOE	KE	MSSDE	MSSLDE	MSLNDE
15	$\lvert Bias\rvert(\hat{\rho})$	$0.3509^{\{1\}}$	$0.3695^{\{3\}}$	$0.3873^{\{5\}}$	$0.3692^{\{2\}}$	$0.3898^{\{7\}}$	$1.4679^{\{13\}}$	$0.3730^{\{4\}}$	$0.4065^{\{8\}}$	$0.4404^{\{12\}}$	$0.4089^{\{9\}}$	$1.6868^{\{14\}}$	$1.7490^{\{15\}}$	$0.4304^{\{10\}}$	$0.3875^{\{6\}}$	$0.4327^{\{11\}}$
	MSE $(\hat{\rho})$	$0.2073^{\{1\}}$	$0.2238^{\{3\}}$	$0.2477^{\{6\}}$	$0.2083^{\{2\}}$	$0.2478^{\{7\}}$	$2.1705^{\{13\}}$	$0.2331^{\{4\}}$	$0.3097^{\{12\}}$	$0.3061^{\{11\}}$	$0.2526^{\{8\}}$	$21.4004^{\{15\}}$	$3.0590^{\{14\}}$	$0.2873^{\{9\}}$	$0.2440^{\{5\}}$	$0.2909^{\{10\}}$
	MRE $(\hat{\rho})$	$0.2005^{\{1\}}$	$0.2112^{\{3\}}$	$0.2213^{\{5\}}$	$0.2109^{\{2\}}$	$0.2227^{\{7\}}$	$0.8388^{\{13\}}$	$0.2131^{\{4\}}$	$0.2323^{\{8\}}$	$0.2517^{\{12\}}$	$0.2336^{\{9\}}$	$0.9639^{\{14\}}$	$0.9994^{\{15\}}$	$0.2459^{\{10\}}$	$0.2214^{\{6\}}$	$0.2472^{\{11\}}$
	D_{abs}	$0.0560^{\{1\}}$	$0.0597^{\{2\}}$	$0.0622^{\{6\}}$	$0.0607^{\{4\}}$	$0.0630^{\{7\}}$	$0.3298^{\{14\}}$	$0.0601^{\{3\}}$	$0.0640^{\{8\}}$	$0.0705^{\{10\}}$	$0.0678^{\{9\}}$	$0.1048^{\{13\}}$	$0.4988^{\{15\}}$	$0.0716^{\{11\}}$	$0.0622^{\{5\}}$	$0.0720^{\{12\}}$
	D_{max}	$0.0811^{\{1\}}$	$0.0864^{\{2\}}$	$0.0899^{\{5\}}$	$0.0888^{\{4\}}$	$0.0910^{\{7\}}$	$0.5284^{\{14\}}$	$0.0872^{\{3\}}$	$0.0928^{\{8\}}$	$0.1047^{\{12\}}$	$0.0979^{\{9\}}$	$0.1682^{\{13\}}$	$0.9424^{\{15\}}$	$0.1040^{\{10\}}$	$0.0908^{\{6\}}$	$0.1046^{\{11\}}$
	$\sum$Ranks	$5^{\{1\}}$	$13^{\{2\}}$	$27^{\{5\}}$	$14^{\{3\}}$	$35^{\{7\}}$	$67^{\{13\}}$	$18^{\{4\}}$	$44^{\{8\}}$	$57^{\{12\}}$	$44^{\{8\}}$	$69^{\{14\}}$	$74^{\{15\}}$	$50^{\{10\}}$	$28^{\{6\}}$	$55^{\{11\}}$
50	$\lvert Bias\rvert(\hat{\rho})$	$0.1392^{\{1\}}$	$0.1507^{\{2\}}$	$0.1582^{\{5\}}$	$0.1529^{\{4\}}$	$0.1594^{\{6\}}$	$1.5109^{\{14\}}$	$0.1517^{\{3\}}$	$0.1763^{\{8\}}$	$0.1819^{\{10\}}$	$0.1766^{\{9\}}$	$0.3383^{\{13\}}$	$1.7490^{\{15\}}$	$0.2431^{\{11\}}$	$0.1733^{\{7\}}$	$0.2451^{\{12\}}$
	MSE $(\hat{\rho})$	$0.0296^{\{1\}}$	$0.0363^{\{3\}}$	$0.0425^{\{5\}}$	$0.0336^{\{2\}}$	$0.0429^{\{6\}}$	$2.2850^{\{14\}}$	$0.0379^{\{4\}}$	$0.0526^{\{10\}}$	$0.0506^{\{9\}}$	$0.0466^{\{8\}}$	$0.4512^{\{13\}}$	$3.0590^{\{15\}}$	$0.0946^{\{11\}}$	$0.0432^{\{7\}}$	$0.0963^{\{12\}}$
	MRE $(\hat{\rho})$	$0.0795^{\{1\}}$	$0.0861^{\{2\}}$	$0.0904^{\{5\}}$	$0.0874^{\{4\}}$	$0.0911^{\{6\}}$	$0.8634^{\{14\}}$	$0.0867^{\{3\}}$	$0.1007^{\{8\}}$	$0.1039^{\{10\}}$	$0.1009^{\{9\}}$	$0.1933^{\{13\}}$	$0.9994^{\{15\}}$	$0.1389^{\{11\}}$	$0.0990^{\{7\}}$	$0.1400^{\{12\}}$
	D_{abs}	$0.0229^{\{1\}}$	$0.0250^{\{2\}}$	$0.0262^{\{5\}}$	$0.0255^{\{4\}}$	$0.0265^{\{6\}}$	$0.3438^{\{14\}}$	$0.0251^{\{3\}}$	$0.0291^{\{8\}}$	$0.0304^{\{10\}}$	$0.0296^{\{9\}}$	$0.0476^{\{13\}}$	$0.5036^{\{15\}}$	$0.0400^{\{11\}}$	$0.0287^{\{7\}}$	$0.0404^{\{12\}}$
	D_{max}	$0.0340^{\{1\}}$	$0.0368^{\{2\}}$	$0.0385^{\{5\}}$	$0.0379^{\{4\}}$	$0.0389^{\{6\}}$	$0.5624^{\{14\}}$	$0.0370^{\{3\}}$	$0.0428^{\{8\}}$	$0.0451^{\{10\}}$	$0.0438^{\{9\}}$	$0.0712^{\{13\}}$	$0.9786^{\{15\}}$	$0.0597^{\{11\}}$	$0.0426^{\{7\}}$	$0.0601^{\{12\}}$
	$\sum$Ranks	$5^{\{1\}}$	$11^{\{2\}}$	$25^{\{5\}}$	$18^{\{4\}}$	$30^{\{6\}}$	$70^{\{14\}}$	$16^{\{3\}}$	$42^{\{8\}}$	$49^{\{10\}}$	$44^{\{9\}}$	$65^{\{13\}}$	$75^{\{15\}}$	$55^{\{11\}}$	$35^{\{7\}}$	$60^{\{12\}}$
120	$\lvert Bias\rvert(\hat{\rho})$	$0.1056^{\{2\}}$	$0.1117^{\{4\}}$	$0.1178^{\{6\}}$	$0.1034^{\{1\}}$	$0.1191^{\{7\}}$	$1.5169^{\{14\}}$	$0.1114^{\{3\}}$	$0.1325^{\{10\}}$	$0.1195^{\{8\}}$	$0.1171^{\{5\}}$	$0.2391^{\{13\}}$	$1.7490^{\{15\}}$	$0.1520^{\{11\}}$	$0.1226^{\{9\}}$	$0.1523^{\{12\}}$
	MSE $(\hat{\rho})$	$0.0176^{\{2\}}$	$0.0201^{\{4\}}$	$0.0223^{\{6\}}$	$0.0170^{\{1\}}$	$0.0226^{\{8\}}$	$2.3019^{\{14\}}$	$0.0195^{\{3\}}$	$0.0278^{\{10\}}$	$0.0219^{\{5\}}$	$0.0223^{\{7\}}$	$0.1349^{\{13\}}$	$3.0590^{\{15\}}$	$0.0333^{\{11\}}$	$0.0227^{\{9\}}$	$0.0335^{\{12\}}$
	MRE $(\hat{\rho})$	$0.0603^{\{2\}}$	$0.0639^{\{4\}}$	$0.0673^{\{6\}}$	$0.0591^{\{1\}}$	$0.0681^{\{7\}}$	$0.8668^{\{14\}}$	$0.0637^{\{3\}}$	$0.0757^{\{10\}}$	$0.0683^{\{8\}}$	$0.0669^{\{5\}}$	$0.1366^{\{13\}}$	$0.9994^{\{15\}}$	$0.0868^{\{11\}}$	$0.0701^{\{9\}}$	$0.0870^{\{12\}}$
	D_{abs}	$0.0174^{\{2\}}$	$0.0185^{\{4\}}$	$0.0194^{\{6\}}$	$0.0171^{\{1\}}$	$0.0196^{\{7\}}$	$0.3427^{\{14\}}$	$0.0183^{\{3\}}$	$0.0217^{\{10\}}$	$0.0197^{\{8\}}$	$0.0194^{\{5\}}$	$0.0364^{\{13\}}$	$0.4976^{\{15\}}$	$0.0251^{\{11\}}$	$0.0202^{\{9\}}$	$0.0252^{\{12\}}$
	D_{max}	$0.0258^{\{2\}}$	$0.0273^{\{4\}}$	$0.0288^{\{6\}}$	$0.0255^{\{1\}}$	$0.0291^{\{7\}}$	$0.5675^{\{14\}}$	$0.0272^{\{3\}}$	$0.0323^{\{10\}}$	$0.0293^{\{8\}}$	$0.0288^{\{5\}}$	$0.0544^{\{13\}}$	$0.9877^{\{15\}}$	$0.0373^{\{11\}}$	$0.0301^{\{9\}}$	$0.0374^{\{12\}}$
	$\sum$Ranks	$10^{\{2\}}$	$20^{\{4\}}$	$30^{\{6\}}$	$5^{\{1\}}$	$36^{\{7\}}$	$70^{\{14\}}$	$15^{\{3\}}$	$50^{\{10\}}$	$37^{\{8\}}$	$27^{\{5\}}$	$65^{\{13\}}$	$75^{\{15\}}$	$55^{\{11\}}$	$45^{\{9\}}$	$60^{\{12\}}$
180	$\lvert Bias\rvert(\hat{\rho})$	$0.0751^{\{1\}}$	$0.0835^{\{3\}}$	$0.0897^{\{7\}}$	$0.0774^{\{2\}}$	$0.0896^{\{6\}}$	$1.5182^{\{14\}}$	$0.0844^{\{4\}}$	$0.1018^{\{9\}}$	$0.1047^{\{10\}}$	$0.0922^{\{8\}}$	$0.1530^{\{13\}}$	$1.7490^{\{15\}}$	$0.1263^{\{11\}}$	$0.0876^{\{5\}}$	$0.1268^{\{12\}}$
	MSE $(\hat{\rho})$	$0.0088^{\{1\}}$	$0.0100^{\{3\}}$	$0.0115^{\{5\}}$	$0.0092^{\{2\}}$	$0.0115^{\{6\}}$	$2.3059^{\{14\}}$	$0.0102^{\{4\}}$	$0.0150^{\{9\}}$	$0.0158^{\{10\}}$	$0.0136^{\{8\}}$	$0.0404^{\{13\}}$	$3.0590^{\{15\}}$	$0.0268^{\{11\}}$	$0.0125^{\{7\}}$	$0.0270^{\{12\}}$
	MRE $(\hat{\rho})$	$0.0429^{\{1\}}$	$0.0477^{\{3\}}$	$0.0512^{\{7\}}$	$0.0442^{\{2\}}$	$0.0512^{\{6\}}$	$0.8676^{\{14\}}$	$0.0482^{\{4\}}$	$0.0582^{\{9\}}$	$0.0598^{\{10\}}$	$0.0527^{\{8\}}$	$0.0875^{\{13\}}$	$0.9994^{\{15\}}$	$0.0721^{\{11\}}$	$0.0501^{\{5\}}$	$0.0725^{\{12\}}$
	D_{abs}	$0.0124^{\{1\}}$	$0.0139^{\{3\}}$	$0.0149^{\{6\}}$	$0.0129^{\{2\}}$	$0.0149^{\{7\}}$	$0.3444^{\{14\}}$	$0.0140^{\{4\}}$	$0.0169^{\{9\}}$	$0.0175^{\{10\}}$	$0.0153^{\{8\}}$	$0.0248^{\{13\}}$	$0.5002^{\{15\}}$	$0.0208^{\{11\}}$	$0.0145^{\{5\}}$	$0.0209^{\{12\}}$
	D_{max}	$0.0184^{\{1\}}$	$0.0205^{\{3\}}$	$0.0220^{\{6\}}$	$0.0191^{\{2\}}$	$0.0220^{\{7\}}$	$0.5687^{\{14\}}$	$0.0207^{\{4\}}$	$0.0249^{\{9\}}$	$0.0258^{\{10\}}$	$0.0227^{\{8\}}$	$0.0368^{\{13\}}$	$0.9903^{\{15\}}$	$0.0309^{\{11\}}$	$0.0216^{\{5\}}$	$0.0310^{\{12\}}$
	$\sum$Ranks	$5^{\{1\}}$	$15^{\{3\}}$	$31^{\{6\}}$	$10^{\{2\}}$	$32^{\{7\}}$	$70^{\{14\}}$	$20^{\{4\}}$	$45^{\{9\}}$	$50^{\{10\}}$	$40^{\{8\}}$	$65^{\{13\}}$	$75^{\{15\}}$	$55^{\{11\}}$	$27^{\{5\}}$	$60^{\{12\}}$
250	$\lvert Bias\rvert(\hat{\rho})$	$0.0773^{\{1\}}$	$0.0865^{\{5\}}$	$0.0904^{\{6\}}$	$0.0786^{\{2\}}$	$0.0905^{\{7\}}$	$1.5199^{\{14\}}$	$0.0865^{\{4\}}$	$0.1026^{\{10\}}$	$0.0983^{\{9\}}$	$0.0830^{\{3\}}$	$0.1721^{\{13\}}$	$1.7490^{\{15\}}$	$0.1099^{\{11\}}$	$0.0955^{\{8\}}$	$0.1101^{\{12\}}$
	MSE $(\hat{\rho})$	$0.0093^{\{1\}}$	$0.0117^{\{4\}}$	$0.0129^{\{6\}}$	$0.0096^{\{2\}}$	$0.0129^{\{7\}}$	$2.3104^{\{14\}}$	$0.0118^{\{5\}}$	$0.0168^{\{10\}}$	$0.0152^{\{9\}}$	$0.0108^{\{3\}}$	$0.0646^{\{13\}}$	$3.0590^{\{15\}}$	$0.0197^{\{11\}}$	$0.0135^{\{8\}}$	$0.0198^{\{12\}}$
	MRE $(\hat{\rho})$	$0.0442^{\{1\}}$	$0.0494^{\{5\}}$	$0.0517^{\{6\}}$	$0.0449^{\{2\}}$	$0.0517^{\{7\}}$	$0.8685^{\{14\}}$	$0.0494^{\{4\}}$	$0.0586^{\{10\}}$	$0.0562^{\{9\}}$	$0.0474^{\{3\}}$	$0.0984^{\{13\}}$	$0.9994^{\{15\}}$	$0.0628^{\{11\}}$	$0.0545^{\{8\}}$	$0.0629^{\{12\}}$
	D_{abs}	$0.0128^{\{1\}}$	$0.0143^{\{5\}}$	$0.0150^{\{6\}}$	$0.0131^{\{2\}}$	$0.0150^{\{7\}}$	$0.3453^{\{14\}}$	$0.0143^{\{4\}}$	$0.0170^{\{10\}}$	$0.0162^{\{9\}}$	$0.0138^{\{3\}}$	$0.0273^{\{13\}}$	$0.5006^{\{15\}}$	$0.0182^{\{11\}}$	$0.0159^{\{8\}}$	$0.0183^{\{12\}}$
	D_{max}	$0.0190^{\{1\}}$	$0.0212^{\{5\}}$	$0.0222^{\{6\}}$	$0.0194^{\{2\}}$	$0.0222^{\{7\}}$	$0.5699^{\{14\}}$	$0.0212^{\{4\}}$	$0.0251^{\{10\}}$	$0.0241^{\{9\}}$	$0.0204^{\{3\}}$	$0.0406^{\{13\}}$	$0.9918^{\{15\}}$	$0.0270^{\{11\}}$	$0.0235^{\{8\}}$	$0.0270^{\{12\}}$
	$\sum$Ranks	$5^{\{1\}}$	$24^{\{5\}}$	$30^{\{6\}}$	$10^{\{2\}}$	$35^{\{7\}}$	$70^{\{14\}}$	$21^{\{4\}}$	$50^{\{10\}}$	$45^{\{9\}}$	$15^{\{3\}}$	$65^{\{13\}}$	$75^{\{15\}}$	$55^{\{11\}}$	$40^{\{8\}}$	$60^{\{12\}}$
350	$\lvert Bias\rvert(\hat{\rho})$	$0.0652^{\{1\}}$	$0.0732^{\{4\}}$	$0.0790^{\{8\}}$	$0.0653^{\{2\}}$	$0.0791^{\{9\}}$	$1.5210^{\{14\}}$	$0.0722^{\{3\}}$	$0.0848^{\{10\}}$	$0.0766^{\{7\}}$	$0.0765^{\{6\}}$	$0.1495^{\{13\}}$	$1.7490^{\{15\}}$	$0.1001^{\{11\}}$	$0.0763^{\{5\}}$	$0.1003^{\{12\}}$
	MSE $(\hat{\rho})$	$0.0062^{\{1\}}$	$0.0084^{\{4\}}$	$0.0098^{\{9\}}$	$0.0062^{\{2\}}$	$0.0098^{\{8\}}$	$2.3139^{\{14\}}$	$0.0084^{\{3\}}$	$0.0115^{\{10\}}$	$0.0088^{\{5\}}$	$0.0089^{\{7\}}$	$0.0668^{\{13\}}$	$3.0590^{\{15\}}$	$0.0145^{\{11\}}$	$0.0088^{\{6\}}$	$0.0146^{\{12\}}$
	MRE $(\hat{\rho})$	$0.0373^{\{1\}}$	$0.0418^{\{4\}}$	$0.0451^{\{8\}}$	$0.0373^{\{2\}}$	$0.0452^{\{9\}}$	$0.8692^{\{14\}}$	$0.0413^{\{3\}}$	$0.0484^{\{10\}}$	$0.0438^{\{7\}}$	$0.0437^{\{6\}}$	$0.0854^{\{13\}}$	$0.9994^{\{15\}}$	$0.0572^{\{11\}}$	$0.0436^{\{5\}}$	$0.0573^{\{12\}}$
	D_{abs}	$0.0108^{\{1\}}$	$0.0121^{\{4\}}$	$0.0130^{\{8\}}$	$0.0108^{\{2\}}$	$0.0131^{\{9\}}$	$0.3450^{\{14\}}$	$0.0119^{\{3\}}$	$0.0140^{\{10\}}$	$0.0126^{\{5\}}$	$0.0126^{\{6\}}$	$0.0233^{\{13\}}$	$0.4979^{\{15\}}$	$0.0166^{\{11\}}$	$0.0127^{\{7\}}$	$0.0166^{\{12\}}$
	D_{max}	$0.0160^{\{1\}}$	$0.0179^{\{4\}}$	$0.0193^{\{8\}}$	$0.0161^{\{2\}}$	$0.0194^{\{9\}}$	$0.5711^{\{14\}}$	$0.0177^{\{3\}}$	$0.0207^{\{10\}}$	$0.0188^{\{6\}}$	$0.0188^{\{7\}}$	$0.0347^{\{13\}}$	$0.9927^{\{15\}}$	$0.0246^{\{11\}}$	$0.0188^{\{5\}}$	$0.0246^{\{12\}}$
	$\sum$Ranks	$5^{\{1\}}$	$20^{\{4\}}$	$41^{\{8\}}$	$10^{\{2\}}$	$44^{\{9\}}$	$70^{\{14\}}$	$15^{\{3\}}$	$50^{\{10\}}$	$30^{\{6\}}$	$32^{\{7\}}$	$65^{\{13\}}$	$75^{\{15\}}$	$55^{\{11\}}$	$28^{\{5\}}$	$60^{\{12\}}$

Table 4. Partial and overall ranks for all estimation methods of the `Obulezi` distribution from Table 3.

n	Metric	MLE	ADE	CVME	MPSE	OLSE	RTADE	WLSE	LTADE	MSADE	MSALDE	ADSOE	KE	MSSDE	MSSLDE	MSLNDE
15	$\lvert Bias\rvert(\hat{\rho})$	1.0	3.0	5.0	2.0	7.0	13.0	4.0	8.0	12.0	9.0	14.0	15.0	10.0	6.0	11.0
	MSE $(\hat{\rho})$	1.0	3.0	6.0	2.0	7.0	13.0	4.0	12.0	11.0	8.0	15.0	14.0	9.0	5.0	10.0
	MRE $(\hat{\rho})$	1.0	3.0	5.0	2.0	7.0	13.0	4.0	8.0	12.0	9.0	14.0	15.0	10.0	6.0	11.0
	D_{abs}	1.0	2.0	6.0	4.0	7.0	14.0	3.0	8.0	10.0	9.0	13.0	15.0	11.0	5.0	12.0
	D_{max}	1.0	2.0	5.0	4.0	7.0	14.0	3.0	8.0	12.0	9.0	13.0	15.0	10.0	6.0	11.0
	$\sum$Ranks	$5^{\{1\}}$	$13^{\{2\}}$	$27^{\{5\}}$	$14^{\{3\}}$	$35^{\{7\}}$	$67^{\{13\}}$	$18^{\{4\}}$	$44^{\{8\}}$	$57^{\{12\}}$	$44^{\{9\}}$	$69^{\{14\}}$	$74^{\{15\}}$	$50^{\{10\}}$	$28^{\{6\}}$	$55^{\{11\}}$
50	$\lvert Bias\rvert(\hat{\rho})$	1.0	2.0	5.0	4.0	6.0	14.0	3.0	8.0	10.0	9.0	13.0	15.0	11.0	7.0	12.0
	MSE $(\hat{\rho})$	1.0	3.0	5.0	2.0	6.0	14.0	4.0	10.0	9.0	8.0	13.0	15.0	11.0	7.0	12.0
	MRE $(\hat{\rho})$	1.0	2.0	5.0	4.0	6.0	14.0	3.0	8.0	10.0	9.0	13.0	15.0	11.0	7.0	12.0
	D_{abs}	1.0	2.0	5.0	4.0	6.0	14.0	3.0	8.0	10.0	9.0	13.0	15.0	11.0	7.0	12.0
	D_{max}	1.0	2.0	5.0	4.0	6.0	14.0	3.0	8.0	10.0	9.0	13.0	15.0	11.0	7.0	12.0
	$\sum$Ranks	$5^{\{1\}}$	$11^{\{2\}}$	$25^{\{5\}}$	$18^{\{4\}}$	$30^{\{6\}}$	$70^{\{14\}}$	$16^{\{3\}}$	$42^{\{8\}}$	$49^{\{10\}}$	$44^{\{9\}}$	$65^{\{13\}}$	$75^{\{15\}}$	$55^{\{11\}}$	$35^{\{7\}}$	$60^{\{12\}}$
120	$\lvert Bias\rvert(\hat{\rho})$	2.0	4.0	6.0	1.0	7.0	14.0	3.0	10.0	8.0	5.0	13.0	15.0	11.0	9.0	12.0
	MSE $(\hat{\rho})$	2.0	4.0	6.0	1.0	8.0	14.0	3.0	10.0	5.0	7.0	13.0	15.0	11.0	9.0	12.0
	MRE $(\hat{\rho})$	2.0	4.0	6.0	1.0	7.0	14.0	3.0	10.0	8.0	5.0	13.0	15.0	11.0	9.0	12.0
	D_{abs}	2.0	4.0	6.0	1.0	7.0	14.0	3.0	10.0	8.0	5.0	13.0	15.0	11.0	9.0	12.0
	D_{max}	2.0	4.0	6.0	1.0	7.0	14.0	3.0	10.0	8.0	5.0	13.0	15.0	11.0	9.0	12.0
	$\sum$Ranks	$10^{\{2\}}$	$20^{\{4\}}$	$30^{\{6\}}$	$5^{\{1\}}$	$36^{\{7\}}$	$70^{\{14\}}$	$15^{\{3\}}$	$50^{\{10\}}$	$37^{\{8\}}$	$27^{\{5\}}$	$65^{\{13\}}$	$75^{\{15\}}$	$55^{\{11\}}$	$45^{\{9\}}$	$60^{\{12\}}$
180	$\lvert Bias\rvert(\hat{\rho})$	1.0	3.0	7.0	2.0	6.0	14.0	4.0	9.0	10.0	8.0	13.0	15.0	11.0	5.0	12.0
	MSE $(\hat{\rho})$	1.0	3.0	5.0	2.0	6.0	14.0	4.0	9.0	10.0	8.0	13.0	15.0	11.0	7.0	12.0
	MRE $(\hat{\rho})$	1.0	3.0	7.0	2.0	6.0	14.0	4.0	9.0	10.0	8.0	13.0	15.0	11.0	5.0	12.0
	D_{abs}	1.0	3.0	6.0	2.0	7.0	14.0	4.0	9.0	10.0	8.0	13.0	15.0	11.0	5.0	12.0
	D_{max}	1.0	3.0	6.0	2.0	7.0	14.0	4.0	9.0	10.0	8.0	13.0	15.0	11.0	5.0	12.0
	$\sum$Ranks	$5^{\{1\}}$	$15^{\{3\}}$	$31^{\{6\}}$	$10^{\{2\}}$	$32^{\{7\}}$	$70^{\{14\}}$	$20^{\{4\}}$	$45^{\{9\}}$	$50^{\{10\}}$	$40^{\{8\}}$	$65^{\{13\}}$	$75^{\{15\}}$	$55^{\{11\}}$	$27^{\{5\}}$	$60^{\{12\}}$
250	$\lvert Bias\rvert(\hat{\rho})$	1.0	5.0	6.0	2.0	7.0	14.0	4.0	10.0	9.0	3.0	13.0	15.0	11.0	8.0	12.0
	MSE $(\hat{\rho})$	1.0	4.0	6.0	2.0	7.0	14.0	5.0	10.0	9.0	3.0	13.0	15.0	11.0	8.0	12.0
	MRE $(\hat{\rho})$	1.0	5.0	6.0	2.0	7.0	14.0	4.0	10.0	9.0	3.0	13.0	15.0	11.0	8.0	12.0
	D_{abs}	1.0	5.0	6.0	2.0	7.0	14.0	4.0	10.0	9.0	3.0	13.0	15.0	11.0	8.0	12.0
	D_{max}	1.0	5.0	6.0	2.0	7.0	14.0	4.0	10.0	9.0	3.0	13.0	15.0	11.0	8.0	12.0
	$\sum$Ranks	$5^{\{1\}}$	$24^{\{5\}}$	$30^{\{6\}}$	$10^{\{2\}}$	$35^{\{7\}}$	$70^{\{14\}}$	$21^{\{4\}}$	$50^{\{10\}}$	$45^{\{9\}}$	$15^{\{3\}}$	$65^{\{13\}}$	$75^{\{15\}}$	$55^{\{11\}}$	$40^{\{8\}}$	$60^{\{12\}}$
350	$\lvert Bias\rvert(\hat{\rho})$	1.0	4.0	8.0	2.0	9.0	14.0	3.0	10.0	7.0	6.0	13.0	15.0	11.0	5.0	12.0
	MSE $(\hat{\rho})$	1.0	4.0	9.0	2.0	8.0	14.0	3.0	10.0	5.0	7.0	13.0	15.0	11.0	6.0	12.0
	MRE $(\hat{\rho})$	1.0	4.0	8.0	2.0	9.0	14.0	3.0	10.0	7.0	6.0	13.0	15.0	11.0	5.0	12.0
	D_{abs}	1.0	4.0	8.0	2.0	9.0	14.0	3.0	10.0	5.0	6.0	13.0	15.0	11.0	7.0	12.0
	D_{max}	1.0	4.0	8.0	2.0	9.0	14.0	3.0	10.0	6.0	7.0	13.0	15.0	11.0	5.0	12.0
	$\sum$Ranks	$5^{\{1\}}$	$20^{\{4\}}$	$41^{\{8\}}$	$10^{\{2\}}$	$44^{\{9\}}$	$70^{\{14\}}$	$15^{\{3\}}$	$50^{\{10\}}$	$30^{\{6\}}$	$32^{\{7\}}$	$65^{\{13\}}$	$75^{\{15\}}$	$55^{\{11\}}$	$28^{\{5\}}$	$60^{\{12\}}$

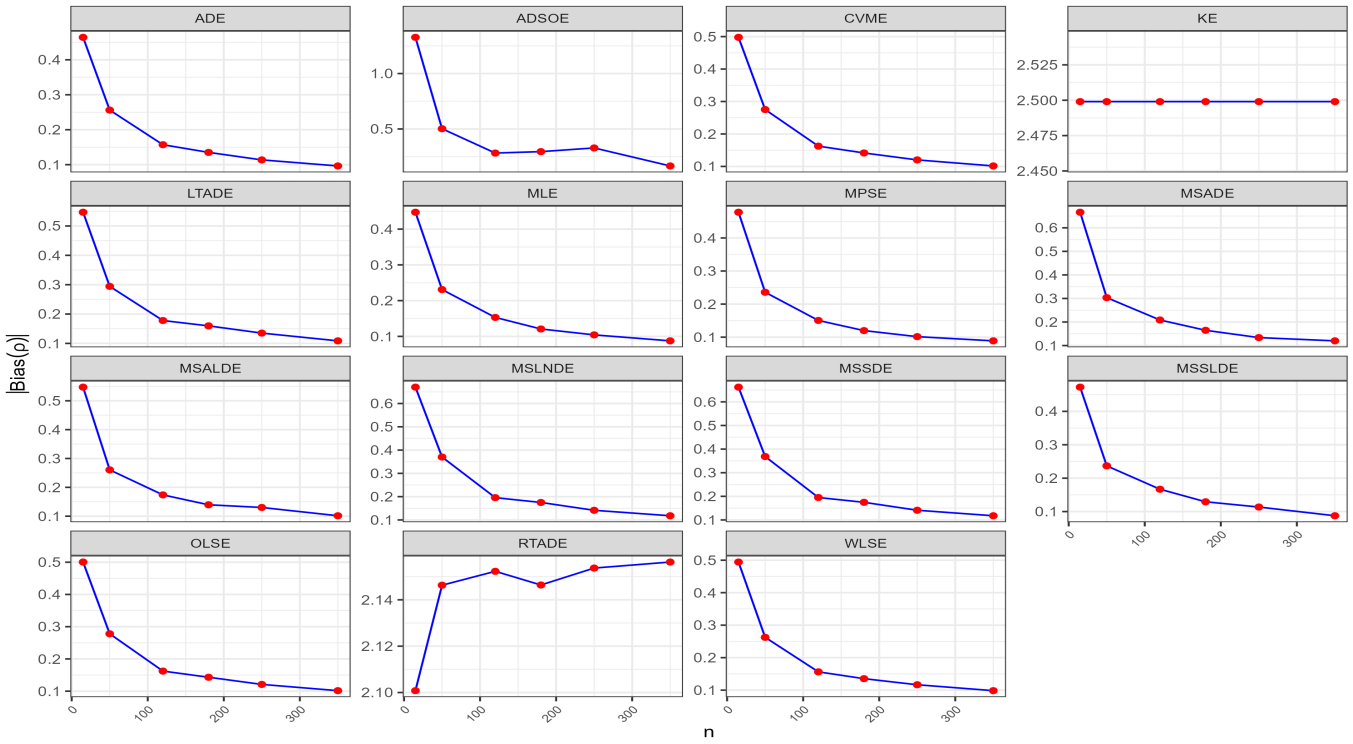

Figure 7. Graphical representations for the Bias values presented in Table 5.

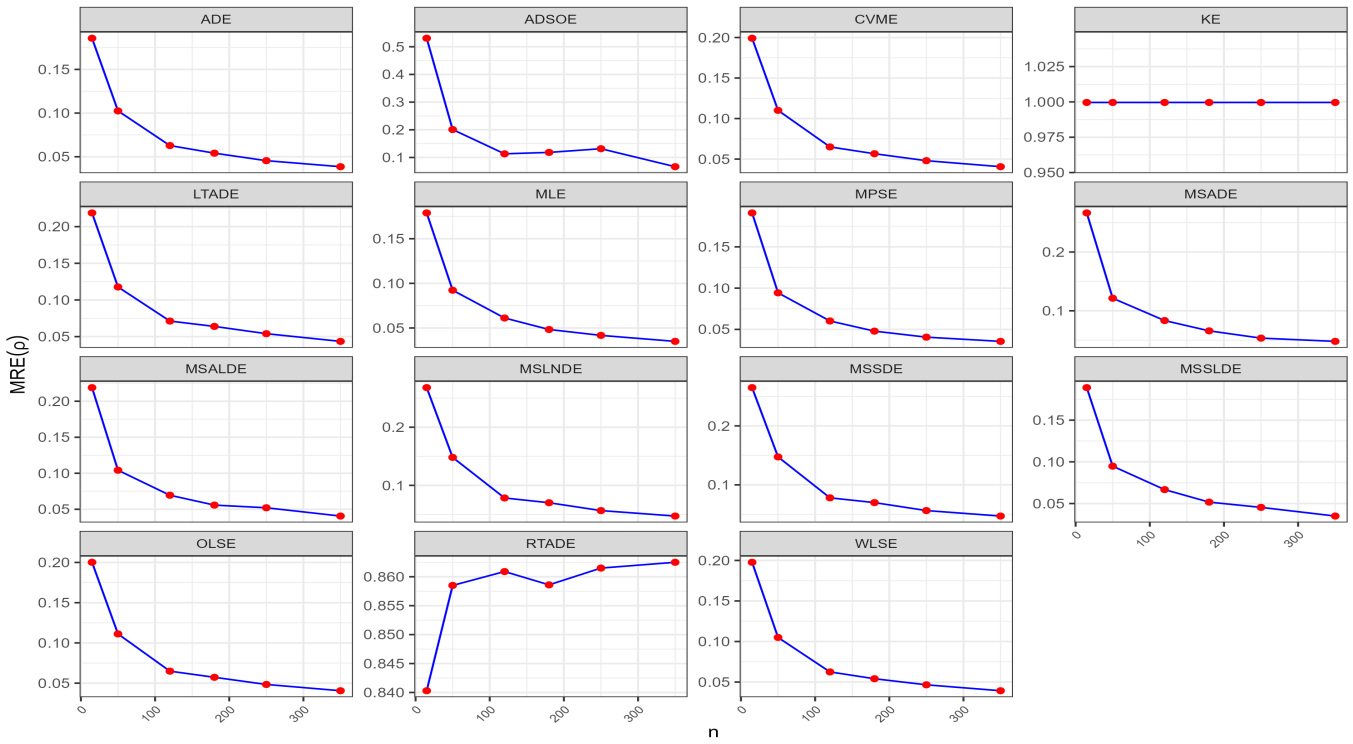

Figure 8. Graphical representations for the MRE values presented in Table 5.

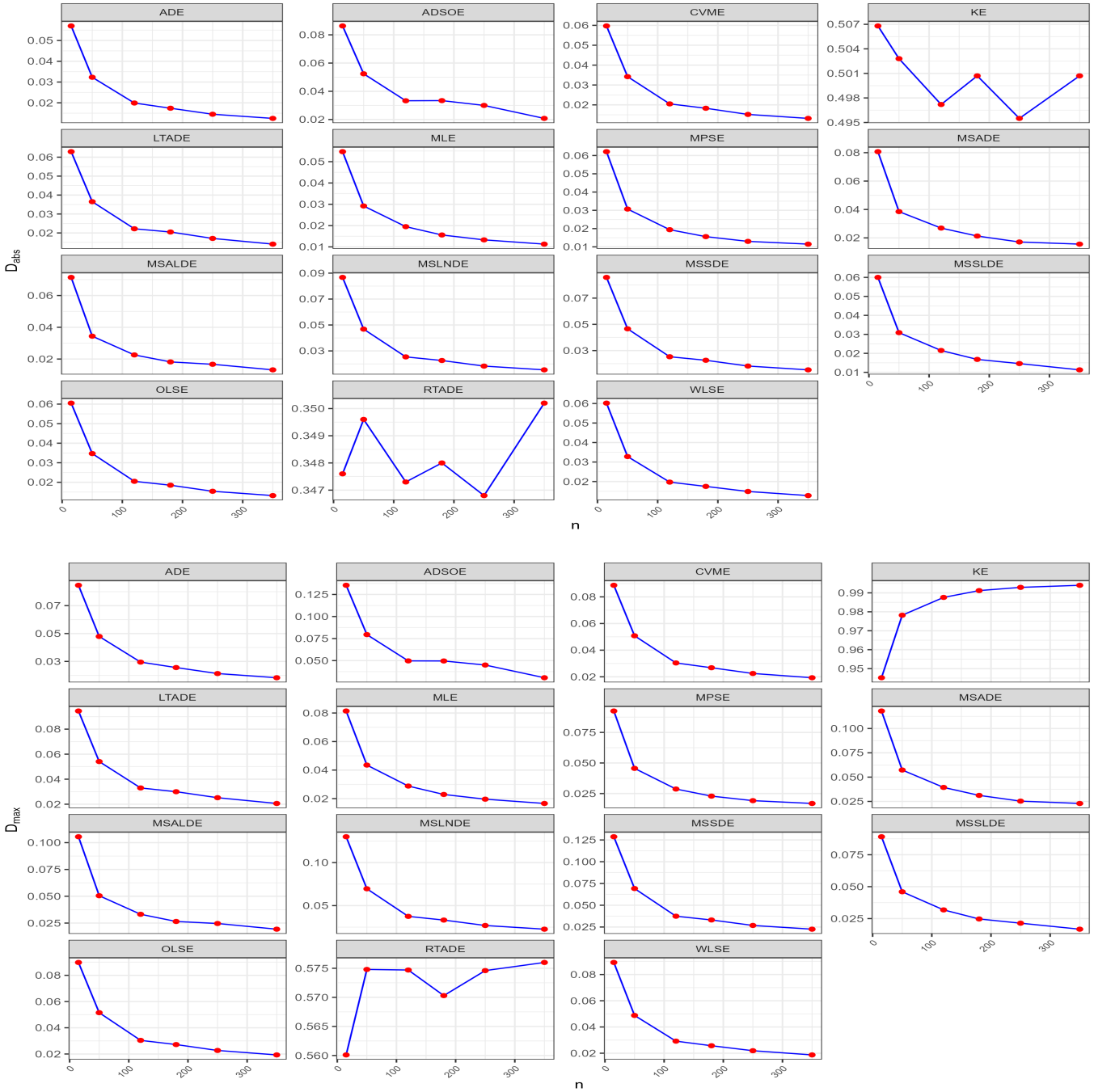

Figure 9. Graphical representations for the D_{abs} and D_{max} values presented in Table 5.

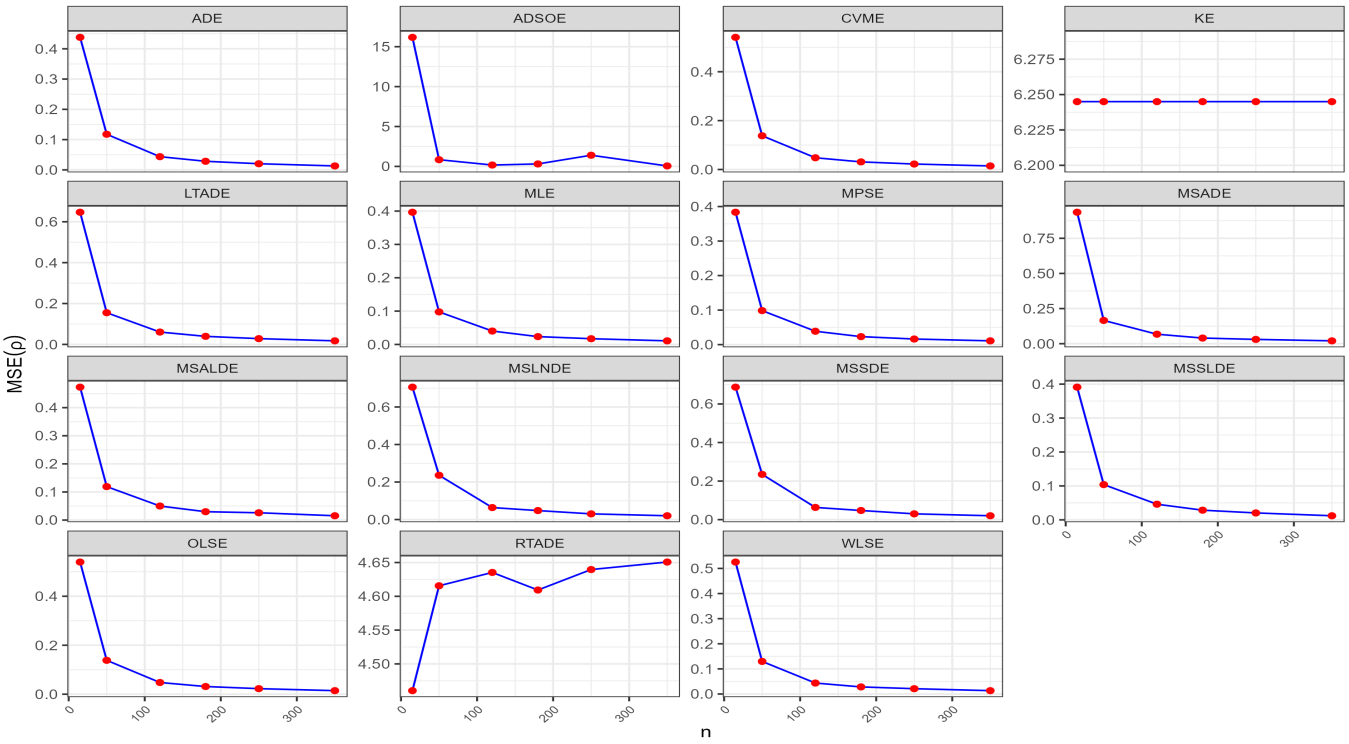

Figure 10. Graphical representations for the MSE values presented in Table 5.

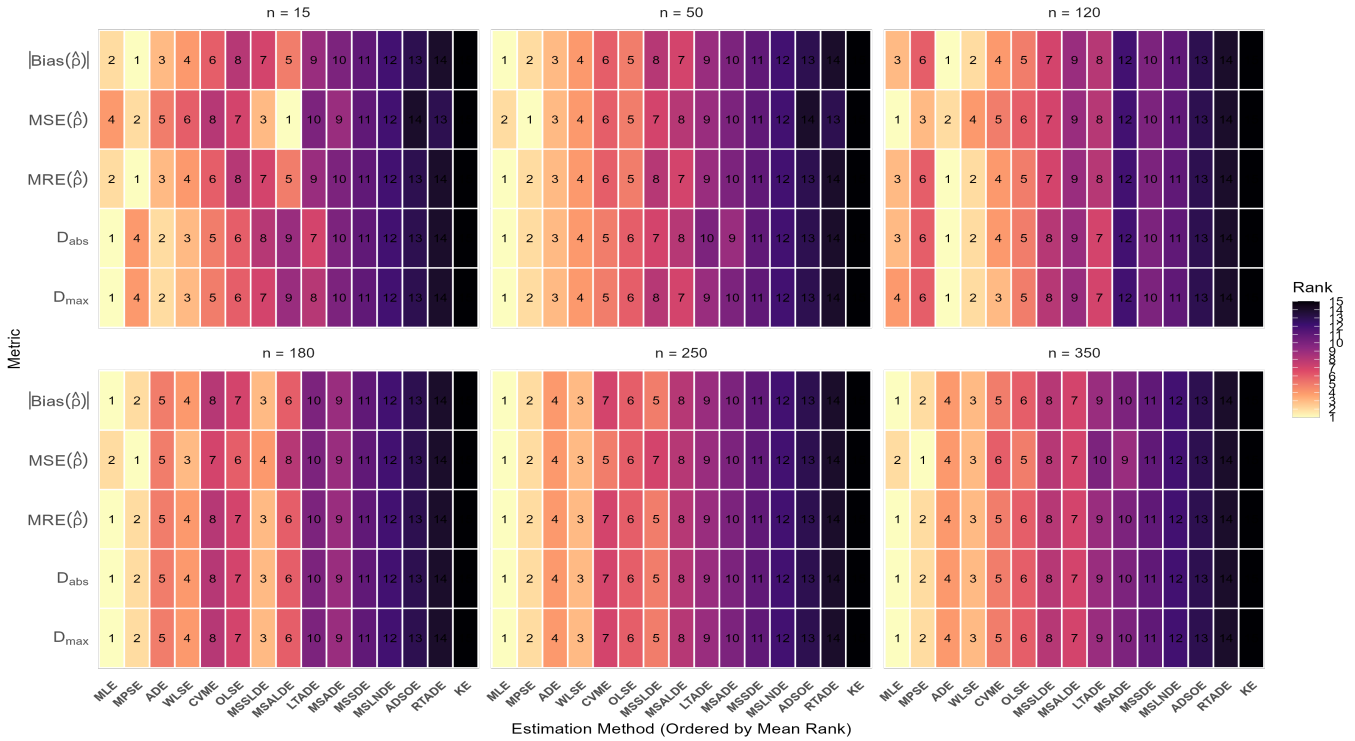

Figure 11. Partial Rank Heatmap for Simulation 5

Table 5. Numerical values of simulation measures for $\rho = 2.50$.

n	Metric	MLE	ADE	CVME	MPSE	OLSE	RTADE	WLSE	LTADE	MSADE	MSALDE	ADSOE	KE	MSSDE	MSSLDE	MSLNDE
15	$\lvert Bias\rvert(\hat{\rho})$	$0.4472^{\{1\}}$	$0.4643^{\{2\}}$	$0.4977^{\{6\}}$	$0.4778^{\{4\}}$	$0.5005^{\{7\}}$	$2.1008^{\{14\}}$	$0.4943^{\{5\}}$	$0.5468^{\{8\}}$	$0.6662^{\{11\}}$	$0.5473^{\{9\}}$	$1.3268^{\{13\}}$	$2.4990^{\{15\}}$	$0.6623^{\{10\}}$	$0.4725^{\{3\}}$	$0.6703^{\{12\}}$
	MSE $(\hat{\rho})$	$0.3965^{\{3\}}$	$0.4379^{\{4\}}$	$0.5409^{\{8\}}$	$0.3835^{\{1\}}$	$0.5396^{\{7\}}$	$4.4604^{\{13\}}$	$0.5254^{\{6\}}$	$0.6466^{\{9\}}$	$0.9354^{\{12\}}$	$0.4730^{\{5\}}$	$16.1725^{\{15\}}$	$6.2450^{\{14\}}$	$0.6872^{\{10\}}$	$0.3911^{\{2\}}$	$0.7058^{\{11\}}$
	MRE $(\hat{\rho})$	$0.1789^{\{1\}}$	$0.1857^{\{2\}}$	$0.1991^{\{6\}}$	$0.1911^{\{4\}}$	$0.2002^{\{7\}}$	$0.8403^{\{14\}}$	$0.1977^{\{5\}}$	$0.2187^{\{8\}}$	$0.2665^{\{11\}}$	$0.2189^{\{9\}}$	$0.5307^{\{13\}}$	$0.9996^{\{15\}}$	$0.2649^{\{10\}}$	$0.1890^{\{3\}}$	$0.2681^{\{12\}}$
	D_{abs}	$0.0547^{\{1\}}$	$0.0570^{\{2\}}$	$0.0597^{\{3\}}$	$0.0621^{\{7\}}$	$0.0605^{\{6\}}$	$0.3476^{\{14\}}$	$0.0602^{\{5\}}$	$0.0629^{\{8\}}$	$0.0807^{\{10\}}$	$0.0714^{\{9\}}$	$0.0863^{\{12\}}$	$0.5068^{\{15\}}$	$0.0858^{\{11\}}$	$0.0600^{\{4\}}$	$0.0867^{\{13\}}$
	D_{max}	$0.0814^{\{1\}}$	$0.0846^{\{2\}}$	$0.0887^{\{3\}}$	$0.0925^{\{7\}}$	$0.0898^{\{6\}}$	$0.5601^{\{14\}}$	$0.0892^{\{5\}}$	$0.0945^{\{8\}}$	$0.1180^{\{10\}}$	$0.1055^{\{9\}}$	$0.1354^{\{13\}}$	$0.9452^{\{15\}}$	$0.1287^{\{11\}}$	$0.0891^{\{4\}}$	$0.1301^{\{12\}}$
	$\sum$Ranks	$7^{\{1\}}$	$12^{\{2\}}$	$26^{\{5\}}$	$23^{\{4\}}$	$33^{\{7\}}$	$69^{\{14\}}$	$26^{\{5\}}$	$41^{\{8\}}$	$54^{\{11\}}$	$41^{\{8\}}$	$66^{\{13\}}$	$74^{\{15\}}$	$52^{\{10\}}$	$16^{\{3\}}$	$60^{\{12\}}$
50	$\lvert Bias\rvert(\hat{\rho})$	$0.2309^{\{1\}}$	$0.2562^{\{4\}}$	$0.2753^{\{7\}}$	$0.2358^{\{2\}}$	$0.2780^{\{8\}}$	$2.1463^{\{14\}}$	$0.2626^{\{6\}}$	$0.2943^{\{9\}}$	$0.3035^{\{10\}}$	$0.2605^{\{5\}}$	$0.5024^{\{13\}}$	$2.4990^{\{15\}}$	$0.3686^{\{11\}}$	$0.2369^{\{3\}}$	$0.3702^{\{12\}}$
	MSE $(\hat{\rho})$	$0.0977^{\{1\}}$	$0.1177^{\{4\}}$	$0.1380^{\{7\}}$	$0.0985^{\{2\}}$	$0.1384^{\{8\}}$	$4.6156^{\{14\}}$	$0.1298^{\{6\}}$	$0.1550^{\{9\}}$	$0.1655^{\{10\}}$	$0.1191^{\{5\}}$	$0.8418^{\{13\}}$	$6.2450^{\{15\}}$	$0.2348^{\{11\}}$	$0.1039^{\{3\}}$	$0.2360^{\{12\}}$
	MRE $(\hat{\rho})$	$0.0923^{\{1\}}$	$0.1025^{\{4\}}$	$0.1101^{\{7\}}$	$0.0943^{\{2\}}$	$0.1112^{\{8\}}$	$0.8585^{\{14\}}$	$0.1050^{\{6\}}$	$0.1177^{\{9\}}$	$0.1214^{\{10\}}$	$0.1042^{\{5\}}$	$0.2009^{\{13\}}$	$0.9996^{\{15\}}$	$0.1474^{\{11\}}$	$0.0948^{\{3\}}$	$0.1481^{\{12\}}$
	D_{abs}	$0.0292^{\{1\}}$	$0.0323^{\{4\}}$	$0.0342^{\{6\}}$	$0.0307^{\{2\}}$	$0.0347^{\{8\}}$	$0.3496^{\{14\}}$	$0.0328^{\{5\}}$	$0.0365^{\{9\}}$	$0.0385^{\{10\}}$	$0.0344^{\{7\}}$	$0.0524^{\{13\}}$	$0.5028^{\{15\}}$	$0.0466^{\{11\}}$	$0.0309^{\{3\}}$	$0.0468^{\{12\}}$
	D_{max}	$0.0435^{\{1\}}$	$0.0479^{\{4\}}$	$0.0508^{\{7\}}$	$0.0456^{\{2\}}$	$0.0515^{\{8\}}$	$0.5748^{\{14\}}$	$0.0488^{\{5\}}$	$0.0541^{\{9\}}$	$0.0573^{\{10\}}$	$0.0505^{\{6\}}$	$0.0795^{\{13\}}$	$0.9782^{\{15\}}$	$0.0692^{\{11\}}$	$0.0460^{\{3\}}$	$0.0696^{\{12\}}$
	$\sum$Ranks	$5^{\{1\}}$	$20^{\{4\}}$	$34^{\{7\}}$	$10^{\{2\}}$	$40^{\{8\}}$	$70^{\{14\}}$	$28^{\{5\}}$	$45^{\{9\}}$	$50^{\{10\}}$	$28^{\{5\}}$	$65^{\{13\}}$	$75^{\{15\}}$	$55^{\{11\}}$	$15^{\{3\}}$	$60^{\{12\}}$
120	$\lvert Bias\rvert(\hat{\rho})$	$0.1530^{\{2\}}$	$0.1571^{\{4\}}$	$0.1625^{\{6\}}$	$0.1505^{\{1\}}$	$0.1623^{\{5\}}$	$2.1523^{\{14\}}$	$0.1563^{\{3\}}$	$0.1779^{\{9\}}$	$0.2086^{\{12\}}$	$0.1738^{\{8\}}$	$0.2830^{\{13\}}$	$2.4990^{\{15\}}$	$0.1950^{\{10\}}$	$0.1669^{\{7\}}$	$0.1957^{\{11\}}$
	MSE $(\hat{\rho})$	$0.0402^{\{2\}}$	$0.0436^{\{3\}}$	$0.0480^{\{7\}}$	$0.0387^{\{1\}}$	$0.0478^{\{6\}}$	$4.6353^{\{14\}}$	$0.0437^{\{4\}}$	$0.0604^{\{9\}}$	$0.0675^{\{12\}}$	$0.0500^{\{8\}}$	$0.1734^{\{13\}}$	$6.2450^{\{15\}}$	$0.0634^{\{10\}}$	$0.0461^{\{5\}}$	$0.0638^{\{11\}}$
	MRE $(\hat{\rho})$	$0.0612^{\{2\}}$	$0.0628^{\{4\}}$	$0.0650^{\{6\}}$	$0.0602^{\{1\}}$	$0.0649^{\{5\}}$	$0.8609^{\{14\}}$	$0.0625^{\{3\}}$	$0.0712^{\{9\}}$	$0.0834^{\{12\}}$	$0.0695^{\{8\}}$	$0.1132^{\{13\}}$	$0.9996^{\{15\}}$	$0.0780^{\{10\}}$	$0.0667^{\{7\}}$	$0.0783^{\{11\}}$
	D_{abs}	$0.0195^{\{2\}}$	$0.0199^{\{4\}}$	$0.0205^{\{6\}}$	$0.0194^{\{1\}}$	$0.0205^{\{5\}}$	$0.3473^{\{14\}}$	$0.0197^{\{3\}}$	$0.0222^{\{8\}}$	$0.0269^{\{12\}}$	$0.0226^{\{9\}}$	$0.0333^{\{13\}}$	$0.4972^{\{15\}}$	$0.0253^{\{10\}}$	$0.0215^{\{7\}}$	$0.0254^{\{11\}}$
	D_{max}	$0.0288^{\{2\}}$	$0.0295^{\{4\}}$	$0.0304^{\{6\}}$	$0.0287^{\{1\}}$	$0.0304^{\{5\}}$	$0.5747^{\{14\}}$	$0.0292^{\{3\}}$	$0.0330^{\{8\}}$	$0.0394^{\{12\}}$	$0.0332^{\{9\}}$	$0.0497^{\{13\}}$	$0.9876^{\{15\}}$	$0.0374^{\{10\}}$	$0.0318^{\{7\}}$	$0.0375^{\{11\}}$
	$\sum$Ranks	$10^{\{2\}}$	$19^{\{4\}}$	$31^{\{6\}}$	$5^{\{1\}}$	$26^{\{5\}}$	$70^{\{14\}}$	$16^{\{3\}}$	$43^{\{9\}}$	$60^{\{12\}}$	$42^{\{8\}}$	$65^{\{13\}}$	$75^{\{15\}}$	$50^{\{10\}}$	$33^{\{7\}}$	$55^{\{11\}}$
180	$\lvert Bias\rvert(\hat{\rho})$	$0.1207^{\{2\}}$	$0.1352^{\{4\}}$	$0.1415^{\{7\}}$	$0.1198^{\{1\}}$	$0.1432^{\{8\}}$	$2.1464^{\{14\}}$	$0.1353^{\{5\}}$	$0.1597^{\{9\}}$	$0.1648^{\{10\}}$	$0.1395^{\{6\}}$	$0.2958^{\{13\}}$	$2.4990^{\{15\}}$	$0.1747^{\{11\}}$	$0.1293^{\{3\}}$	$0.1751^{\{12\}}$
	MSE $(\hat{\rho})$	$0.0235^{\{2\}}$	$0.0284^{\{4\}}$	$0.0311^{\{7\}}$	$0.0231^{\{1\}}$	$0.0314^{\{8\}}$	$4.6093^{\{14\}}$	$0.0283^{\{3\}}$	$0.0394^{\{9\}}$	$0.0401^{\{10\}}$	$0.0298^{\{6\}}$	$0.3091^{\{13\}}$	$6.2450^{\{15\}}$	$0.0474^{\{11\}}$	$0.0285^{\{5\}}$	$0.0478^{\{12\}}$
	MRE $(\hat{\rho})$	$0.0483^{\{2\}}$	$0.0541^{\{4\}}$	$0.0566^{\{7\}}$	$0.0479^{\{1\}}$	$0.0573^{\{8\}}$	$0.8586^{\{14\}}$	$0.0541^{\{5\}}$	$0.0639^{\{9\}}$	$0.0659^{\{10\}}$	$0.0558^{\{6\}}$	$0.1183^{\{13\}}$	$0.9996^{\{15\}}$	$0.0699^{\{11\}}$	$0.0517^{\{3\}}$	$0.0701^{\{12\}}$
	D_{abs}	$0.0156^{\{1\}}$	$0.0174^{\{4\}}$	$0.0183^{\{7\}}$	$0.0156^{\{2\}}$	$0.0185^{\{8\}}$	$0.3480^{\{14\}}$	$0.0175^{\{5\}}$	$0.0205^{\{9\}}$	$0.0213^{\{10\}}$	$0.0182^{\{6\}}$	$0.0334^{\{13\}}$	$0.5007^{\{15\}}$	$0.0226^{\{11\}}$	$0.0168^{\{3\}}$	$0.0226^{\{12\}}$
	D_{max}	$0.0229^{\{1\}}$	$0.0256^{\{4\}}$	$0.0268^{\{7\}}$	$0.0229^{\{2\}}$	$0.0272^{\{8\}}$	$0.5703^{\{14\}}$	$0.0257^{\{5\}}$	$0.0300^{\{9\}}$	$0.0312^{\{10\}}$	$0.0265^{\{6\}}$	$0.0496^{\{13\}}$	$0.9912^{\{15\}}$	$0.0331^{\{11\}}$	$0.0247^{\{3\}}$	$0.0332^{\{12\}}$
	$\sum$Ranks	$8^{\{2\}}$	$20^{\{4\}}$	$35^{\{7\}}$	$7^{\{1\}}$	$40^{\{8\}}$	$70^{\{14\}}$	$23^{\{5\}}$	$45^{\{9\}}$	$50^{\{10\}}$	$30^{\{6\}}$	$65^{\{13\}}$	$75^{\{15\}}$	$55^{\{11\}}$	$17^{\{3\}}$	$60^{\{12\}}$
250	$\lvert Bias\rvert(\hat{\rho})$	$0.1042^{\{2\}}$	$0.1137^{\{4\}}$	$0.1201^{\{6\}}$	$0.1015^{\{1\}}$	$0.1210^{\{7\}}$	$2.1537^{\{14\}}$	$0.1166^{\{5\}}$	$0.1351^{\{10\}}$	$0.1338^{\{9\}}$	$0.1302^{\{8\}}$	$0.3290^{\{13\}}$	$2.4990^{\{15\}}$	$0.1411^{\{11\}}$	$0.1136^{\{3\}}$	$0.1414^{\{12\}}$
	MSE $(\hat{\rho})$	$0.0172^{\{2\}}$	$0.0203^{\{3\}}$	$0.0223^{\{6\}}$	$0.0162^{\{1\}}$	$0.0227^{\{7\}}$	$4.6396^{\{14\}}$	$0.0212^{\{5\}}$	$0.0282^{\{9\}}$	$0.0306^{\{12\}}$	$0.0260^{\{8\}}$	$1.3998^{\{13\}}$	$6.2450^{\{15\}}$	$0.0301^{\{10\}}$	$0.0204^{\{4\}}$	$0.0303^{\{11\}}$
	MRE $(\hat{\rho})$	$0.0417^{\{2\}}$	$0.0455^{\{4\}}$	$0.0480^{\{6\}}$	$0.0406^{\{1\}}$	$0.0484^{\{7\}}$	$0.8615^{\{14\}}$	$0.0466^{\{5\}}$	$0.0540^{\{10\}}$	$0.0535^{\{9\}}$	$0.0521^{\{8\}}$	$0.1316^{\{13\}}$	$0.9996^{\{15\}}$	$0.0564^{\{11\}}$	$0.0454^{\{3\}}$	$0.0566^{\{12\}}$
	D_{abs}	$0.0133^{\{2\}}$	$0.0145^{\{3\}}$	$0.0152^{\{6\}}$	$0.0130^{\{1\}}$	$0.0154^{\{7\}}$	$0.3468^{\{14\}}$	$0.0149^{\{5\}}$	$0.0171^{\{10\}}$	$0.0171^{\{9\}}$	$0.0167^{\{8\}}$	$0.0300^{\{13\}}$	$0.4955^{\{15\}}$	$0.0182^{\{11\}}$	$0.0146^{\{4\}}$	$0.0183^{\{12\}}$
	D_{max}	$0.0196^{\{2\}}$	$0.0213^{\{3\}}$	$0.0225^{\{6\}}$	$0.0192^{\{1\}}$	$0.0227^{\{7\}}$	$0.5746^{\{14\}}$	$0.0219^{\{5\}}$	$0.0252^{\{9\}}$	$0.0253^{\{10\}}$	$0.0246^{\{8\}}$	$0.0450^{\{13\}}$	$0.9929^{\{15\}}$	$0.0268^{\{11\}}$	$0.0214^{\{4\}}$	$0.0269^{\{12\}}$
	$\sum$Ranks	$10^{\{2\}}$	$17^{\{3\}}$	$30^{\{6\}}$	$5^{\{1\}}$	$35^{\{7\}}$	$70^{\{14\}}$	$25^{\{5\}}$	$48^{\{9\}}$	$49^{\{10\}}$	$40^{\{8\}}$	$65^{\{13\}}$	$75^{\{15\}}$	$54^{\{11\}}$	$18^{\{4\}}$	$59^{\{12\}}$
350	$\lvert Bias\rvert(\hat{\rho})$	$0.0875^{\{1\}}$	$0.0964^{\{4\}}$	$0.1015^{\{7\}}$	$0.0888^{\{3\}}$	$0.1016^{\{8\}}$	$2.1563^{\{14\}}$	$0.0984^{\{5\}}$	$0.1087^{\{9\}}$	$0.1200^{\{12\}}$	$0.1015^{\{6\}}$	$0.1667^{\{13\}}$	$2.4990^{\{15\}}$	$0.1178^{\{10\}}$	$0.0875^{\{2\}}$	$0.1180^{\{11\}}$
	MSE $(\hat{\rho})$	$0.0108^{\{1\}}$	$0.0130^{\{4\}}$	$0.0145^{\{6\}}$	$0.0109^{\{2\}}$	$0.0145^{\{7\}}$	$4.6507^{\{14\}}$	$0.0134^{\{5\}}$	$0.0174^{\{9\}}$	$0.0203^{\{12\}}$	$0.0154^{\{8\}}$	$0.0591^{\{13\}}$	$6.2450^{\{15\}}$	$0.0202^{\{10\}}$	$0.0121^{\{3\}}$	$0.0202^{\{11\}}$
	MRE $(\hat{\rho})$	$0.0350^{\{1\}}$	$0.0386^{\{4\}}$	$0.0406^{\{7\}}$	$0.0355^{\{3\}}$	$0.0406^{\{8\}}$	$0.8625^{\{14\}}$	$0.0393^{\{5\}}$	$0.0435^{\{9\}}$	$0.0480^{\{12\}}$	$0.0406^{\{6\}}$	$0.0667^{\{13\}}$	$0.9996^{\{15\}}$	$0.0471^{\{10\}}$	$0.0350^{\{2\}}$	$0.0472^{\{11\}}$
	D_{abs}	$0.0113^{\{1\}}$	$0.0125^{\{4\}}$	$0.0132^{\{7\}}$	$0.0115^{\{3\}}$	$0.0132^{\{8\}}$	$0.3502^{\{14\}}$	$0.0128^{\{5\}}$	$0.0141^{\{9\}}$	$0.0156^{\{12\}}$	$0.0132^{\{6\}}$	$0.0208^{\{13\}}$	$0.5007^{\{15\}}$	$0.0153^{\{10\}}$	$0.0113^{\{2\}}$	$0.0154^{\{11\}}$
	D_{max}	$0.0166^{\{1\}}$	$0.0183^{\{4\}}$	$0.0193^{\{6\}}$	$0.0169^{\{3\}}$	$0.0193^{\{7\}}$	$0.5760^{\{14\}}$	$0.0187^{\{5\}}$	$0.0206^{\{9\}}$	$0.0229^{\{12\}}$	$0.0193^{\{8\}}$	$0.0306^{\{13\}}$	$0.9940^{\{15\}}$	$0.0225^{\{10\}}$	$0.0167^{\{2\}}$	$0.0226^{\{11\}}$
	$\sum$Ranks	$5^{\{1\}}$	$20^{\{4\}}$	$33^{\{6\}}$	$14^{\{3\}}$	$38^{\{8\}}$	$70^{\{14\}}$	$25^{\{5\}}$	$45^{\{9\}}$	$60^{\{12\}}$	$34^{\{7\}}$	$65^{\{13\}}$	$75^{\{15\}}$	$50^{\{10\}}$	$11^{\{2\}}$	$55^{\{11\}}$

Table 6. Partial and overall ranks for all estimation methods of the `Obulezi` distribution from Table 5.

n	Metric	MLE	ADE	CVME	MPSE	OLSE	RTADE	WLSE	LTADE	MSADE	MSALDE	ADSOE	KE	MSSDE	MSSLDE	MSLNDE
15	$\lvert Bias\rvert(\hat{\rho})$	1.0	2.0	6.0	4.0	7.0	14.0	5.0	8.0	10.0	9.0	13.0	15.0	11.0	3.0	12.0
	MSE $(\hat{\rho})$	3.0	4.0	8.0	1.0	7.0	13.0	6.0	9.0	10.0	5.0	15.0	14.0	12.0	2.0	11.0
	MRE $(\hat{\rho})$	1.0	2.0	6.0	4.0	7.0	14.0	5.0	8.0	10.0	9.0	13.0	15.0	11.0	3.0	12.0
	D_{abs}	1.0	2.0	3.0	7.0	6.0	14.0	5.0	8.0	11.0	9.0	12.0	15.0	10.0	4.0	13.0
	D_{max}	1.0	2.0	3.0	7.0	6.0	14.0	5.0	8.0	11.0	9.0	13.0	15.0	10.0	4.0	12.0
	$\sum$Ranks	$7^{\{1\}}$	$12^{\{2\}}$	$26^{\{5\}}$	$23^{\{4\}}$	$33^{\{7\}}$	$69^{\{14\}}$	$26^{\{6\}}$	$41^{\{8\}}$	$52^{\{10\}}$	$41^{\{9\}}$	$66^{\{13\}}$	$74^{\{15\}}$	$54^{\{11\}}$	$16^{\{3\}}$	$60^{\{12\}}$
50	$\lvert Bias\rvert(\hat{\rho})$	1.0	4.0	7.0	2.0	8.0	14.0	6.0	9.0	11.0	5.0	13.0	15.0	10.0	3.0	12.0
	MSE $(\hat{\rho})$	1.0	4.0	7.0	2.0	8.0	14.0	6.0	9.0	11.0	5.0	13.0	15.0	10.0	3.0	12.0
	MRE $(\hat{\rho})$	1.0	4.0	7.0	2.0	8.0	14.0	6.0	9.0	11.0	5.0	13.0	15.0	10.0	3.0	12.0
	D_{abs}	1.0	4.0	6.0	2.0	8.0	14.0	5.0	9.0	11.0	7.0	13.0	15.0	10.0	3.0	12.0
	D_{max}	1.0	4.0	7.0	2.0	8.0	14.0	5.0	9.0	11.0	6.0	13.0	15.0	10.0	3.0	12.0
	$\sum$Ranks	$5^{\{1\}}$	$20^{\{4\}}$	$34^{\{7\}}$	$10^{\{2\}}$	$40^{\{8\}}$	$70^{\{14\}}$	$28^{\{5\}}$	$45^{\{9\}}$	$55^{\{11\}}$	$28^{\{6\}}$	$65^{\{13\}}$	$75^{\{15\}}$	$50^{\{10\}}$	$15^{\{3\}}$	$60^{\{12\}}$
120	$\lvert Bias\rvert(\hat{\rho})$	2.0	4.0	6.0	1.0	5.0	14.0	3.0	9.0	10.0	8.0	13.0	15.0	12.0	7.0	11.0
	MSE $(\hat{\rho})$	2.0	3.0	7.0	1.0	6.0	14.0	4.0	9.0	10.0	8.0	13.0	15.0	12.0	5.0	11.0
	MRE $(\hat{\rho})$	2.0	4.0	6.0	1.0	5.0	14.0	3.0	9.0	10.0	8.0	13.0	15.0	12.0	7.0	11.0
	D_{abs}	2.0	4.0	6.0	1.0	5.0	14.0	3.0	8.0	10.0	9.0	13.0	15.0	12.0	7.0	11.0
	D_{max}	2.0	4.0	6.0	1.0	5.0	14.0	3.0	8.0	10.0	9.0	13.0	15.0	12.0	7.0	11.0
	$\sum$Ranks	$10^{\{2\}}$	$19^{\{4\}}$	$31^{\{6\}}$	$5^{\{1\}}$	$26^{\{5\}}$	$70^{\{14\}}$	$16^{\{3\}}$	$43^{\{9\}}$	$50^{\{10\}}$	$42^{\{8\}}$	$65^{\{13\}}$	$75^{\{15\}}$	$60^{\{12\}}$	$33^{\{7\}}$	$55^{\{11\}}$
180	$\lvert Bias\rvert(\hat{\rho})$	2.0	4.0	7.0	1.0	8.0	14.0	5.0	9.0	11.0	6.0	13.0	15.0	10.0	3.0	12.0
	MSE $(\hat{\rho})$	2.0	4.0	7.0	1.0	8.0	14.0	3.0	9.0	11.0	6.0	13.0	15.0	10.0	5.0	12.0
	MRE $(\hat{\rho})$	2.0	4.0	7.0	1.0	8.0	14.0	5.0	9.0	11.0	6.0	13.0	15.0	10.0	3.0	12.0
	D_{abs}	1.0	4.0	7.0	2.0	8.0	14.0	5.0	9.0	11.0	6.0	13.0	15.0	10.0	3.0	12.0
	D_{max}	1.0	4.0	7.0	2.0	8.0	14.0	5.0	9.0	11.0	6.0	13.0	15.0	10.0	3.0	12.0
	$\sum$Ranks	$8^{\{2\}}$	$20^{\{4\}}$	$35^{\{7\}}$	$7^{\{1\}}$	$40^{\{8\}}$	$70^{\{14\}}$	$23^{\{5\}}$	$45^{\{9\}}$	$55^{\{11\}}$	$30^{\{6\}}$	$65^{\{13\}}$	$75^{\{15\}}$	$50^{\{10\}}$	$17^{\{3\}}$	$60^{\{12\}}$
250	$\lvert Bias\rvert(\hat{\rho})$	2.0	4.0	6.0	1.0	7.0	14.0	5.0	10.0	11.0	8.0	13.0	15.0	9.0	3.0	12.0
	MSE $(\hat{\rho})$	2.0	3.0	6.0	1.0	7.0	14.0	5.0	9.0	10.0	8.0	13.0	15.0	12.0	4.0	11.0
	MRE $(\hat{\rho})$	2.0	4.0	6.0	1.0	7.0	14.0	5.0	10.0	11.0	8.0	13.0	15.0	9.0	3.0	12.0
	D_{abs}	2.0	3.0	6.0	1.0	7.0	14.0	5.0	10.0	11.0	8.0	13.0	15.0	9.0	4.0	12.0
	D_{max}	2.0	3.0	6.0	1.0	7.0	14.0	5.0	9.0	11.0	8.0	13.0	15.0	10.0	4.0	12.0
	$\sum$Ranks	$10^{\{2\}}$	$17^{\{3\}}$	$30^{\{6\}}$	$5^{\{1\}}$	$35^{\{7\}}$	$70^{\{14\}}$	$25^{\{5\}}$	$48^{\{9\}}$	$54^{\{11\}}$	$40^{\{8\}}$	$65^{\{13\}}$	$75^{\{15\}}$	$49^{\{10\}}$	$18^{\{4\}}$	$59^{\{12\}}$
350	$\lvert Bias\rvert(\hat{\rho})$	1.0	4.0	7.0	3.0	8.0	14.0	5.0	9.0	10.0	6.0	13.0	15.0	12.0	2.0	11.0
	MSE $(\hat{\rho})$	1.0	4.0	6.0	2.0	7.0	14.0	5.0	9.0	10.0	8.0	13.0	15.0	12.0	3.0	11.0
	MRE $(\hat{\rho})$	1.0	4.0	7.0	3.0	8.0	14.0	5.0	9.0	10.0	6.0	13.0	15.0	12.0	2.0	11.0
	D_{abs}	1.0	4.0	7.0	3.0	8.0	14.0	5.0	9.0	10.0	6.0	13.0	15.0	12.0	2.0	11.0
	D_{max}	1.0	4.0	6.0	3.0	7.0	14.0	5.0	9.0	10.0	8.0	13.0	15.0	12.0	2.0	11.0
	$\sum$Ranks	$5^{\{1\}}$	$20^{\{4\}}$	$33^{\{6\}}$	$14^{\{3\}}$	$38^{\{8\}}$	$70^{\{14\}}$	$25^{\{5\}}$	$45^{\{9\}}$	$50^{\{10\}}$	$34^{\{7\}}$	$65^{\{13\}}$	$75^{\{15\}}$	$60^{\{12\}}$	$11^{\{2\}}$	$55^{\{11\}}$

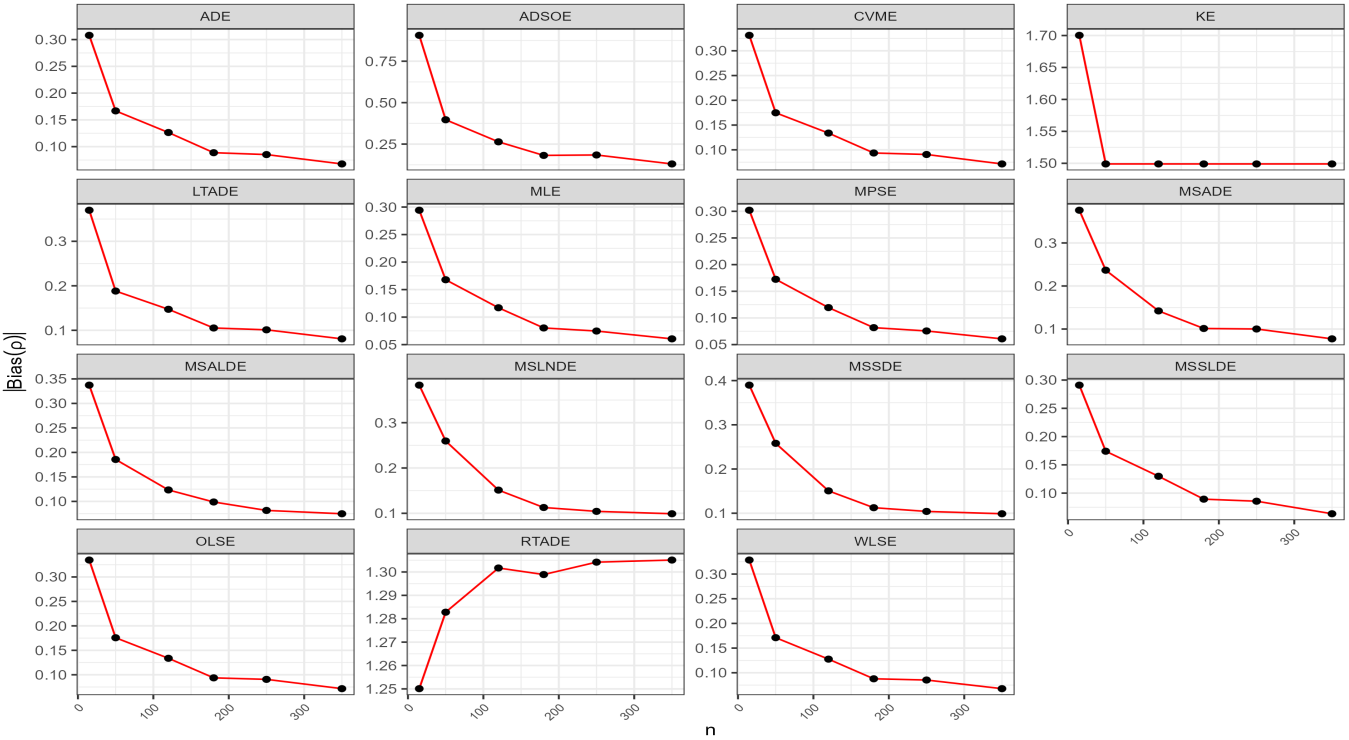

Figure 12. Graphical representations for the Bias values presented in Table 7.

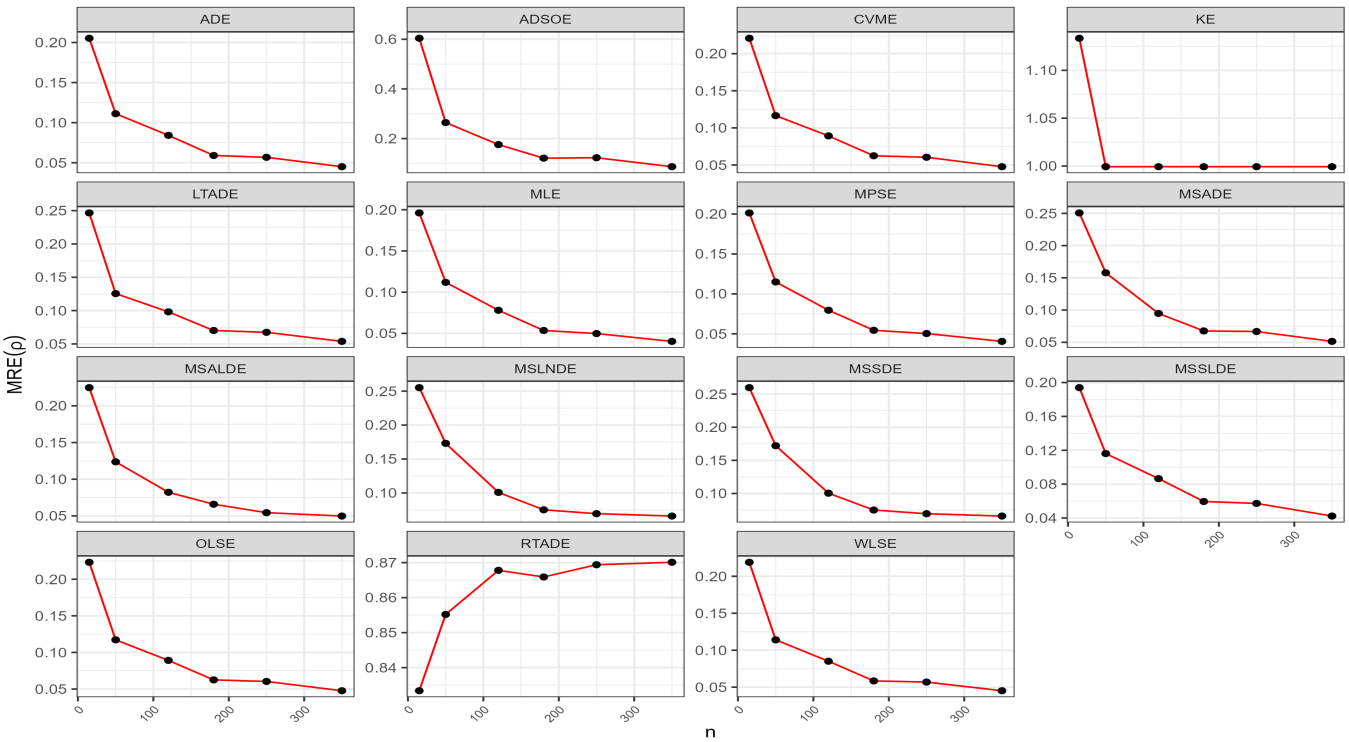

Figure 13. Graphical representations for the MRE values presented in Table 7.

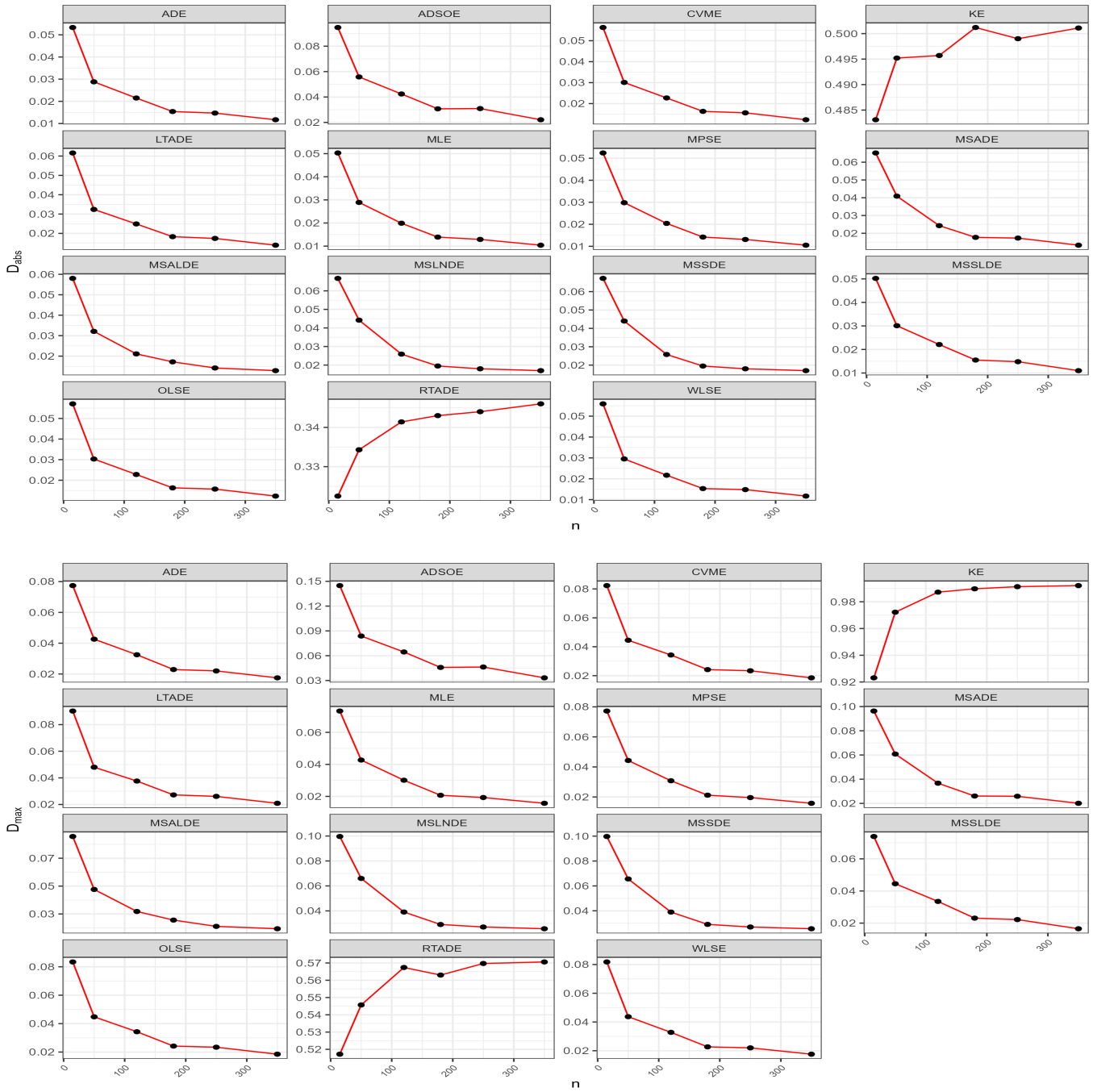

Figure 14. Graphical representations for the D_{abs} and D_{max} values presented in Table 7.

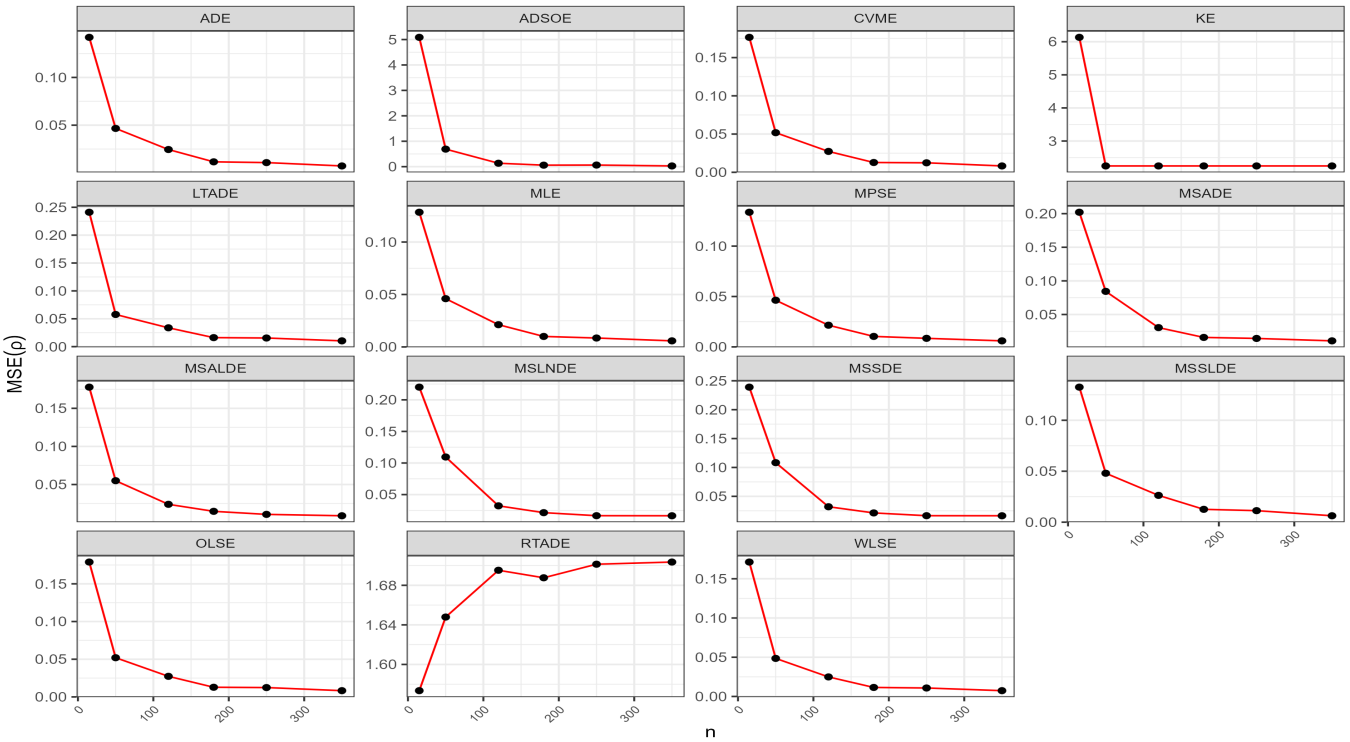

Figure 15. Graphical representations for the MSE values presented in Table 7.

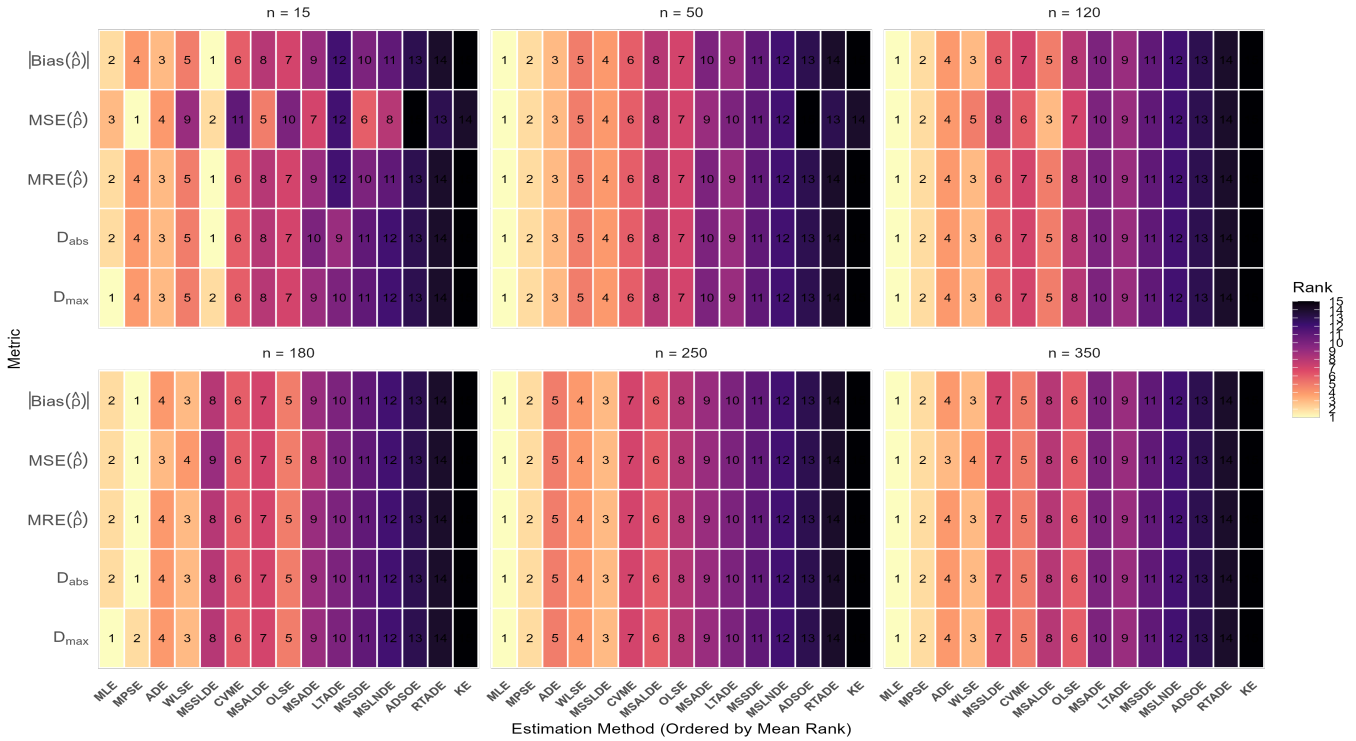

Figure 16. Partial Rank Heatmap for Simulation 7

Table 7. Numerical values of simulation measures for $\rho = 1.50$.

n	Metric	MLE	ADE	CVME	MPSE	OLSE	RTADE	WLSE	LTADE	MSADE	MSALDE	ADSOE	KE	MSSDE	MSSLDE	MSLNDE
15	$\lvert Bias\rvert(\hat{\rho})$	$0.2942^{\{2\}}$	$0.3079^{\{4\}}$	$0.3312^{\{6\}}$	$0.3020^{\{3\}}$	$0.3346^{\{7\}}$	$1.2501^{\{14\}}$	$0.3284^{\{5\}}$	$0.3698^{\{9\}}$	$0.3760^{\{10\}}$	$0.3373^{\{8\}}$	$0.9061^{\{13\}}$	$1.7003^{\{15\}}$	$0.3897^{\{12\}}$	$0.2910^{\{1\}}$	$0.3829^{\{11\}}$
	MSE $(\hat{\rho})$	$0.1284^{\{1\}}$	$0.1420^{\{4\}}$	$0.1765^{\{6\}}$	$0.1336^{\{3\}}$	$0.1789^{\{8\}}$	$1.5735^{\{13\}}$	$0.1713^{\{5\}}$	$0.2411^{\{12\}}$	$0.2021^{\{9\}}$	$0.1778^{\{7\}}$	$5.0869^{\{14\}}$	$6.1332^{\{15\}}$	$0.2390^{\{11\}}$	$0.1325^{\{2\}}$	$0.2201^{\{10\}}$
	MRE $(\hat{\rho})$	$0.1961^{\{2\}}$	$0.2053^{\{4\}}$	$0.2208^{\{6\}}$	$0.2014^{\{3\}}$	$0.2231^{\{7\}}$	$0.8334^{\{14\}}$	$0.2189^{\{5\}}$	$0.2466^{\{9\}}$	$0.2507^{\{10\}}$	$0.2249^{\{8\}}$	$0.6041^{\{13\}}$	$1.1335^{\{15\}}$	$0.2598^{\{12\}}$	$0.1940^{\{1\}}$	$0.2552^{\{11\}}$
	D_{abs}	$0.0503^{\{2\}}$	$0.0533^{\{4\}}$	$0.0563^{\{6\}}$	$0.0524^{\{3\}}$	$0.0571^{\{7\}}$	$0.3225^{\{14\}}$	$0.0559^{\{5\}}$	$0.0616^{\{9\}}$	$0.0652^{\{10\}}$	$0.0580^{\{8\}}$	$0.0947^{\{13\}}$	$0.4831^{\{15\}}$	$0.0672^{\{12\}}$	$0.0502^{\{1\}}$	$0.0667^{\{11\}}$
	D_{max}	$0.0733^{\{1\}}$	$0.0774^{\{4\}}$	$0.0823^{\{6\}}$	$0.0772^{\{3\}}$	$0.0834^{\{7\}}$	$0.5172^{\{14\}}$	$0.0818^{\{5\}}$	$0.0902^{\{9\}}$	$0.0963^{\{10\}}$	$0.0856^{\{8\}}$	$0.1448^{\{13\}}$	$0.9231^{\{15\}}$	$0.0997^{\{12\}}$	$0.0739^{\{2\}}$	$0.0996^{\{11\}}$
	$\sum$Ranks	$8^{\{2\}}$	$20^{\{4\}}$	$30^{\{6\}}$	$15^{\{3\}}$	$36^{\{7\}}$	$69^{\{14\}}$	$25^{\{5\}}$	$48^{\{9\}}$	$49^{\{10\}}$	$39^{\{8\}}$	$66^{\{13\}}$	$75^{\{15\}}$	$59^{\{12\}}$	$7^{\{1\}}$	$54^{\{11\}}$
50	$\lvert Bias\rvert(\hat{\rho})$	$0.1679^{\{2\}}$	$0.1668^{\{1\}}$	$0.1748^{\{6\}}$	$0.1725^{\{4\}}$	$0.1757^{\{7\}}$	$1.2828^{\{14\}}$	$0.1711^{\{3\}}$	$0.1882^{\{9\}}$	$0.2367^{\{10\}}$	$0.1856^{\{8\}}$	$0.3968^{\{13\}}$	$1.4990^{\{15\}}$	$0.2581^{\{11\}}$	$0.1741^{\{5\}}$	$0.2596^{\{12\}}$
	MSE $(\hat{\rho})$	$0.0460^{\{1\}}$	$0.0466^{\{3\}}$	$0.0518^{\{6\}}$	$0.0463^{\{2\}}$	$0.0520^{\{7\}}$	$1.6479^{\{14\}}$	$0.0485^{\{5\}}$	$0.0577^{\{9\}}$	$0.0844^{\{10\}}$	$0.0550^{\{8\}}$	$0.6897^{\{13\}}$	$2.2470^{\{15\}}$	$0.1083^{\{11\}}$	$0.0480^{\{4\}}$	$0.1095^{\{12\}}$
	MRE $(\hat{\rho})$	$0.1119^{\{2\}}$	$0.1112^{\{1\}}$	$0.1165^{\{6\}}$	$0.1150^{\{4\}}$	$0.1172^{\{7\}}$	$0.8552^{\{14\}}$	$0.1140^{\{3\}}$	$0.1255^{\{9\}}$	$0.1578^{\{10\}}$	$0.1237^{\{8\}}$	$0.2645^{\{13\}}$	$0.9993^{\{15\}}$	$0.1721^{\{11\}}$	$0.1161^{\{5\}}$	$0.1731^{\{12\}}$
	D_{abs}	$0.0289^{\{2\}}$	$0.0288^{\{1\}}$	$0.0301^{\{6\}}$	$0.0298^{\{4\}}$	$0.0303^{\{7\}}$	$0.3343^{\{14\}}$	$0.0295^{\{3\}}$	$0.0324^{\{9\}}$	$0.0409^{\{10\}}$	$0.0321^{\{8\}}$	$0.0558^{\{13\}}$	$0.4952^{\{15\}}$	$0.0440^{\{11\}}$	$0.0301^{\{5\}}$	$0.0442^{\{12\}}$
	D_{max}	$0.0427^{\{2\}}$	$0.0426^{\{1\}}$	$0.0445^{\{6\}}$	$0.0443^{\{4\}}$	$0.0448^{\{7\}}$	$0.5457^{\{14\}}$	$0.0437^{\{3\}}$	$0.0480^{\{9\}}$	$0.0608^{\{10\}}$	$0.0476^{\{8\}}$	$0.0838^{\{13\}}$	$0.9722^{\{15\}}$	$0.0656^{\{11\}}$	$0.0445^{\{5\}}$	$0.0660^{\{12\}}$
	$\sum$Ranks	$9^{\{2\}}$	$7^{\{1\}}$	$30^{\{6\}}$	$18^{\{4\}}$	$35^{\{7\}}$	$70^{\{14\}}$	$17^{\{3\}}$	$45^{\{9\}}$	$50^{\{10\}}$	$40^{\{8\}}$	$65^{\{13\}}$	$75^{\{15\}}$	$55^{\{11\}}$	$24^{\{5\}}$	$60^{\{12\}}$
120	$\lvert Bias\rvert(\hat{\rho})$	$0.1170^{\{1\}}$	$0.1264^{\{4\}}$	$0.1338^{\{8\}}$	$0.1194^{\{2\}}$	$0.1337^{\{7\}}$	$1.3017^{\{14\}}$	$0.1276^{\{5\}}$	$0.1472^{\{10\}}$	$0.1421^{\{9\}}$	$0.1234^{\{3\}}$	$0.2636^{\{13\}}$	$1.4990^{\{15\}}$	$0.1506^{\{11\}}$	$0.1298^{\{6\}}$	$0.1512^{\{12\}}$
	MSE $(\hat{\rho})$	$0.0212^{\{1\}}$	$0.0245^{\{4\}}$	$0.0273^{\{8\}}$	$0.0215^{\{2\}}$	$0.0273^{\{7\}}$	$1.6952^{\{14\}}$	$0.0249^{\{5\}}$	$0.0338^{\{12\}}$	$0.0305^{\{9\}}$	$0.0240^{\{3\}}$	$0.1349^{\{13\}}$	$2.2470^{\{15\}}$	$0.0320^{\{10\}}$	$0.0263^{\{6\}}$	$0.0322^{\{11\}}$
	MRE $(\hat{\rho})$	$0.0780^{\{1\}}$	$0.0842^{\{4\}}$	$0.0892^{\{8\}}$	$0.0796^{\{2\}}$	$0.0891^{\{7\}}$	$0.8678^{\{14\}}$	$0.0851^{\{5\}}$	$0.0981^{\{10\}}$	$0.0947^{\{9\}}$	$0.0822^{\{3\}}$	$0.1757^{\{13\}}$	$0.9993^{\{15\}}$	$0.1004^{\{11\}}$	$0.0865^{\{6\}}$	$0.1008^{\{12\}}$
	D_{abs}	$0.0199^{\{1\}}$	$0.0215^{\{4\}}$	$0.0227^{\{7\}}$	$0.0204^{\{2\}}$	$0.0228^{\{8\}}$	$0.3414^{\{14\}}$	$0.0217^{\{5\}}$	$0.0249^{\{10\}}$	$0.0243^{\{9\}}$	$0.0211^{\{3\}}$	$0.0424^{\{13\}}$	$0.4957^{\{15\}}$	$0.0258^{\{11\}}$	$0.0221^{\{6\}}$	$0.0259^{\{12\}}$
	D_{max}	$0.0301^{\{1\}}$	$0.0325^{\{4\}}$	$0.0343^{\{7\}}$	$0.0308^{\{2\}}$	$0.0343^{\{8\}}$	$0.5674^{\{14\}}$	$0.0328^{\{5\}}$	$0.0376^{\{10\}}$	$0.0367^{\{9\}}$	$0.0318^{\{3\}}$	$0.0645^{\{13\}}$	$0.9872^{\{15\}}$	$0.0390^{\{11\}}$	$0.0335^{\{6\}}$	$0.0391^{\{12\}}$
	$\sum$Ranks	$5^{\{1\}}$	$20^{\{4\}}$	$38^{\{8\}}$	$10^{\{2\}}$	$37^{\{7\}}$	$70^{\{14\}}$	$25^{\{5\}}$	$52^{\{10\}}$	$45^{\{9\}}$	$15^{\{3\}}$	$65^{\{13\}}$	$75^{\{15\}}$	$54^{\{11\}}$	$30^{\{6\}}$	$59^{\{12\}}$
180	$\lvert Bias\rvert(\hat{\rho})$	$0.0803^{\{1\}}$	$0.0887^{\{4\}}$	$0.0936^{\{6\}}$	$0.0818^{\{2\}}$	$0.0937^{\{7\}}$	$1.2989^{\{14\}}$	$0.0878^{\{3\}}$	$0.1052^{\{10\}}$	$0.1013^{\{9\}}$	$0.0988^{\{8\}}$	$0.1817^{\{13\}}$	$1.4990^{\{15\}}$	$0.1125^{\{11\}}$	$0.0893^{\{5\}}$	$0.1128^{\{12\}}$
	MSE $(\hat{\rho})$	$0.0100^{\{1\}}$	$0.0116^{\{4\}}$	$0.0128^{\{6\}}$	$0.0104^{\{2\}}$	$0.0128^{\{7\}}$	$1.6876^{\{14\}}$	$0.0115^{\{3\}}$	$0.0162^{\{10\}}$	$0.0159^{\{9\}}$	$0.0148^{\{8\}}$	$0.0590^{\{13\}}$	$2.2470^{\{15\}}$	$0.0213^{\{11\}}$	$0.0126^{\{5\}}$	$0.0214^{\{12\}}$
	MRE $(\hat{\rho})$	$0.0535^{\{1\}}$	$0.0591^{\{4\}}$	$0.0624^{\{6\}}$	$0.0545^{\{2\}}$	$0.0625^{\{7\}}$	$0.8659^{\{14\}}$	$0.0585^{\{3\}}$	$0.0701^{\{10\}}$	$0.0676^{\{9\}}$	$0.0659^{\{8\}}$	$0.1211^{\{13\}}$	$0.9993^{\{15\}}$	$0.0750^{\{11\}}$	$0.0595^{\{5\}}$	$0.0752^{\{12\}}$
	D_{abs}	$0.0139^{\{1\}}$	$0.0154^{\{4\}}$	$0.0163^{\{6\}}$	$0.0142^{\{2\}}$	$0.0163^{\{7\}}$	$0.3430^{\{14\}}$	$0.0153^{\{3\}}$	$0.0183^{\{10\}}$	$0.0177^{\{9\}}$	$0.0172^{\{8\}}$	$0.0307^{\{13\}}$	$0.5012^{\{15\}}$	$0.0195^{\{11\}}$	$0.0155^{\{5\}}$	$0.0195^{\{12\}}$
	D_{max}	$0.0207^{\{1\}}$	$0.0229^{\{4\}}$	$0.0242^{\{6\}}$	$0.0212^{\{2\}}$	$0.0242^{\{7\}}$	$0.5630^{\{14\}}$	$0.0227^{\{3\}}$	$0.0272^{\{10\}}$	$0.0261^{\{9\}}$	$0.0256^{\{8\}}$	$0.0458^{\{13\}}$	$0.9897^{\{15\}}$	$0.0291^{\{11\}}$	$0.0231^{\{5\}}$	$0.0291^{\{12\}}$
	$\sum$Ranks	$5^{\{1\}}$	$20^{\{4\}}$	$30^{\{6\}}$	$10^{\{2\}}$	$35^{\{7\}}$	$70^{\{14\}}$	$15^{\{3\}}$	$50^{\{10\}}$	$45^{\{9\}}$	$40^{\{8\}}$	$65^{\{13\}}$	$75^{\{15\}}$	$55^{\{11\}}$	$25^{\{5\}}$	$60^{\{12\}}$
250	$\lvert Bias\rvert(\hat{\rho})$	$0.0747^{\{1\}}$	$0.0852^{\{4\}}$	$0.0906^{\{7\}}$	$0.0756^{\{2\}}$	$0.0906^{\{8\}}$	$1.3042^{\{14\}}$	$0.0853^{\{5\}}$	$0.1011^{\{10\}}$	$0.1001^{\{9\}}$	$0.0816^{\{3\}}$	$0.1843^{\{13\}}$	$1.4990^{\{15\}}$	$0.1041^{\{11\}}$	$0.0857^{\{6\}}$	$0.1043^{\{12\}}$
	MSE $(\hat{\rho})$	$0.0085^{\{1\}}$	$0.0108^{\{5\}}$	$0.0124^{\{8\}}$	$0.0085^{\{2\}}$	$0.0124^{\{7\}}$	$1.7013^{\{14\}}$	$0.0108^{\{4\}}$	$0.0155^{\{10\}}$	$0.0144^{\{9\}}$	$0.0108^{\{3\}}$	$0.0634^{\{13\}}$	$2.2470^{\{15\}}$	$0.0165^{\{11\}}$	$0.0113^{\{6\}}$	$0.0166^{\{12\}}$
	MRE $(\hat{\rho})$	$0.0498^{\{1\}}$	$0.0568^{\{4\}}$	$0.0604^{\{7\}}$	$0.0504^{\{2\}}$	$0.0604^{\{8\}}$	$0.8694^{\{14\}}$	$0.0569^{\{5\}}$	$0.0674^{\{10\}}$	$0.0667^{\{9\}}$	$0.0544^{\{3\}}$	$0.1229^{\{13\}}$	$0.9993^{\{15\}}$	$0.0694^{\{11\}}$	$0.0572^{\{6\}}$	$0.0695^{\{12\}}$
	D_{abs}	$0.0129^{\{1\}}$	$0.0147^{\{4\}}$	$0.0156^{\{7\}}$	$0.0131^{\{2\}}$	$0.0157^{\{8\}}$	$0.3440^{\{14\}}$	$0.0148^{\{5\}}$	$0.0174^{\{10\}}$	$0.0173^{\{9\}}$	$0.0142^{\{3\}}$	$0.0309^{\{13\}}$	$0.4990^{\{15\}}$	$0.0180^{\{11\}}$	$0.0148^{\{6\}}$	$0.0180^{\{12\}}$
	D_{max}	$0.0193^{\{1\}}$	$0.0220^{\{4\}}$	$0.0234^{\{7\}}$	$0.0196^{\{2\}}$	$0.0234^{\{8\}}$	$0.5697^{\{14\}}$	$0.0220^{\{5\}}$	$0.0261^{\{10\}}$	$0.0259^{\{9\}}$	$0.0211^{\{3\}}$	$0.0463^{\{13\}}$	$0.9913^{\{15\}}$	$0.0270^{\{11\}}$	$0.0222^{\{6\}}$	$0.0271^{\{12\}}$
	$\sum$Ranks	$5^{\{1\}}$	$21^{\{4\}}$	$36^{\{7\}}$	$10^{\{2\}}$	$39^{\{8\}}$	$70^{\{14\}}$	$24^{\{5\}}$	$50^{\{10\}}$	$45^{\{9\}}$	$15^{\{3\}}$	$65^{\{13\}}$	$75^{\{15\}}$	$55^{\{11\}}$	$30^{\{6\}}$	$60^{\{12\}}$
350	$\lvert Bias\rvert(\hat{\rho})$	$0.0605^{\{1\}}$	$0.0677^{\{4\}}$	$0.0715^{\{6\}}$	$0.0608^{\{2\}}$	$0.0716^{\{7\}}$	$1.3051^{\{14\}}$	$0.0678^{\{5\}}$	$0.0808^{\{10\}}$	$0.0772^{\{9\}}$	$0.0748^{\{8\}}$	$0.1302^{\{13\}}$	$1.4990^{\{15\}}$	$0.0988^{\{11\}}$	$0.0635^{\{3\}}$	$0.0990^{\{12\}}$
	MSE $(\hat{\rho})$	$0.0058^{\{1\}}$	$0.0073^{\{4\}}$	$0.0083^{\{6\}}$	$0.0060^{\{2\}}$	$0.0083^{\{7\}}$	$1.7035^{\{14\}}$	$0.0074^{\{5\}}$	$0.0104^{\{9\}}$	$0.0108^{\{10\}}$	$0.0090^{\{8\}}$	$0.0284^{\{13\}}$	$2.2470^{\{15\}}$	$0.0164^{\{11\}}$	$0.0063^{\{3\}}$	$0.0165^{\{12\}}$
	MRE $(\hat{\rho})$	$0.0403^{\{1\}}$	$0.0451^{\{4\}}$	$0.0477^{\{6\}}$	$0.0406^{\{2\}}$	$0.0477^{\{7\}}$	$0.8701^{\{14\}}$	$0.0452^{\{5\}}$	$0.0538^{\{10\}}$	$0.0514^{\{9\}}$	$0.0498^{\{8\}}$	$0.0868^{\{13\}}$	$0.9993^{\{15\}}$	$0.0659^{\{11\}}$	$0.0423^{\{3\}}$	$0.0660^{\{12\}}$
	D_{abs}	$0.0104^{\{1\}}$	$0.0117^{\{4\}}$	$0.0123^{\{6\}}$	$0.0105^{\{2\}}$	$0.0123^{\{7\}}$	$0.3460^{\{14\}}$	$0.0117^{\{5\}}$	$0.0139^{\{10\}}$	$0.0133^{\{9\}}$	$0.0129^{\{8\}}$	$0.0221^{\{13\}}$	$0.5011^{\{15\}}$	$0.0170^{\{11\}}$	$0.0110^{\{3\}}$	$0.0170^{\{12\}}$
	D_{max}	$0.0157^{\{1\}}$	$0.0175^{\{4\}}$	$0.0185^{\{6\}}$	$0.0158^{\{2\}}$	$0.0185^{\{7\}}$	$0.5706^{\{14\}}$	$0.0176^{\{5\}}$	$0.0209^{\{10\}}$	$0.0201^{\{9\}}$	$0.0194^{\{8\}}$	$0.0332^{\{13\}}$	$0.9921^{\{15\}}$	$0.0256^{\{11\}}$	$0.0165^{\{3\}}$	$0.0257^{\{12\}}$
	$\sum$Ranks	$5^{\{1\}}$	$20^{\{4\}}$	$30^{\{6\}}$	$10^{\{2\}}$	$35^{\{7\}}$	$70^{\{14\}}$	$25^{\{5\}}$	$49^{\{10\}}$	$46^{\{9\}}$	$40^{\{8\}}$	$65^{\{13\}}$	$75^{\{15\}}$	$55^{\{11\}}$	$15^{\{3\}}$	$60^{\{12\}}$

Table 8. Partial and overall ranks for all estimation methods of the `Obulezi` distribution from Table 7.

n	Metric	MLE	ADE	CVME	MPSE	OLSE	RTADE	WLSE	LTADE	MSADE	MSALDE	ADSOE	KE	MSSDE	MSSLDE	MSLNDE
15	$\|Bias\|(\hat{\rho})$	2.0	4.0	6.0	3.0	7.0	14.0	5.0	9.0	10.0	8.0	13.0	15.0	12.0	1.0	11.0
	MSE $(\hat{\rho})$	1.0	4.0	6.0	3.0	8.0	13.0	5.0	12.0	9.0	7.0	14.0	15.0	11.0	2.0	10.0
	MRE $(\hat{\rho})$	2.0	4.0	6.0	3.0	7.0	14.0	5.0	9.0	10.0	8.0	13.0	15.0	12.0	1.0	11.0
	D_{abs}	2.0	4.0	6.0	3.0	7.0	14.0	5.0	9.0	10.0	8.0	13.0	15.0	12.0	1.0	11.0
	D_{max}	1.0	4.0	6.0	3.0	7.0	14.0	5.0	9.0	10.0	8.0	13.0	15.0	12.0	2.0	11.0
	$\sum$Ranks	$8^{\{2\}}$	$20^{\{4\}}$	$30^{\{6\}}$	$15^{\{3\}}$	$36^{\{7\}}$	$69^{\{14\}}$	$25^{\{5\}}$	$48^{\{9\}}$	$49^{\{10\}}$	$39^{\{8\}}$	$66^{\{13\}}$	$75^{\{15\}}$	$59^{\{12\}}$	$7^{\{1\}}$	$54^{\{11\}}$
50	$\|Bias\|(\hat{\rho})$	2.0	1.0	6.0	4.0	7.0	14.0	3.0	9.0	10.0	8.0	13.0	15.0	11.0	5.0	12.0
	MSE $(\hat{\rho})$	1.0	3.0	6.0	2.0	7.0	14.0	5.0	9.0	10.0	8.0	13.0	15.0	11.0	4.0	12.0
	MRE $(\hat{\rho})$	2.0	1.0	6.0	4.0	7.0	14.0	3.0	9.0	10.0	8.0	13.0	15.0	11.0	5.0	12.0
	D_{abs}	2.0	1.0	6.0	4.0	7.0	14.0	3.0	9.0	10.0	8.0	13.0	15.0	11.0	5.0	12.0
	D_{max}	2.0	1.0	6.0	4.0	7.0	14.0	3.0	9.0	10.0	8.0	13.0	15.0	11.0	5.0	12.0
	$\sum$Ranks	$9^{\{2\}}$	$7^{\{1\}}$	$30^{\{6\}}$	$18^{\{4\}}$	$35^{\{7\}}$	$70^{\{14\}}$	$17^{\{3\}}$	$45^{\{9\}}$	$50^{\{10\}}$	$40^{\{8\}}$	$65^{\{13\}}$	$75^{\{15\}}$	$55^{\{11\}}$	$24^{\{5\}}$	$60^{\{12\}}$
120	$\|Bias\|(\hat{\rho})$	1.0	4.0	8.0	2.0	7.0	14.0	5.0	10.0	9.0	3.0	13.0	15.0	11.0	6.0	12.0
	MSE $(\hat{\rho})$	1.0	4.0	8.0	2.0	7.0	14.0	5.0	12.0	9.0	3.0	13.0	15.0	10.0	6.0	11.0
	MRE $(\hat{\rho})$	1.0	4.0	8.0	2.0	7.0	14.0	5.0	10.0	9.0	3.0	13.0	15.0	11.0	6.0	12.0
	D_{abs}	1.0	4.0	7.0	2.0	8.0	14.0	5.0	10.0	9.0	3.0	13.0	15.0	11.0	6.0	12.0
	D_{max}	1.0	4.0	7.0	2.0	8.0	14.0	5.0	10.0	9.0	3.0	13.0	15.0	11.0	6.0	12.0
	$\sum$Ranks	$5^{\{1\}}$	$20^{\{4\}}$	$38^{\{8\}}$	$10^{\{2\}}$	$37^{\{7\}}$	$70^{\{14\}}$	$25^{\{5\}}$	$52^{\{10\}}$	$45^{\{9\}}$	$15^{\{3\}}$	$65^{\{13\}}$	$75^{\{15\}}$	$54^{\{11\}}$	$30^{\{6\}}$	$59^{\{12\}}$
180	$\|Bias\|(\hat{\rho})$	1.0	4.0	6.0	2.0	7.0	14.0	3.0	10.0	9.0	8.0	13.0	15.0	11.0	5.0	12.0
	MSE $(\hat{\rho})$	1.0	4.0	6.0	2.0	7.0	14.0	3.0	10.0	9.0	8.0	13.0	15.0	11.0	5.0	12.0
	MRE $(\hat{\rho})$	1.0	4.0	6.0	2.0	7.0	14.0	3.0	10.0	9.0	8.0	13.0	15.0	11.0	5.0	12.0
	D_{abs}	1.0	4.0	6.0	2.0	7.0	14.0	3.0	10.0	9.0	8.0	13.0	15.0	11.0	5.0	12.0
	D_{max}	1.0	4.0	6.0	2.0	7.0	14.0	3.0	10.0	9.0	8.0	13.0	15.0	11.0	5.0	12.0
	$\sum$Ranks	$5^{\{1\}}$	$20^{\{4\}}$	$30^{\{6\}}$	$10^{\{2\}}$	$35^{\{7\}}$	$70^{\{14\}}$	$15^{\{3\}}$	$50^{\{10\}}$	$45^{\{9\}}$	$40^{\{8\}}$	$65^{\{13\}}$	$75^{\{15\}}$	$55^{\{11\}}$	$25^{\{5\}}$	$60^{\{12\}}$
250	$\|Bias\|(\hat{\rho})$	1.0	4.0	7.0	2.0	8.0	14.0	5.0	10.0	9.0	3.0	13.0	15.0	11.0	6.0	12.0
	MSE $(\hat{\rho})$	1.0	5.0	8.0	2.0	7.0	14.0	4.0	10.0	9.0	3.0	13.0	15.0	11.0	6.0	12.0
	MRE $(\hat{\rho})$	1.0	4.0	7.0	2.0	8.0	14.0	5.0	10.0	9.0	3.0	13.0	15.0	11.0	6.0	12.0
	D_{abs}	1.0	4.0	7.0	2.0	8.0	14.0	5.0	10.0	9.0	3.0	13.0	15.0	11.0	6.0	12.0
	D_{max}	1.0	4.0	7.0	2.0	8.0	14.0	5.0	10.0	9.0	3.0	13.0	15.0	11.0	6.0	12.0
	$\sum$Ranks	$5^{\{1\}}$	$21^{\{4\}}$	$36^{\{7\}}$	$10^{\{2\}}$	$39^{\{8\}}$	$70^{\{14\}}$	$24^{\{5\}}$	$50^{\{10\}}$	$45^{\{9\}}$	$15^{\{3\}}$	$65^{\{13\}}$	$75^{\{15\}}$	$55^{\{11\}}$	$30^{\{6\}}$	$60^{\{12\}}$
350	$\|Bias\|(\hat{\rho})$	1.0	4.0	6.0	2.0	7.0	14.0	5.0	10.0	9.0	8.0	13.0	15.0	11.0	3.0	12.0
	MSE $(\hat{\rho})$	1.0	4.0	6.0	2.0	7.0	14.0	5.0	9.0	10.0	8.0	13.0	15.0	11.0	3.0	12.0
	MRE $(\hat{\rho})$	1.0	4.0	6.0	2.0	7.0	14.0	5.0	10.0	9.0	8.0	13.0	15.0	11.0	3.0	12.0
	D_{abs}	1.0	4.0	6.0	2.0	7.0	14.0	5.0	10.0	9.0	8.0	13.0	15.0	11.0	3.0	12.0
	D_{max}	1.0	4.0	6.0	2.0	7.0	14.0	5.0	10.0	9.0	8.0	13.0	15.0	11.0	3.0	12.0
	$\sum$Ranks	$5^{\{1\}}$	$20^{\{4\}}$	$30^{\{6\}}$	$10^{\{2\}}$	$35^{\{7\}}$	$70^{\{14\}}$	$25^{\{5\}}$	$49^{\{10\}}$	$46^{\{9\}}$	$40^{\{8\}}$	$65^{\{13\}}$	$75^{\{15\}}$	$55^{\{11\}}$	$15^{\{3\}}$	$60^{\{12\}}$

The plot, Figure 16, is a partial rank heatmap comparing fifteen estimation methods across five metrics for the Obulezi distribution at six different sample sizes (n) for simulation case 7. Lighter colors (yellow/peach) represent Rank 1 (best performance), while darker colors (purple/black) represent the worst rank. The D_{abs} and D_{max} goodness-of-fit metrics show consistent high ranks (light colors) for a few methods, notably OLSE, WLSE, and LTADE, across all sample sizes.

For the parameter $\rho = 1.50$ of the `Obulezi` distribution in Tables 7 and 8, the MLE and the MPSE demonstrate the best overall performance, especially at larger sample sizes. The MLE achieves the overall first rank for $n = 120, 180, 250$, and 350, while the MPSE is its most frequent and consistent challenger, securing the second overall rank in those same four cases. For the smallest sample size ($n = 15$), the MSSLDE is the top performer, followed by the MLE. For $n = 50$, the ADE edges out the MLE for the first rank. Across all sample sizes, these handful of top methods consistently yield the lowest values for all metrics, including Mean Squared Error (MSE) and bias measures.

A positive general trend is observed across all estimation methods: the numerical values for all bias and error measures systematically decrease as the sample size increases from $n = 15$ to $n = 350$. This confirms the consistency of all estimators, showing that they become more accurate and precise with more data. At the other end of the spectrum, the RTADE and the KE consistently perform the worst, yielding the highest numerical values and occupying the last two positions in the overall rankings across every sample size. The plots in Figures 12, 13, 15 and 14 align perfectly with the results in Tables 7 and 8.

6. Applications

In this section, `Obulezi` distribution is deployed in three lifetime data scenarios in an attempt to demonstrate its competitive advantage in modeling lifetime events. Data I represents the time to failure of 18 electronic devices studied by [39]. It is presented in Table 9.

Table 9. Data I

5	11	21	31	46	75	98	122	145
165	195	224	245	293	321	330	350	420

Table 10 contains Data II, which is the failure times (in weeks) of 50 components, first studied by [16]

Table 10. Data II

0.013	0.065	0.111	0.111	0.163	0.309	0.426	0.535	0.684	0.747
0.997	1.284	1.304	1.647	1.829	2.336	2.838	3.269	3.977	3.981
4.520	4.789	4.849	5.202	5.291	5.349	5.911	6.018	6.427	6.456
6.572	7.023	7.087	7.291	7.787	8.596	9.388	10.261	10.713	11.658
13.006	13.388	13.842	17.152	17.283	19.418	23.471	24.777	32.795	48.105

Data III represents the intervals between failures (in hours) of the air conditioning system of a fleet of 13 Boeing 720 jet airplanes. This data has been studied by [4] and it is reported in Table 11.

Table 11. Data III

1	4	11	16	18	18	18	24	31	39	46	51	54	63
68	77	80	82	97	106	111	141	142	163	191	206	216	

Table 12. Summary Statistics

Measures	Data I	Data II	Data III
n	18	50	27
Q_1	53.25	1.38975	21
Q_3	281	10.04275	108.5
IQR	227.75	8.653	87.5
Outlier	-	23.471, 24.777 32.795, 48.105	-
Mean	172.0556	7.82102	76.81481
Median	155	5.32	63
Standard Deviation	131.5265	9.2063	63.71272
Variance	17299.23	84.75597	4059.311
Range	405	48.092	215
Skewness	0.3157486	2.306048	0.802352
Kurtosis	1.850757	9.408282	2.573307

Based on the summary statistics in Table 12, Data II has the largest sample size ($n = 50$), followed by Data III ($n = 27$), with Data I ($n = 18$) being the smallest. Across all datasets, the Mean is greater than the Median and the Skewness is positive (ranging from 0.32 to 2.31), indicating that all distributions are right-skewed. Data II exhibits the most extreme characteristics, showing the strongest skewness (2.306) and the highest kurtosis (9.408), suggesting it is the most peaked and has the longest right tail, which is further supported by the presence of four outliers. In contrast, Data I is the least skewed (0.316) and is the only dataset that is platykurtic (less peaked, 1.851). Regarding variability, Data I is the most spread out, possessing the largest standard deviation (131.53), while Data II shows the least variability (Standard Deviation: 9.21), despite containing the most outliers.

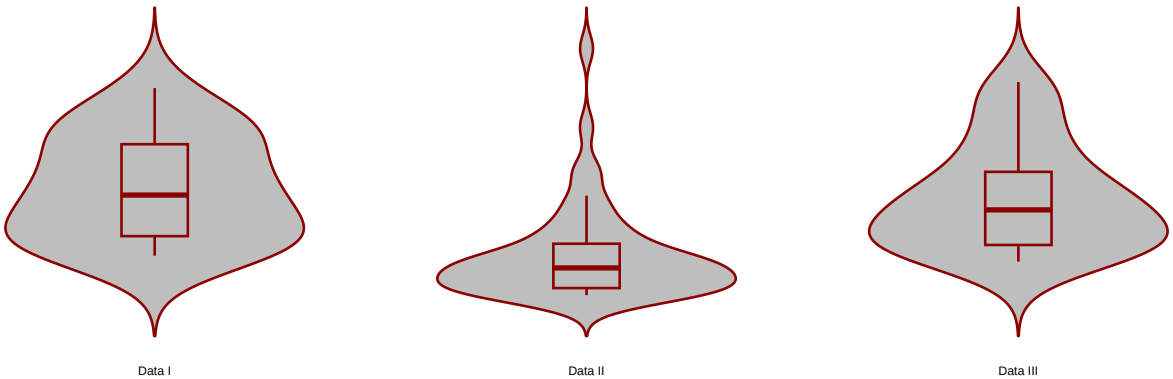

Figure 17. Boxplot superimposed on Violin plot

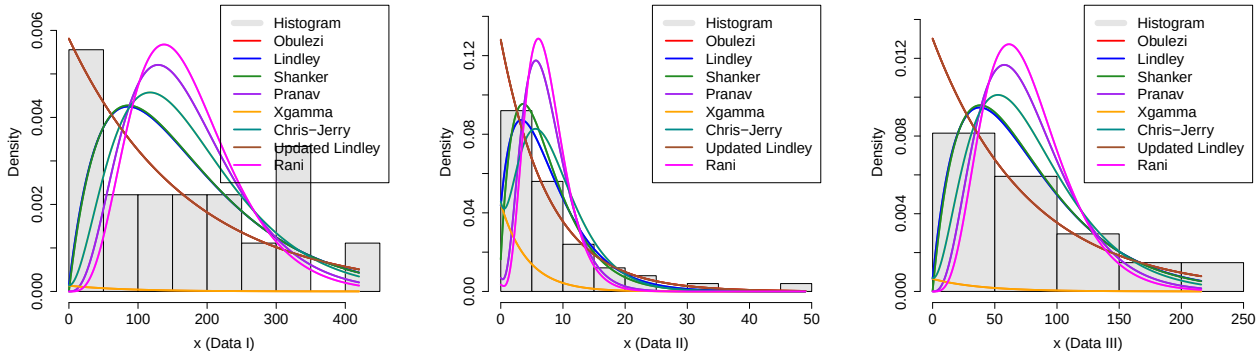

Figure 18. Density superimposed on Histogram

Figures 17 reveal essentially that there is no datapoint in Data I and Data III that constitutes an extreme value. However, the Data III is positively skewed from the histogram shape in Figure 18 with four outliers.

The proposed `Obulezi` distribution is compared to other well-known one-parameter distributions namely, Lindley [9], Shanker [19], Pranav [8], xgamma [17] and Chris-Jerry [13] distributions.

Table 13. Measures of fitness and model performance

Data	Model	LL	AIC	CAIC	BIC	HQIC	W	A	KS	p-value
Data I	`Obulezi`	-110.66	223.3214	223.5714	224.2118	223.4442	0.0596	0.3970	0.1249	0.9090
	Lindley	-112.70	227.3903	227.6403	228.2806	227.5130	0.0579	0.3884	0.1743	0.5855
	Shanker	-112.93	227.8534	228.1034	252.4220	227.9762	0.0591	0.3940	0.1768	0.5674
	Pranav	-124.77	251.5316	251.7816	396.0415	251.6544	0.0589	0.3929	0.2542	0.1635
	xgamma	-196.58	395.1511	395.4011	236.0435	395.2739	0.0540	0.3796	0.2761	0.1052
	Chris-Jerry	-116.58	235.1532	235.4032	224.2118	235.2759	0.0552	0.3829	0.2289	0.2601
	Updated Lindley	-110.66	223.3214	223.5714	266.7010	223.4442	0.0596	0.3970	0.1251	0.9083
	Rani	-131.91	265.8106	266.0606	309.5947	265.9334	0.0588	0.3928	0.2659	0.1299
Data II	`Obulezi`	-152.84	307.6827	307.7661	309.5947	308.4108	0.0658	0.3295	0.1089	0.5933
	Lindley	-161.28	324.5580	324.6413	326.4700	325.2861	0.0430	0.2431	0.1806	0.0767
	Shanker	-168.00	-168.00	338.0077	338.0910	339.9197	338.7358	0.0047	0.2652	0.0378
	Pranav	-200.27	402.5387	402.6220	404.4507	403.2668	0.0570	0.4351	0.2750	0.0010
	xgamma	-264.94	495.8862	495.9695	497.7982	496.6143	0.0522	0.3135	0.3270	4.539×10^{-5}
	Chris-Jerry	-166.39	334.7810	334.8643	336.6930	335.5091	0.0485	0.3192	0.2172	0.0179
	Updated Lindley	-152.83	307.6628	307.7462	309.5749	308.3910	0.0659	0.3299	0.1087	0.5956
	Rani	-219.52	441.0358	441.1191	442.9478	441.7639	0.0720	0.5579	0.2951	0.0003
Data III	`Obulezi`	-144.22	290.4355	290.5955	291.7313	290.8208	0.0248	0.1988	0.0801	0.9951
	Lindley	-146.53	295.0621	295.2221	296.3579	295.4474	0.0234	0.1851	0.1728	0.3956
	Shanker	-147.33	296.6522	296.8122	297.9481	297.0376	0.0245	0.1959	0.1782	0.3580
	Pranav	-164.53	331.0565	331.2165	332.3523	331.4418	0.0244	0.1947	0.2580	0.0550
	xgamma	-251.69	505.3899	505.5499	506.6858	505.7753	0.0269	0.2109	0.3031	0.0140
	Chris-Jerry	-150.65	303.3020	303.4620	304.5979	303.6874	0.0258	0.2006	0.2227	0.1375
	Updated Lindley	-144.22	290.4355	290.5955	291.7313	290.8208	0.0248	0.1988	0.0803	0.9950
	Rani	-174.96	351.9206	352.0806	353.2165	352.3060	0.0243	0.1944	0.2790	0.0299

Based on the goodness-of-fit and model performance measures—where in Table 13, a lower value is desirable for LL (highest absolute value), AIC, CAIC, BIC, HQIC, W, A, and KS statistic, and a higher

value is desirable for the p-value—the `Obulezi` and Updated Lindley models consistently emerge as the best performers across all three datasets (Data I, Data II, and Data III), often having identical or nearly identical metrics, with the Updated Lindley model specifically having a very slight edge in the KS p-value for Data II and Data III. For instance, in Data I, both models share the highest LL (−110.66) and lowest information criteria (e.g., AIC 223.3214) and W (0.0596) and A (0.3970), with the Updated Lindley model having the highest p-value (0.9083) compared to `Obulezi`'s (0.9090). Conversely, the xgamma model is unequivocally the worst performer across all three datasets, consistently yielding the lowest LL (highest absolute value), highest information criteria, and worst goodness-of-fit statistics (highest W, A, and KS statistic) coupled with the lowest and most significant p-values, such as the extremely low p-value of 4.539×10^{-5} for Data II, indicating a very poor fit.

Table 14. Parameter Estimation for the Datasets

Data	Method	MLE	ADE	CVME	OLSE	MPSE	RTADE	WLSE	LTADE	MSADE	MSALDE	ADSOE	KE	MSSDE	MSSLDE	MSLNDE
Data I	Obulezi	0.0058 (0.0014)	0.0052 (0.0017)	0.0050 (0.0019)	0.0049 (0.0018)	0.0055 (0.0015)	0.0013 (0.0005)	0.0052 (0.0018)	0.0051 (0.0022)	0.0058 (0.0020)	0.0056 (0.0017)	0.0058 (0.0074)	0.0054 (0.0019)	0.0057 (0.0022)	0.0051 (0.0016)	0.0057 (0.0021)
	Lindley	0.0116 (0.0019)	0.0114 (0.0020)	0.0108 (0.0021)	0.0106 (0.0021)	0.0111 (0.0019)	0.0030 (0.0012)	0.0107 (0.0021)	0.0140 (0.0023)	0.0105 (0.0025)	0.0111 (0.0022)	0.0322 (0.0082)	0.0125 (0.0021)	0.0098 (0.0027)	0.0123 (0.0022)	0.0098 (0.0027)
	Shanker	0.0116 (0.0019)	0.0115 (0.0022)	0.0108 (0.0023)	0.0107 (0.0023)	0.0112 (0.0020)	0.0030 (0.0012)	0.0107 (0.0023)	0.0142 (0.0026)	0.0105 (0.0027)	0.0111 (0.0022)	0.0363 (0.0072)	0.0126 (0.0024)	0.0098 (0.0030)	0.0125 (0.0022)	0.0098 (0.0030)
	Pranav	0.0232 (0.0027)	0.0235 (0.0029)	0.0222 (0.0031)	0.0220 (0.0031)	0.0226 (0.0028)	0.0065 (0.0025)	0.0212 (0.0030)	0.0494 (0.0034)	0.0183 (0.0038)	0.0197 (0.0031)	0.0755 (0.0084)	0.0269 (0.0031)	0.0175 (0.0040)	0.0277 (0.0030)	0.0175 (0.0041)
	Xgamma	0.0116 (0.0019)	0.0171 (0.0017)	0.0164 (0.0019)	0.0162 (0.0019)	0.0161 (0.0016)	0.0048 (0.0012)	0.0158 (0.0018)	0.0246 (0.0020)	0.0131 (0.0021)	0.0148 (0.0018)	0.0594 (0.0050)	0.0196 (0.0019)	0.0137 (0.0023)	0.0181 (0.0017)	0.0137 (0.0023)
	Chris-Jerry	0.0170 (0.0024)	0.0173 (0.0026)	0.0165 (0.0027)	0.0163 (0.0027)	0.0163 (0.0024)	0.0048 (0.0019)	0.0159 (0.0027)	0.0256 (0.0029)	0.0132 (0.0032)	0.0148 (0.0026)	0.0693 (0.0077)	0.0198 (0.0028)	0.0137 (0.0037)	0.0186 (0.0025)	0.0137 (0.0035)
	Updated Lindley	0.0058 (0.0014)	0.0052 (0.0017)	0.0050 (0.0020)	0.0049 (0.0020)	0.0055 (0.0014)	0.0013 (0.0004)	0.0052 (0.0019)	0.0051 (0.0024)	0.0058 (0.0021)	0.0056 (0.0016)	0.0058 (0.0092)	0.0054 (0.0020)	0.0057 (0.0022)	0.0051 (0.0016)	0.0057 (0.0022)
	Rani	0.0291 (0.0031)	0.0295 (0.0030)	0.0280 (0.0032)	0.0277 (0.0032)	0.0283 (0.0029)	0.0083 (0.0035)	0.0266 (0.0031)	0.0812 (0.0035)	0.0216 (0.0037)	0.0244 (0.0033)	0.0811 (0.0073)	0.0335 (0.0032)	0.0211 (0.0043)	0.0353 (0.0033)	0.0211 (0.0047)
Data II	Obulezi	0.1289 (0.0185)	0.1401 (0.0229)	0.1384 (0.0246)	0.1377 (0.0245)	0.1199 (0.0203)	0.0148 (0.0055)	0.1373 (0.0233)	0.1551 (0.0272)	0.1409 (0.0262)	NAN	0.3236 (0.0935)	0.1523 (0.0250)	0.1227 (0.0276)	NAN	0.1228 (0.0280)
	Lindley	0.2317 (0.0234)	0.2703 (0.0269)	0.2737 (0.0287)	0.2727 (0.0287)	0.2192 (0.0242)	0.0243 (0.0143)	0.2697 (0.0275)	0.3346 (0.0319)	0.2167 (0.0327)	NAN	0.5386 (0.1089)	0.3152 (0.0292)	0.2394 (0.0342)	NAN	0.2396 (0.0345)
	Shanker	0.2589 (0.0248)	0.2991 (0.0258)	0.2982 (0.0269)	0.2974 (0.0269)	0.2449 (0.0245)	0.0223 (0.0154)	0.2938 (0.0260)	0.3994 (0.0287)	0.2674 (0.0330)	NAN	0.5421 (0.0598)	0.3538 (0.0272)	0.2518 (0.0346)	NAN	0.2519 (0.0351)
	Pranav	0.5300 (0.0361)	0.6474 (0.0376)	0.6560 (0.0388)	0.6551 (0.0388)	0.5060 (0.0367)	0.0341 (0.0407)	0.6499 (0.0380)	0.6582 (0.0418)	0.4455 (0.0465)	NAN	0.6582 (0.0854)	0.6582 (0.0397)	0.5324 (0.0481)	NAN	0.5322 (0.0484)
	Xgamma	0.2339 (0.0238)	0.3707 (0.0210)	0.3891 (0.0219)	0.3882 (0.0219)	0.2917 (0.0196)	0.0382 (0.0143)	0.3844 (0.0212)	0.4469 (0.0243)	0.3400 (0.0258)	NAN	0.5955 (0.0938)	0.4094 (0.0225)	0.3648 (0.0273)	NAN	0.3649 (0.0275)
	Chris-Jerry	0.3266 (0.0287)	0.4060 (0.0314)	0.4281 (0.0328)	0.4267 (0.0327)	0.3111 (0.0296)	0.0336 (0.0205)	0.4226 (0.0319)	0.5214 (0.0361)	0.3584 (0.0361)	NAN	0.6001 (0.1172)	0.4697 (0.0339)	0.3810 (0.0400)	NAN	0.3809 (0.0415)
	Updated Lindley	0.1282 (0.0183)	0.1391 (0.0207)	0.1373 (0.0221)	0.1367 (0.0220)	0.1194 (0.0185)	0.0148 (0.0054)	0.1363 (0.0211)	0.1537 (0.0256)	0.1400 (0.0239)	NAN	0.3164 (0.1062)	0.1509 (0.0231)	0.1220 (0.0263)	NAN	0.1221 (0.0264)
	Rani	0.6621 (0.0407)	0.7084 (0.0424)	0.7084 (0.0439)	0.7084 (0.0440)	0.6337 (0.0405)	0.0755 (0.0541)	0.7084 (0.0425)	0.7084 (0.0468)	0.5407 (0.0539)	NAN	0.7083 (0.0824)	0.7084 (0.0446)	0.6711 (0.0578)	NAN	0.6709 (0.0582)
Data III	Obulezi	0.0130 (0.0025)	0.0121 (0.0027)	0.0119 (0.0029)	0.0118 (0.0029)	0.0117 (0.0025)	0.0026 (0.0008)	0.0120 (0.0028)	0.0118 (0.0034)	0.0125 (0.0032)	NAN	0.0123 (0.0146)	0.0124 (0.0030)	0.0125 (0.0034)	NAN	0.0125 (0.0035)
	Lindley	0.0257 (0.0035)	0.0266 (0.0037)	0.0267 (0.0040)	0.0265 (0.0040)	0.0235 (0.0034)	0.0055 (0.0022)	0.0261 (0.0038)	0.0315 (0.0043)	0.0237 (0.0047)	NAN	0.0629 (0.0148)	0.0300 (0.0040)	0.0242 (0.0051)	NAN	0.0243 (0.0051)
	Shanker	0.0260 (0.0035)	0.0270 (0.0040)	0.0270 (0.0043)	0.0269 (0.0043)	0.0238 (0.0036)	0.0055 (0.0021)	0.0264 (0.0041)	0.0324 (0.0047)	0.0238 (0.0049)	NAN	0.0976 (0.0109)	0.0307 (0.0043)	0.0244 (0.0056)	NAN	0.0244 (0.0056)
	Pranav	0.0521 (0.0050)	0.0573 (0.0052)	0.0572 (0.0055)	0.0569 (0.0055)	0.0480 (0.0050)	0.0107 (0.0049)	0.0559 (0.0053)	0.0926 (0.0059)	0.0399 (0.0064)	NAN	0.1467 (0.0162)	0.0674 (0.0055)	0.0546 (0.0072)	NAN	0.0548 (0.0074)
	Xgamma	0.0257 (0.0035)	0.0402 (0.0030)	0.0411 (0.0032)	0.0409 (0.0032)	0.0339 (0.0029)	0.0082 (0.0023)	0.0402 (0.0031)	0.0526 (0.0034)	0.0311 (0.0037)	NAN	0.0877 (0.0122)	0.0466 (0.0032)	0.0393 (0.0040)	NAN	0.0395 (0.0040)
	Chris-Jerry	0.0377 (0.0043)	0.0409 (0.0042)	0.0416 (0.0044)	0.0414 (0.0044)	0.0344 (0.0040)	0.0082 (0.0033)	0.0407 (0.0043)	0.0552 (0.0050)	0.0312 (0.0054)	NAN	0.1126 (0.0178)	0.0483 (0.0045)	0.0393 (0.0056)	NAN	0.0395 (0.0055)
	Updated Lindley	0.0130 (0.0025)	0.0121 (0.0029)	0.0119 (0.0031)	0.0118 (0.0031)	0.0117 (0.0025)	0.0026 (0.0008)	0.0120 (0.0030)	0.0118 (0.0036)	0.0125 (0.0034)	NAN	0.0123 (0.0123)	0.0124 (0.0032)	0.0125 (0.0038)	NAN	0.0125 (0.0038)
	Rani	0.0651 (0.0056)	0.0130 (0.0058)	0.0130 (0.0060)	0.0130 (0.0060)	0.0130 (0.0056)	0.0130 (0.0064)	0.0130 (0.0059)	0.0130 (0.0066)	0.0130 (0.0076)	0.0130 (0.0063)	0.0130 (0.0150)	0.0130 (0.0062)	0.0130 (0.0080)	0.0130 (0.0061)	0.0130 (0.0081)

From Table 14, the standard errors (SE), which measure the precision of the parameter estimates, reveals that the RTADE method is consistently the best estimator across all three datasets and all distributions, as it frequently yields the absolute lowest SE values (e.g., 0.0004 for the Updated Lindley distribution in Data I, and 0.0008 for `Obulezi` and Updated Lindley in Data III). Conversely, the ADSOE method is clearly the worst estimator, as it almost always results in the absolute highest standard errors across all distributions and datasets (e.g., 0.0092 for Updated Lindley in Data I, 0.1172 for Chris-Jerry in Data II, and 0.0178 for Chris-Jerry in Data III), indicating the least precise estimates. While the MLE is often considered a benchmark, this empirical study shows that the RTADE is overwhelmingly superior in terms of precision, demonstrating that distance-based methods can outperform classical methods for these specific models and datasets. The "NAN" (Not a Number) values appearing in the table for the MSALDE, MSSLDE, and MSLNDE estimation methods for Data II and Data III indicate a complete failure of these methods to yield a valid parameter estimate for the respective distributions. This outcome most commonly arises from the numerical optimization algorithms either failing to converge to a solution or encountering computational

instabilities (such as taking the logarithm of a non-positive value) due to the nature of the data or the complexity of the estimation equations. In the context of evaluating estimator performance, the presence of NAN marks these three methods as unviable and unusable for the distributions applied to Data II and Data III, making them the least reliable choices compared to all other methods listed.

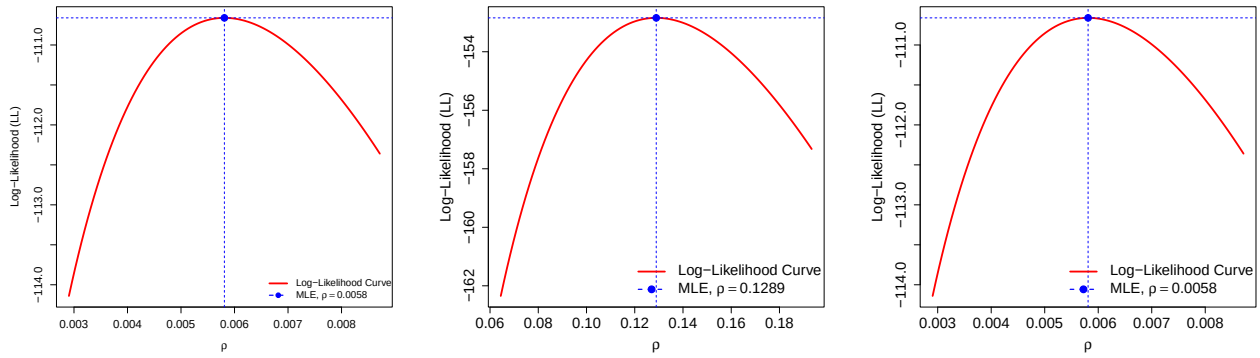

Figure 19. Negative Log-likelihood Profile for `Obulezi`(ρ) distribution

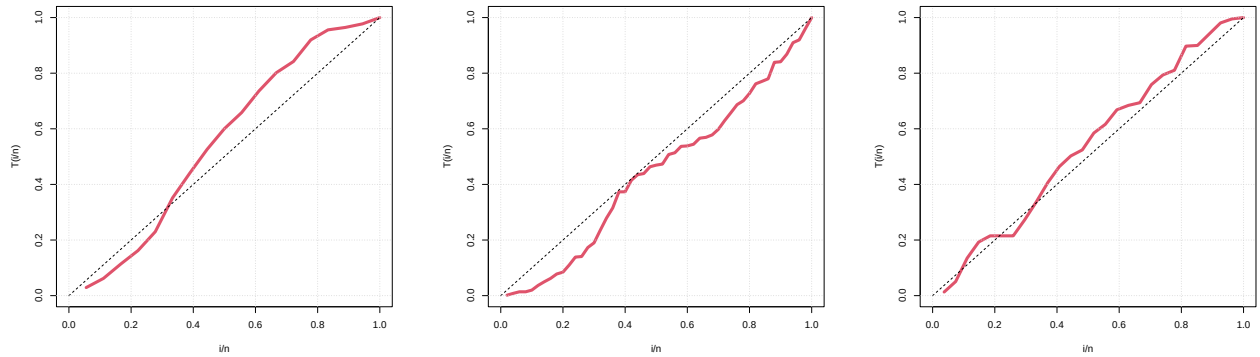

Figure 20. Total Time on Test (TTT) plots

Figure 19 displays the Log-likelihood Profile for the `Obulezi` parameter ρ for the three datasets. The characteristic reversed U-shape of each curve, with a clear and well-defined minimum, indicates that the maximum likelihood estimate (MLE) of ρ is unique and stable for all three datasets. The red dashed line and the red point in each plot pinpoint the exact value of the MLE where the negative log-likelihood is minimized, confirming the reliability of the estimation process for the `Obulezi` distribution.

Figure 20 shows the Total Time on Test (TTT) plots for the three datasets. The TTT plots are a graphical method used to assess the shape of the hazard rate function. For Data I, the TTT curve is a strictly increasing failure rate (IFR). For Data II, the TTT plot indicates a non-monotonic, showing an initial increase in the hazard rate, followed by a period where the hazard rate stabilizes or slightly decreases, and then an increase again toward the end. This suggests a complex failure process, but the main visual characteristic is that the hazard rate is not strictly monotonic (neither purely increasing nor purely decreasing). The TTT plot for Data III suggests a non-monotonic hazard rate, predominantly characterized by an Increasing Failure Rate (IFR) after a very brief initial period. The overall pattern is consistent with a bathtub-shaped hazard

function where the wear-out phase dominates.

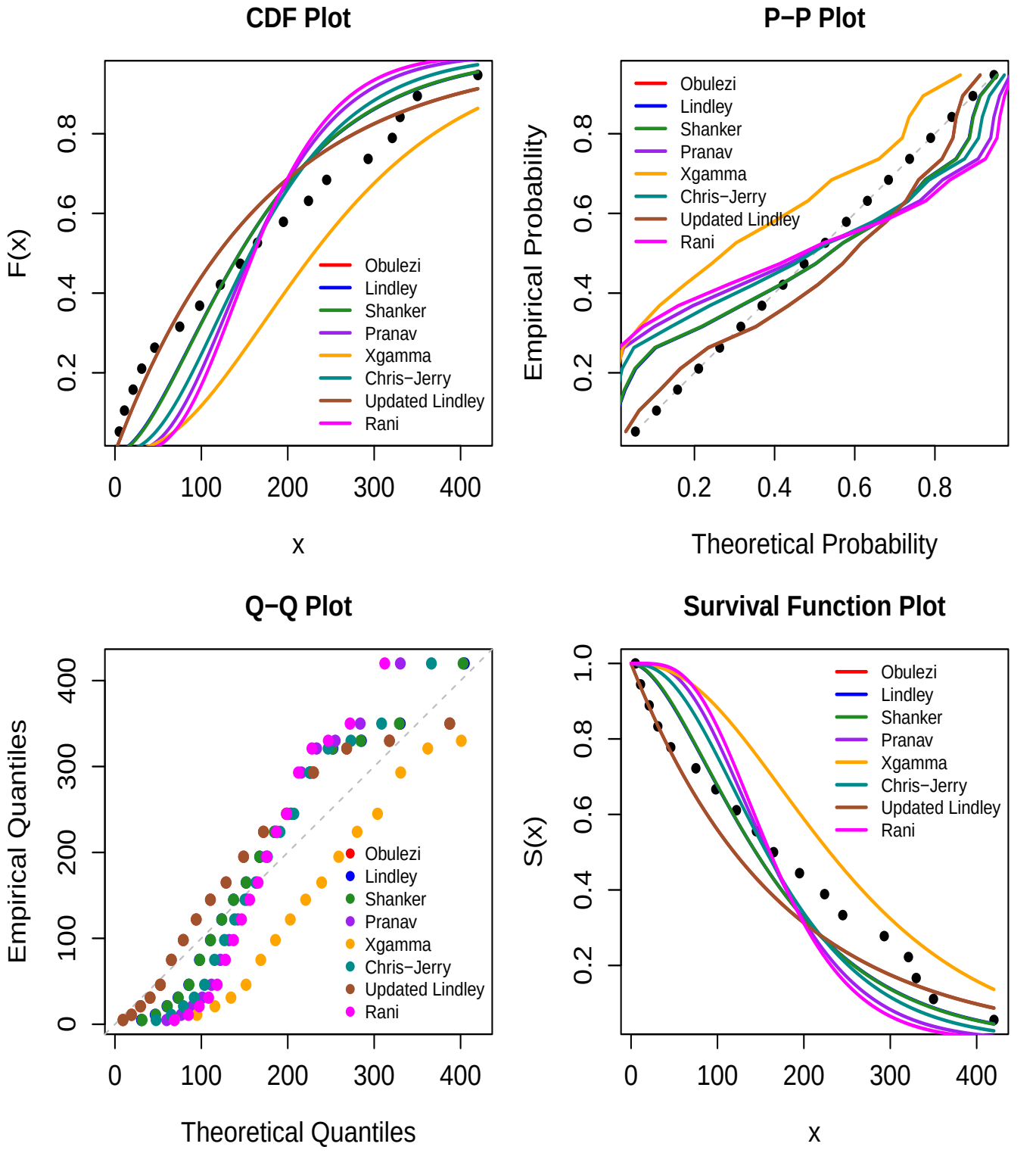

Figure 21. CDF, Probability-Probability (P-P), Quantile-Quantile (Q-Q) and Survival function plots for Data I

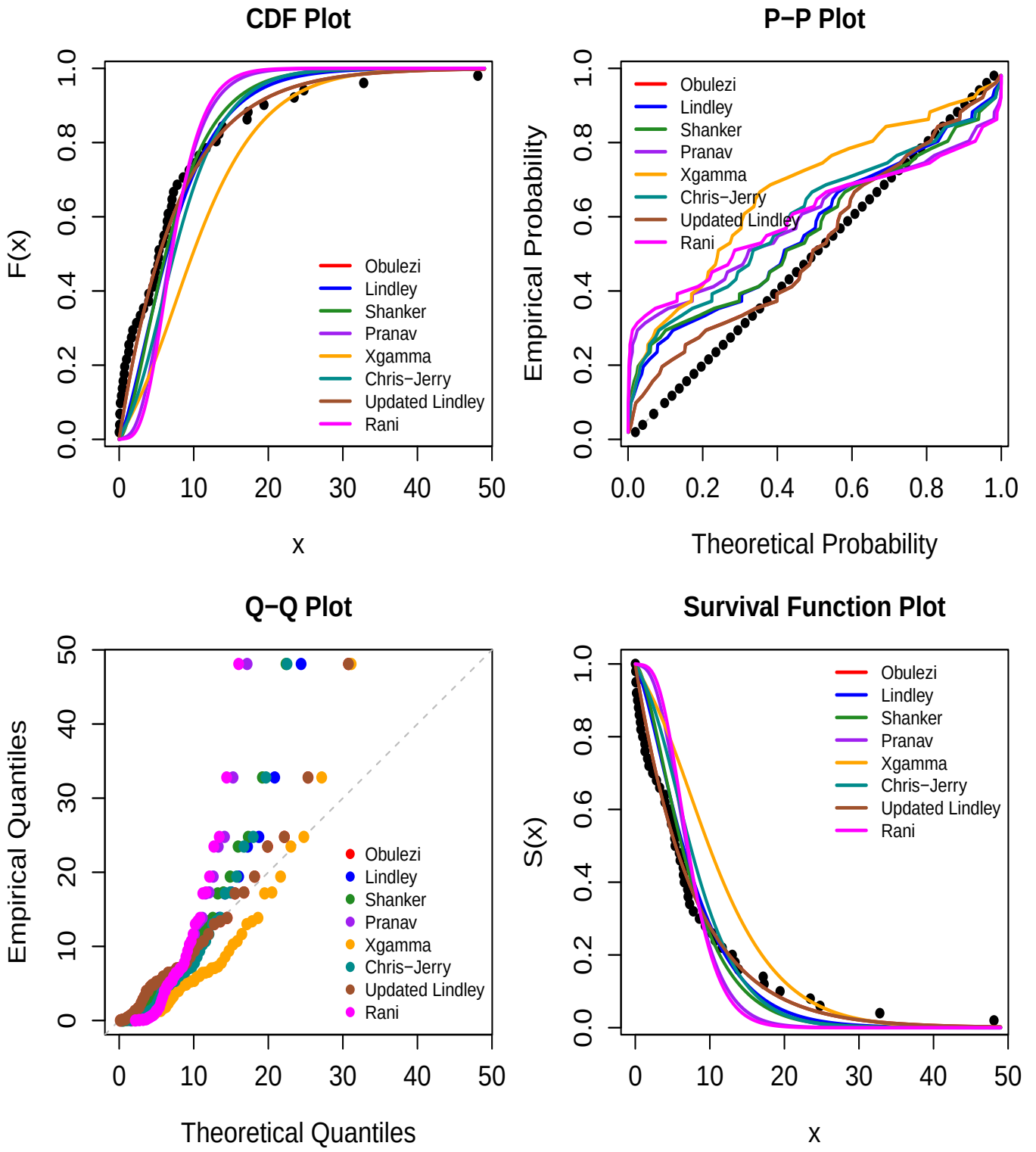

Figure 22. CDF, Probability-Probability (P-P), Quantile-Quantile (Q-Q) and Survival function plots for Data II

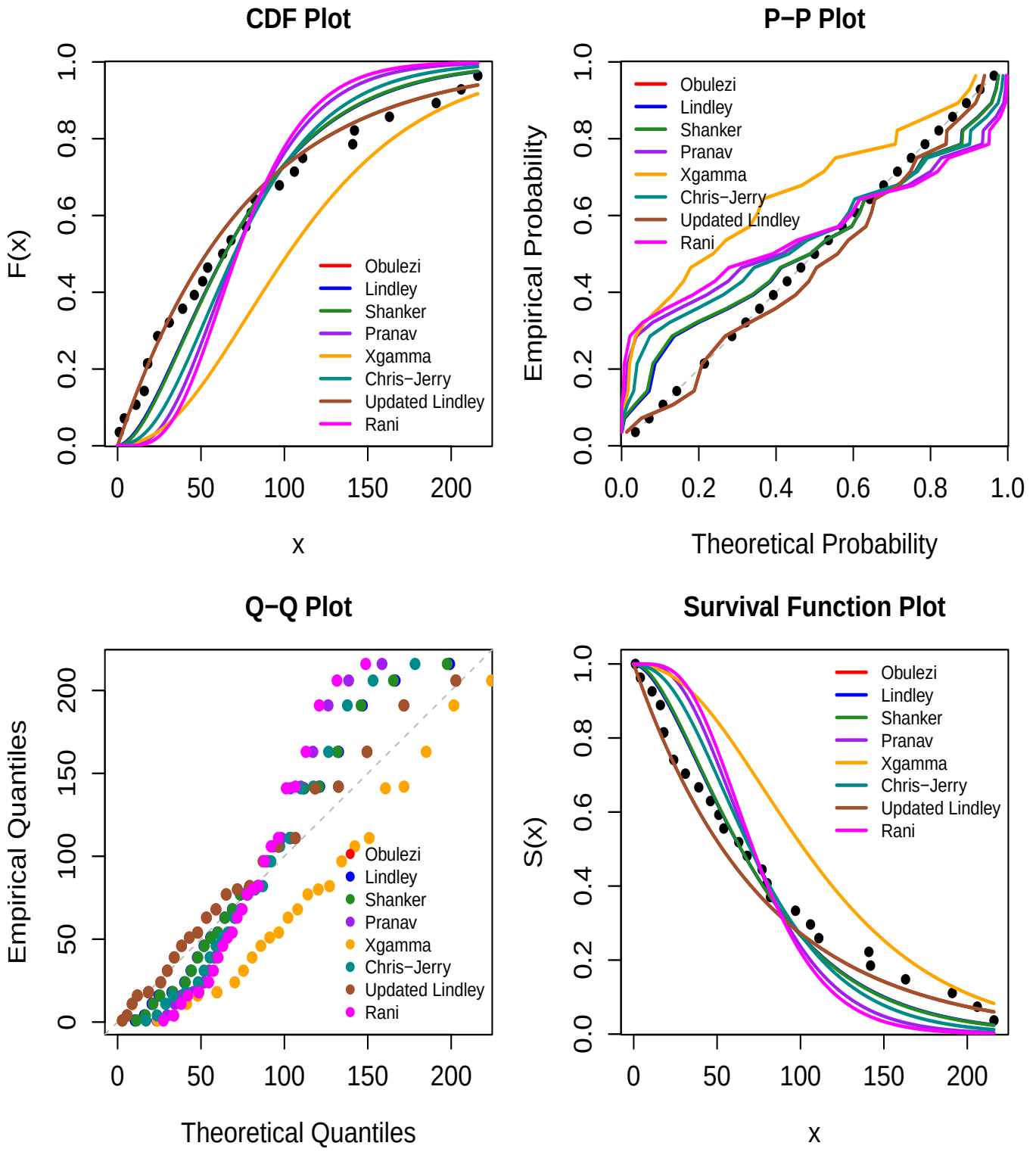

Figure 23. CDF, Probability-Probability (P-P), Quantile-Quantile (Q-Q) and Survival function plots for Data III

The goodness-of-fit plots for Data I, Data II and Data III in Figures 21, 22, and 23 respectively visually

confirm the statistical findings, demonstrating how well each theoretical distribution fits the empirical data. Across all four plots—the CDF Plot, Probability-Probability (P-P) Plot, Quantile-Quantile (Q-Q) Plot, and Survival Function Plot—the `Obulezi` and Updated Lindley distributions are visually the best-fitting models as their lines lie closest to the empirical data points (in the CDF and Survival plots) or are tightest around the diagonal reference line (in the P-P and Q-Q plots). Specifically, in the Q-Q plot, the points for `Obulezi` and Updated Lindley are the nearest to the dashed diagonal line, indicating that their theoretical quantiles closely match the empirical quantiles. Conversely, the xgamma distribution consistently shows the worst fit, as its line (yellow) is the furthest from the empirical data points in the CDF and Survival plots, and its quantiles (in the Q-Q plot) and probabilities (in the P-P plot) deviate most significantly from the diagonal line, confirming its poor performance.

7. Conclusion and Future Work

In this study, we successfully introduced and rigorously analyzed the `Obulezi` distribution, a novel, single-parameter continuous probability model formulated to enhance the flexibility and descriptive power of distributions in the Lindley class. We derived and explored several essential mathematical properties, including the complete and incomplete moments, the moment generating function, the mean residual life function, and the stress-strength reliability function, demonstrating the model's analytical tractability. We also established that the distribution is stochastically ordered with respect to its scale parameter, ρ.

A major contribution of this work lies in the extensive evaluation of parameter estimation methods. We not only utilized the Maximum Likelihood Estimator (MLE) but also employed fourteen competing estimation techniques (a total of 15 methods) in both simulation studies and real-data applications across three distinct datasets. Crucially, the empirical analysis demonstrated the `Obulezi` distribution's significant practical utility in modeling diverse lifetime datasets. The Log-likelihood profiles confirmed the uniqueness and stability of the parameter estimation via the Maximum Likelihood method. Furthermore, graphical assessment via Quantile-Quantile (Q-Q) plots showed a close fit between the theoretical `Obulezi` model and the observed data across varying scales, providing strong visual validation. The TTT plots consistently suggested that the distribution is particularly effective for modeling phenomena exhibiting an increasing failure rate (IFR), a feature common in certain reliability and survival studies where initial mortality is low. Ultimately, the `Obulezi` distribution presents itself as a parsimonious, robust, and highly competitive alternative to established single-parameter models like the Exponential and Lindley distributions for modeling positively skewed lifetime data.

The comprehensive framework established here opens several promising avenues for future research:

(a) Since the `Obulezi` distribution can only model the IFR, introducing an additional shape parameter will enhance its flexibility, and ultimately make it fit a decreasing failure rate (DFR) situation.

(b) Generalization and Extension: Future work could involve introducing one or more additional shape or scale parameters to create a generalized or flexible version of the `Obulezi` distribution. This will enhance its flexibility to model more complex non-monotonic hazard rate patterns, such as bathtub or unimodal shapes, expanding its applicability beyond DHR data.

(c) Discrete Compounding: Following the tradition of the Lindley family, the `Obulezi` distribution can be used as a compounding distribution with a discrete model, such as the Poisson or Binomial, to generate new count distributions (e.g., the Poisson-Obulezi distribution). This would allow the model

to be applied in fields like quality control and reliability, where discrete count data (e.g., number of failures) are common.

(d) Bivariate and Multivariate Forms: Developing bivariate or multivariate extensions of the `Obulezi` distribution would allow it to model dependent survival times, making it valuable for analyses in fields like clinical trials or reliability engineering involving paired or grouped data.

(e) Bayesian Inference and Regression: Exploring Bayesian estimation methods for the parameter ρ, potentially using different prior distributions, would provide a robust alternative to classical MLE. Additionally, integrating the `Obulezi` distribution into a regression framework would allow for modeling the effect of covariates on the lifetime variable.

Authors' Contributions

O. J. O. : Conceptualization, Methodology, Software, Validation, Formal Analysis, Investigation, Resources, Data Curation, Writing – Original Draft Preparation, Writing – Review & Editing, Visualization, Supervision, Project Administration, and Funding Acquisition.

Data Availability Statement

The data used in this study is provided within the manuscript.

Conflicts of Interest

The author declares no conflict of interest.

Acknowledgments

I acknowledge the profound memory of my late father, `Mr. Obulezi Marcus Ehisianya`, whose spirit continues to inspire my work. Though he did not live to see this achievement, the `Obulezi` distribution is formulated in his honor and stands as a permanent tribute to his life and legacy.

Funding

This research received no external funding.

References

1.Aijaz, A., Jallal, M., Ain, S. Q. U., and Tripathi, R. (2020). The hamza distribution with statistical properties and applications. *Asian journal of probability and statistics*, 8(1):28–42.

2.Echebiri, U. V. and Mbegbu, J. I. (2022). Juchez probability distribution: Properties and applications. *Asian Journal of Probability and Statistics*, 20(2):56–71.

3.Ekemezie, D.-F. N. and Obulezi, O. J. (2024). The fav-jerry distribution: Another member in the lindley class with applications. *Earthline Journal of Mathematical Sciences*, 14(4):793–816.

4.El Gazar, A. M., Metwally, D. S., Elgarhy, M., and El-Desouky, B. S. (2025). Truncated transmuted exponential distribution with different estimation methods and applications. *Journal of Multidisciplinary Applied Natural Science*.

5.Elechi, O., Okereke, E. W., Chukwudi, I. H., Chizoba, K. L., and Wale, O. T. (2022). Iwueze's distribution and its application. *Journal of Applied Mathematics and Physics*, 10(12):3783–3803.

6.Fisher, R. A. (1912). On an absolute criterion for fitting frequency curves. *Messenger of mathematics*, 41:155–156.

7.Fisher, R. A. (1922). On the mathematical foundations of theoretical statistics. *Philosophical transactions of the Royal Society of London. Series A, containing papers of a mathematical or physical character*, 222(594-604):309–368.

8.KK, S. (2018). Pranav distribution with properties and its applications. *Biom Biostat Int J*, 7(3):244–254.

9.Lindley, D. V. (1958). Fiducial distributions and bayes' theorem. *Journal of the Royal Statistical Society. Series B (Methodological)*, pages 102–107.

10.Odom, C. and Ijomah, M. (2019). Odoma distribution and its application. *Asian journal of probability and statistics*, 4(1):1–11.

11.Okereke, E. W. and Uwaeme, O. R. (2025). A new one-parameter distribution with two turning points and bathtub shaped failure rate function. *Journal of Probability and Statistical Science*, 23(1).

12.Onyekwere, C. K., Aguwa, O. C., and Obulezi, O. J. (2025). An updated lindley distribution: Properties, estimation, acceptance sampling, actuarial risk assessment and applications. *Innovation in Statistics and Probability*, 1(1):1–27.

13.Onyekwere, K. C. and Obulezi, O. (2023). Chris-jerry distribution and its applications. *Asian Journal of Probability and Statistics*, 20(1):16–30.

14.Oramulu, D. O., Etaga, H. O., Onuorah, A. J., and Obulezi, O. J. (2023). A new member in the lindley class of distributions with flexible applications. *Sch J Phys Math Stat*, 7:148–159.

15.Radhakrishnan, R., Venkatesan, D., and Prasanth, C. (2025). Sujit distribution and its applications. *International Journal of Agricultural & Statistical Sciences*, 21(1).

16.Razali, A. M. and Al-Wakeel, A. A. (2013). Mixture weibull distributions for fitting failure times data. *Applied Mathematics and Computation*, 219(24):11358–11364.

17.Sen, S., Maiti, S. S., and Chandra, N. (2016). The xgamma distribution: statistical properties and application. *Journal of Modern Applied Statistical Methods*, 15(1):38.

18.Shanker, R. (2015a). Akash distribution and its application. *International Journal of Probability and Statistics*, 4(3):65–75.

19.Shanker, R. (2015b). Shanker distribution and its applications. *International journal of statistics and Applications*, 5(6):338–348.

20.Shanker, R. (2016a). Amarendra distribution and its applications. *American Journal of Mathematics and Statistics*, 6(1):44–56.

21.Shanker, R. (2016b). Aradhana distribution and its applications. *International Journal of Statistics and Applications*, 6(1):23–34.

22.Shanker, R. (2016c). Devya distribution and its applications. *International Journal of Statistics and Applications*, 6(4):189–202.

23.Shanker, R. (2016d). Shambhu distribution and its applications. *International Journal of Probability and Statistics*, 5(2):48–63.

24.Shanker, R. (2016e). Sujatha distribution and its applications. *Statistics in Transition. New Series*, 17(3):391–410.

25.Shanker, R. (2017a). Akshaya distribution and its application. *American Journal of Mathematics and Statistics*, 7(2):51–59.

26.Shanker, R. (2017b). Rama distribution and its application. *International Journal of Statistics and Applications*, 7(1):26–35.

27.Shanker, R. (2017c). Rani distribution and its application. *Biometrics & Biostatistics International Journal*, 6(1):1–10.

28.Shanker, R. (2017d). Suja distribution and its application. *International Journal of Probability and Statistics*, 6(2):11–19.

29.Shanker, R. (2022). Uma distribution with properties and applications. *Biometrics & Biostatistics International Journal*, 11(5):165–169.

30.Shanker, R. (2023a). Komal distribution with properties and application in survival analysis. *Biometrics & Biostatistics International Journal*, 12(2):40–44.

31.Shanker, R. (2023b). Pratibha distribution with properties and application. *Biometr. Biostat. Int. J.*, 12:136–142.

32.Shanker, R. (2025). Shreekant distribution with properties and applications to model stress and strength data from engineering. *Reliability: Theory & Applications*, 20(2 (84)):78–95.

33.Shanker, R. and Shukla, K. (2017). Ishita distribution and its applications. *Biometrics & Biostatistics International Journal*, 5(2):1–9.

34.Shanker, R., Shukla, K., Ranjan, A., and Shanker, R. (2021). Adya distribution with properties and application. *Biometrics & Biostatistics International Journal*, 10(3):81–88.

35.Shanker, R. and Shukla, K. K. (2018). Om distribution with properties and applications. *Reliability: Theory & Applications*, 13(4 (51)):27–41.

36.Shanker, R. and Shukla, K. K. (2020). Kamlesh-rama distribution and its applications. *Journal of Probability and Statistical Science*, 18(1):1–12.

37.Shukla, K. K. (2018). Prakaamy distribution with properties and applications. *JAQM*, 13(3):30–38.

38.Shukla, K. K. and Shanker, R. (2019). Shukla distribution and its application. *Reliability: Theory & Applications*, 14(3):46–55.

39.Xie, M., Tang, Y., and Goh, T. N. (2002). A modified weibull extension with bathtub-shaped failure rate function. *Reliability Engineering & System Safety*, 76(3):279–285.